UNIVERSIDAD AUTONOMA DE MADRID

FACULTAD DE CIENCIAS

Departamento de Biología Molecular

DREAM DIFFERENTLY REGULATES SPINAL AND TRIGEMINAL NOCICEPTION

Tesis Doctoral

Tomaso Benedet

Madrid, 2010

CENTRO NACIONAL DE BIOTECNOLOGIA

CSIC

El trabajo experimental presentado en esta memoria ha sido realizado en el Departamento de Biología Molecular y Celular (Centro Nacional de Biotecnología CNB-CSIC) bajo la dirección de el Dr. José Ramón Naranjo Orovio, gracias a una beca FPI del Ministerio de Ciencia y Tecnología asociada al proyecto: **SAF 2004-06644**

Acknowledgement

PAGINA NUOVA, PENSIERI PIU FRESCHI…

Llevar a cabo este trabajo ha sido posible sólo gracias a la colaboración, el esfuerzo y la cercanía de muchas personas. Algunas han compartido y enriquecido mi día a día, y otras, un poco más lejanas –pero no menos importantes-, han sido mi íntimo apoyo.

En primer lugar, quiero agradecer a mi director de tesis, el Dr. José Ramón Naranjo por haberme dirigido en éste siempre estimulante trabajo y por la confianza que ha depositado en mí en estos años. A la vez, quiero agradecer a la Dra. Britt Mellstrom porque, con su ejemplo, me ha enseñado la importancia del método de trabajo en el desarrollo de un proyecto de investigación.

Las colaboraciones puede que sean el momento en el que la investigación encuentra su sentido más genuino. Durante este trabajo he tenido la oportunidad de colaborar con los grupos dirigidos por el Dr. Carlos Avendaño y el Dr. José Antonio López, a ellos va mi más sentido agradecimiento. Y no puedo olvidar dar las gracias a Carolina y Agi, mis compañeras a la hora desempeñar la parte mas "sucia" de este proyecto.

A lo largo de estos años han pasado muchas personas por el laboratorio, junto a ellos he compartido ésta más que intensa experiencia. Gracias a ellos he aprendido muchas cosas, algunas tienen a que ver con la biología, otras no. Y son muy importantes.
In primis, quiero agradecer un montón a todas las personas que están ahora en el laboratorio y que me han estado apoyando en estos últimos meses de frenesís ciclotímico: Paz, Marcos, Sofía, Vero, Diego y José. ¡ Gracias por haberme aguantado día tras día!
Un GRAZIE también a Rosa a Malgosia y a Clara que me echaron una gran mano y ya no están aquí en el CNB. Y a David que siempre me ha ayudado a moverme por este centro. Y a Judith, que cuando el pasillo de atrás era "nuestro pasillo", me enseñó todas las palabras que no se encuentran en la RAE. Un abrazo CO!

Cuando pienso en el laboratorio, pienso en el departamento y en todos los que curran porque las cosas funcionen, por eso quiero dar las gracias a las chicas de cocina, y a Carlos. Un gracias particular a Socorro, porque uno se siente bien a charlar contigo y por todas las plantas que me has pasado (aun si ninguna a tenido mucha suerte!)
Finalmente quiero dar las gracias a todo el personal del animalario (¡me gusta la música que ponéis!) y a Mercedes que siempre ha sido capaz de aclarar mis líos con los ratones, como un profesional, como un amiga.

Antes de bajar de este taburete imaginario quiero agradecer a Leti y a Gus, porque con vosotros, y gracias a vosotros, he estado màs que en casa en Calle Ayala. A Laura, porque si algun un día entiendo todo lo que dices podré aprender… un mogollón! A Angel que me nutre con pastas de te y con historia de España. A Lali, que sabe lo que es la fuerza y sabe buscarla donde se esconde. A Clara, que todavía no sabe todo lo que dà. A Sofía, porque no te encontré solamente en el labo. Y a Eladio, ¡que cuida a todos los que quiere!

… Due parole in italiano!

Ultimamente, sarà il periodo, penso spesso a quando iniziai a trappolare in un laboratorio! Ho una maglietta rossa che mi ricorda quel periodo. Ci sono in circolazione tre magliette uguali alla mia. Dietro hanno scritte differenti: Cotol, Arnel, Gnol.
Non è stato facile, e forse proprio per questo vi ricordo con tanto affetto. So che è pure grazie a voi che sono arrivato fin qui.

Approfitto di questo spazio dei ringraziamenti, di questo “qui si può”, per fermarmi un secondo e ripensare a tutto l’esercito di comici, spaventati guerrieri che mi hanno accompagnato fino a qui.

[s-e-c-o-n-d-o]

Un bacione in particolare a Maria che mi e’ stata sempre vicina, anche nelle situazioni più improbabili, e che proprio ora è “una e bina”!! E a Bau, perché apro la mail, busso, e tu apri sempre in pochi secondi… e per tutti i km che ti sei fatto per vedermi!

Grazie Paolo&Anna, grazie Anna&Paolo. Anna, ho capito che l'amore esiste in forme molto differenti, a volte strane, ma non per questo meno profonde. Paolo, sei la persona che sa rendere costante il mio cuore.

INDEX

INDEX

ABBREVIATIONS

ABBREVIATIONS

2-AG: 2-Arachidonoylglycerol

AA-NAT: Arylalkylamine N-Acetyltransferase

AMPA: α-Amino-3-Hydroxy-5-Methyl-4-Isoxazolepropionic Acid

AP1: Activator Protein 1

aRNA: Amplified RNA

ASIC (1; 2; 3): Acid Sensing Ion Channel (1; 2; 3)

BDNF: Brain Derived Neurotrophic Factor

BK (1; 2) receptor: Bradykinin (1; 2) receptor

BoNT: Botulinum Neurotoxin

CaMKII: Calmodulin Kinase II

CaRF: Calcium-Response Factor

CaV2.2: Voltage Gated Calcium Channel 2.2

CB1: Cannabinoid receptor type 1

CBP: CREB Binding Protein

CCI: Chronic Constriction Injury

CFA: Complete Freund's Adjuvant

CGRP: Calcitonin Gene Related Peptide

CNS: Central Nervous System

COX: Cyclo-Oxygenase

CRE: cAMP Response Element

CREB: cAMP Response Element Binding Protein

CREM: cAMP Response Element Modulator

CTSL: Cathepsin L

daDREAM: dominant active DREAM

DBNDD2: Dysbindin Domain containing protein 2

DOR: δ Opioid Receptor

DRE: Downstream Regulatory Element

DREAM: Downstream Regulatory Element Antagonist Modulator

DRG: Dorsal Root Ganglion

DR-VRR: Dorsal Root-Ventral Root refex

DTNBP1: Dysbindin

DTT: Dithiothreitol

ER: Endoplasmic Reticulum

ERK (1; 2): External Receptor Kinase (1; 2)

FAM: 6-Carboxyfluorescein

FDR: False Discovery Rate

FKN: Fractalkine

fl-trkB: Full Length trkB

FRA-2: Fos Related Antigen 2

GABA: γ-Aminobutyric Acid

GAPDH: Glyceraldehyde 3-Phosphate Dehydrogenase

GPCR: G Protein-Coupled Receptor

GRK (2; 6): G Protein-Coupled Receptor Kinase (2; 6)

ICER: Inducible cAMP Early Repressor

IL (1β; 2; 4; 6): Interleukin (1β; 2; 4; 6)

IRES: Internal Ribosom Entry Site

JNK: c-Jun N-terminal Kinase

K2P: Two-pore Potassium Channel

KCC2: Potassium Chloride Cotransporter 2

KChIP (1-4): Potassium Channel Interacting Protein (1-4)

KCNK (2; 4; 18): Two Pore Domain Potassium Channel

KID: Kinase Inducible Domain

KOR: κ Opioid Receptor

Kv (4.1; 4.2; 4.3): Voltage Gated Potassium Channel (4.1; 4.2; 4.3)

L1: line 1

L16: line 16

LCD: Leucine, Charged residue-rich Domain

LHVS: Morpholinurea-Leucine-Homophenylalanine-Vinyl Sulfone-Phenyl

LTP: Long Term Potentiation

MAPK: Mitogen-Activated Protein Kinase

MGB: Minor Groove Binder

MGLL: Monoacylglycerol Lipase

mGLU-R: Metabotropic Glutamate Receptor

MOR: μ Opioid Receptor

Nav (1.2; 1.7; 1.8; 1.9): Voltage Gated Sodium Channel

NF-kB: Nuclear Factor-kappaB

NGF: Nerve Growth Factor

NK1 receptor: Neurokinin

NMDA: N-Methyl-D-Aspartate

NR2B: NMDA Receptor 2B

NSF: N-Ethylmaleimide Sensitive Fusion Proteins

NT (4; 4/5): receptor: Neurotrophin (4; 4/5) receptor

ORL: Opioid Receptor Like

PAG: Periaqueductal gray

PAX8: Paired Box Gene 8

PCR: Polymerase Chain Reaction

PDYN: Prodynorphin

PENK: Proenkephalin

PGE2: Prostaglandin E2

PI3K: Phosphatidylinositol-3-Kinase

PKA: Protein Kinase A

PKC: Protein Kinase C

PLC-γ: Phospholipase C-γ

PNOC: Pronociceptin

PNS: Peripheral Nervous System

POMC: Proopiomelanocortin

PS (1; 2): Presenilin (1; 2)

PSD-95: Post Synaptic Density 95

PVDF: Polyvinylidene Fluoride

Q-PCR: Quantitative PCR

RVM: Nucleus Raphe Magnus

SC: Spinal Cord

SDS: Sodium Dodecyl Phosphate

SEM: Standard Error of the Mean

SIA: Stress Induced Analgesia

SNARE: Soluble NSF Attachment Protein Receptors

SUMO: Small Ubiquitin-Like Modifier

SV2 (a; b; c): Synaptic Vesicle 2 (a; b; c)

TBS: Tris Buffered Saline

TBS-T: Tris Buffered Saline-Tween-20

TG: Trigeminal Ganglion

TNF-α: Tumor Necrosis Factor-α

trk (A; B; C): Tropomyosine Receptor Kinase (A; B; C)

TRPA1: Transient Receptor Potential Ankyrin

TRPM8: Transient Receptor Potential Melastatin 8

TRPV (1; 2; 4): Transient Receptor Potential Vanilloid (1; 2; 4)

tr-trkB: Truncated trkB

TTF-1: Thyroid transcription factor-1

Ubc9: Ubiquitin Carrier Protein 9

VPL: Ventral Postero-Lateral

VPM: Ventral Postero-Medial

ABSTRACT

ABSTRACT

The transcriptional repressor DREAM (downstream regulatory element antagonist modulator) controls the expression of prodynorphin and has been involved in the modulation of endogenous responses to pain. To investigate the role of DREAM in nociception we used transgenic mice overexpressing a Ca^{2+}- and cAMP-insensitive DREAM mutant. The DREAM mutant has been previously shown to function as a constitutively cross-dominant active mutant able to block activity-dependent derepression of all DREAM/KChIP family members.

DREAM transgenic mice showed reduced expression of several genes related to pain in spinal cord and DRG, including the different members of the opioid system and BDNF, and they show a state of basal hyperalgesia. Moreover, daDREAM expressing mice fail to develop a normal central sensitization process in response to inflammatory pain. On the other hand, daDREAM do not modify the nocifensive response to neuropathic pain, suggesting that DREAM is not functionally involved in the molecular mechanisms controlling this type of pain.

Overexpression of dominant active mutant DREAM in the trigeminal ganglia also resulted in a phenotype of orofacial hyperalgesia. Genome-wide analysis disclosed several new target genes for DREAM repression in trigeminal neurons, which could be involved in the specific and differential response of these neurons to inflammatory pain.

RESUMENES

RESUMENES

1. INTRODUCCIÓN

La señal dolorosa se genera por la estimulación de fibras aferentes especificas: los nociceptores. Estas neuronas polimodales responden a estímulos de naturaleza térmica, mecánica o química que pueden resultar lesivos para el organismo.

A nivel molecular existen diferentes receptores que pueden convertir los estímulos nocivos en señales nerviosas. Para los estímulos térmicos los más caracterizados son el canal TRPV1, para altas temperaturas, y el canal TRPM8, para bajas temperaturas. La nocicepción mecánica esta mediada por los canales sensibles a ácidos ASIC1, 2 y 3 mientras que las señales químicas son transmitidas fundamentalmente por los canales TRPV1, TRPM8 y TRPA1.

El dolor se define como agudo, cuando surge en respuesta a un estímulo nocivo y dura solo mientras este perdure. Se define crónico, cuando dura más que el estímulo que lo ha generado. Esta hiperalgesia puede tener dos orígenes: inflamatorio o neuropático. En el primer caso se debe a una repuesta adaptativa del sistema nervioso que, para favorecer la protección de un tejido dañado, aumenta la sensibilidad del mismo a los estímulos dolorosos. En el segundo caso , no tiene ningún significado adaptativo y es causada por un daño en el sistema nervioso.

El dolor inflamatorio y el dolor neuropático se caracterizan por una etiología muy distinta y se basan en diferentes mecanismos moleculares y celulares. A pesar de todas sus especificidades estas dos condiciones tienen un origen común: el fenómeno de plasticidad conocido como sensibilización a nivel central. Ésta consiste en una facilitación de la transmisión sináptica en respuesta a una estimulación periférica sostenida.

DREAM, conocida también como KChIP3 o Calsenilina, es una proteína multifuncional que ejerce diferentes papeles en diferentes localizaciones subcelulares. DREAM ha sido estudiada por su interacción con el canal de potasio dependiente de voltaje Kv4 a nivel de la membrana plasmática, su interacción con Presenilinas en la membrana del retículo endoplasmático y su función como represor transcripcional dependiente de calcio en el núcleo.

DREAM regula la expresión del gen de la prodinorfina, precursor de la dinorfina, un péptido fundamental en el control de la transmisión de la señal nociceptiva. El fenotipo hipoalgesico del ratón deficiente de DREAM (Cheng et al., 2002) confirmó la importancia de este factor transcripcional en el control de la propagación de los estímulos dolorosos. Además, estudios sobre la función de los canales de potasio dependientes de voltaje en la respuesta a estímulos nociceptivos (Hu et al., 2006) pusieron en evidencia nuevos posibles papeles de DREAM en el control de la nocicepción.

2. OBJETIVOS

El objetivo global fue caracterizar el papel funcional de DREAM en el control de la nocicepción a nivel de la medula espinal, de los ganglios de la raíz dorsal (GRD) y del ganglio trigémino. En particular hemos tratado de caracterizar:

1. La respuesta basal al dolor en la medula espinal y en los GRD en ratones transgénicos que sobre-expresan un dominante activo de DREAM (ratones daDREAM).

2. La respuesta al dolor crónico (tanto inflamatorio como neuropático) en la medula espinal y en los GRD en los ratones daDREAM.

3. Los cambios transcripcionales impuestos por el daDREAM que influyen en la nocicepción basal.

4. El papel de DREAM en la respuesta molecular al dolor inflamatorio crónico en la medula espinal y en los GRD.

5. El papel de DREAM en la respuesta molecular al dolor en el trigémino.

6. Los genes diana de DREAM que están involucrados en la percepción y la respuesta al dolor en el trigémino.

3. RESULTADOS

En la primera parte de este trabajo de tesis hemos caracterizado desde un punto de visto comportamental y molecular el papel de DREAM en el control de los mecanismos que regulan la percepción dolorosa en la medula espinal y en los ganglios de la raíz dorsal (GRD). Los ratones transgénicos (línea 1) que expresan un mutante dominante activo de DREAM (daDREAM) en estas dos áreas presentan cambios sustanciales en su fenotipo nociceptivo en respuesta a estimulación térmica y a dolor tónico. A nivel molecular los ratones de la línea 1 presentan una bajada generalizada del tono opioide y de la expresión de BDNF.

En nuestro modelo de dolor crónico inflamatorio los ratones de la línea 1 presentan un retraso en el desarrollo de la hiperalgesia inducida por CFA. BDNF es fundamental en los procesos de plasticidad sináptica y su expresión se induce en respuesta a una estimulación dolorosa sostenida. En los ratones transgénicos daDREAM, BDNF tampoco se induce en respuesta a un estimulo inflamatorio. Estos datos moleculares se correlacionan con estudios electrofisiológicos que demuestran como la falta de aporte de BDNF provoca la ausencia de facilitación sináptica en las neuronas del asta dorsal de la medula espinal en los ratones de la línea 1.

Los ratones transgénicos, además, presentan un nivel basal más alto de fosforilación de la quinasa ERK que se puede relacionar con una caída funcional de la inhibición GABAérgica inducida por el mutante dominante activo de DREAM.

En la segunda parte de este trabajo hemos investigado la importancia de DREAM en el control del los fenómenos nociceptivos a nivel del ganglio trigémino, mostrando un fenotipo hiperalgésico facial en los ratones transgénicos daDREAM (líneas 1 y 16). Utilizando un estudio de microarray hemos analizado las diferencias transcripcionales inducidas en neuronas trigeminales por la expresión de daDREAM en los ratones de la línea 16. Esto nos ha permitido caracterizar la tipología de los genes cuya expresión está afectada por daDREAM y aislar un sub-grupo de genes de interés para profundizar con nuestra investigación. Finalmente, hemos analizado la respuesta transcripcional en neuronas trigeminales al dolor inflamatorio incluyendo los genes opioides, BDNF así como los genes seleccionados en nuestro estudio transcriptómico.

4. DISCUSIÓN

En este trabajo de tesis hemos utilizado un modelo de ratón transgénico que sobrexpresa un mutante dominante activo del la proteína DREAM (daDREAM) para el estudio de la funcionalidad de este factor de transcripción en el control de los procesos nociceptivos.

Los ratones transgénicos de la línea 1 presentan una marcada hiperalgesia que se puede relacionar con el efecto de la expresión del mutante daDREAM sobre el sistema opioide en la médula y en el ganglio de la raíz dorsal (GRD). La bajada del tono opioide en estas dos áreas podría deberse a una regulación directa de DREAM sobre los genes que codifican los precursores polipeptídicos y de los receptores opioides o a un efecto indirecto. En este ultimo caso la represión por parte de DREAM de algunos de los promotores de estos genes provocaría una caída generalizada de todo el sistema opioide.

Además, los ratones de la línea 1 presentan una alteración en la expresión de las subunidades del canal de potasio dependiente de voltaje Kv4. Sin embargo, el estudio electrofisiológico no mostró cambios en las corrientes de potasio tipo A mediadas por dichos canales por lo que descartamos que el fenotipo hiperalgésico de los ratones transgénicos pueda atribuirse a una disfunción de los Kv4.

El papel de DREAM es también fundamental en la regulación de los fenómenos de plasticidad sináptica que controlan la respuesta a dolor crónico, en particular a dolor inflamatorio. En este contexto, DREAM es importante porque controla de forma directa la trascripción del gen de BDNF. A su vez, DREAM puede regular de forma indirecta, a través del control sobre el tono GABAérgico de las neuronas del asta dorsal de la medula espinal, el nivel de fosforilación basal de la quinasa ERK.

DREAM participa en la regulación de la percepción dolorosa a nivel del ganglio trigémino. En un estudio transcriptómico hemos podido caracterizar los efectos globales de la sobrexpresión del mutante dominante activo en este área. Analizando en detalle el listado de los genes cuya expresión se ve alterada en los ratones transgénicos hemos podido aislar un grupo de nuevos posibles genes diana de DREAM que pueden estar relacionados con el control de los estímulos nociceptivos.

El análisis de la respuesta molecular a dolor inflamatorio ha evidenciado diferencias en la función que la prodinorfina y BDNF desempeñan en el ganglio trigémino respecto a su papel en la medula o en el DRG

INTRODUCTION

INTRODUCTION

Sensation usually refers to the immediate, relatively unprocessed, result of sensory reception in the eyes, ears, nose, tongue and skin. Perception on the other hand better describes one's ultimate experience of the world and typically involves further processing of the sensory input. In practice, sensation and perception are virtually impossible to separate because they are steps of a continuous process. Thus perception describes the process whereby sensory stimulation is translated into organized experience.

We have a clear example if we analyze a fundamental evolutionary skill such as the experience of pain. The perception of pain warns us of a possible danger but our nervous system is also able to modulate our response to a constant painful sensation to better react to an ongoing threat to our organism. This plasticity is reflected at the molecular level by the possibility of modifying cell responses both transcriptionally and post-translationally.

1. Neuro-anatomy of pain

Pain sensation is generated by the stimulation of specific receptors, the nociceptors (Sherrington, 1906). They are slow adaptation fibers with a high threshold that selectively respond to noxious stimuli and to chemicals released from neighboring traumatized tissues.

Three classes of nociceptors can be distinguished on the basis of the type of stimulus to which they respond (Basbaum, 2000):

Thermal nociceptors: are composed of Aδ and C fibers and are excited by temperature extremes. They can be sub-divided in two groups, those that respond to high temperatures (above 45ºC) and those that respond to noxious cold (below 5ºC)

Mechanical nociceptors: are composed exclusively of Aβ fibers. They are the fastest-conducting nociceptive fibers that respond to painful tactile stimuli, mediating the sensation of sharp and prickling pain.

Polymodal nociceptors: are formed by C fibers only. They respond to a variety of destructive mechanical, thermal or chemical stimuli. Stimulation of these receptors leads to a sensation of persistent burning pain.

Afferent nerves conduct sensory information to the central nervous system (CNS); there are three different kinds of fibers that convey the primary sensory input:

C fibers: are thin unmyelinated fibers (0,2-1,5 μm of diameter), with the slowest conduction velocity of no more the 2 m/s. They account for the perception of persistent burning pain.

Aδ fibers: are thin myelinated fibers (1-5 μm of diameter) with a moderate conduction velocity (1-5 m/s), they are associated with acute pain perception.

Aβ fibers: are myelinated fibers with a diameter that ranges from 6 to 12 μm, they have the highest conductance velocity (from 35 to 75 m/s). These fibers only transmit proprioceptive stimuli.

1.1. Afferent nerves

Afferent nerves can be categorized in two groups, based on where they connect to the central nervous system (CNS); the spinal nerves and the cranial nerves.

Spinal nerves: are mixed nerves formed by sensory and motor neurons. Afferent fibers are connected to the spinal cord through the dorsal root, they are composed of pseudo-unipolar neurons whose soma resides in the dorsal root ganglion (DRG). Shortly after the DRG the afferent fibers fuse with efferent ones that emerge from the spinal cord through the ventral root (Fig. 1 A).

The grey matter of spinal cord is structurally and functionally divided in a system of ten different laminae, the Rexed laminae (Rexed, 1952) (Fig. 1 B); nociceptors are principally in direct contact with laminae I, II, III and V. Pain sensation is mainly projected to the thalamus via three different ascending pathways;

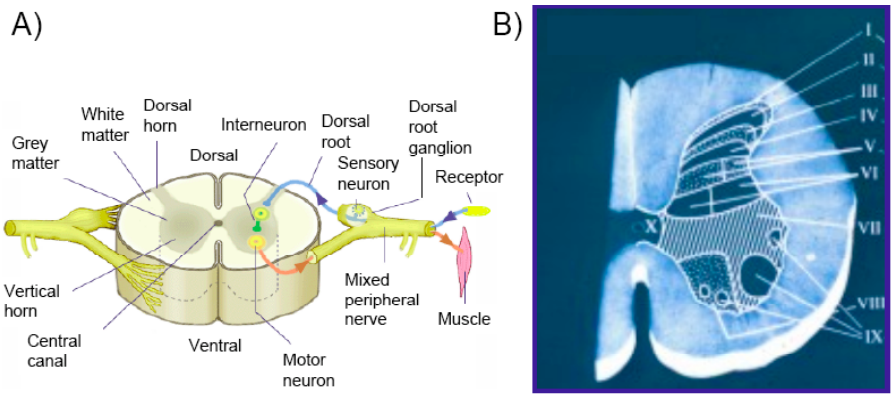

Figure 1. Spinal nerve. A) Schematic representation of a spinal nerve at its insertion site in the spinal cord (Adapted from Mandl et al. 2005). B) The ten Rexed laminae in the grey matter of the lumbar spinal cord (Adapted from Samojen et al. 2001).

Spinothalamic tract; is the most prominent ascending nociceptive pathway in the spinal cord. Neurons in laminae I, V, VI, VII project to the contralateral side of the spinal cord and ascend trough the anterolateral white matter terminating directly in the thalamus.

Spinoreticular tract; axons of neurons in laminae V, VI and VII ascend in the anterolateral quadrant of the spinal cord and terminate in both the thalamus and the reticular formation in the brainstem.

Corticothalamic tract; neurons in this pathway connect to specific nuclei in the thalamus and in the medulla.

Apart from these, there are two pathways that can convey pain stimuli to other brain areas:

Spinomesencephalic tract; projects to the mesencephalic reticular formation, the periaqueductal gray matter and the parabrachial nuclei. This last one in turn, project to the amygdala. This tract is thought to contribute to the affective component of pain.

Spinohypothalamic tract; comprises the axons of neurons in laminae I, V and VIII. It projects directly to supraspinal autonomic control centers and it is thought to activate complex neuroendocrine and cardiovascular responses.

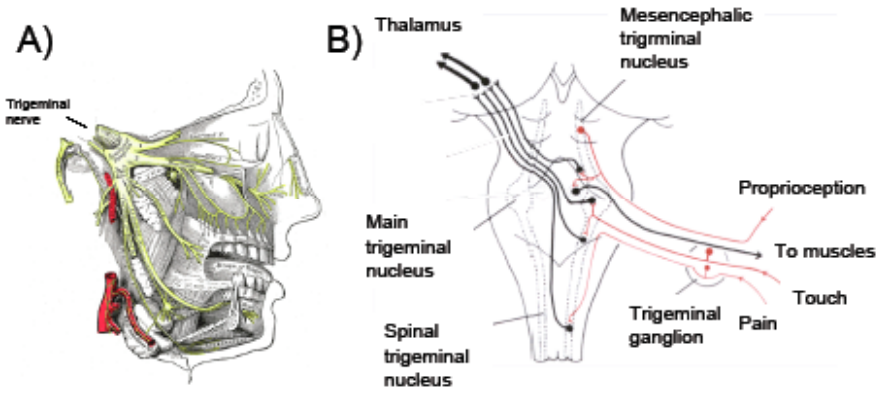

Figure 2. Trigeminal nerve. A) Schematic representation of the trigeminal nerve and of its three major branches. B) Schematic representation of the trigeminal nucleus in the brainstem (Adapted from Gray et al., 1918)

Cranial nerves; this class of nerves is connected to the CNS directly trough the brainstem. There are twelve pairs of cranial nerves, but for the interest of this study we will focus our attention specifically on the fifth member of the family, the trigeminal nerve.

The trigeminal nerve is the largest member of the family, it primarily carries sensory information from the face but it has also certain motor functions. It has three major

branches (the ophthalmic branch, the maxillary branch and the mandibular branch) that converge on the trigeminal ganglia (TG) (Fig. 2 A). This ganglion, analogous to the DRG, is located in the Meckel's cave and contains the somas of the sensory neurons. From the TG a single root enters in the brainstem at the level of the pons, where all the afferent fibers terminate in the trigeminal nucleus. This structure extends throughout the entire brainstem, from the midbrain to the medulla. It is divided in three parts that receive different types of information: the spinal trigeminal nucleus, the main trigeminal nucleus and the mesencephalic trigeminal nucleus (Fig. 2 B). Nociceptors from the trigeminal nerve are grouped together and sent to the spinal trigeminal nucleus, they are connected to the secondary fibers that ascend to the thalamus via the trigemino-thalamic pathway.

1.2. Pain information in the thalamus

The thalamus is a complex structure composed by many different nuclei that connect incoming inputs to different parts of the cortex. Pain information from the spinal cord is mainly directed to the ventral posterolateral nucleus (VPL), while the one from the trigeminal nerve is mainly directed to the ventral posteromedial nucleus (VPM). From the VPL/VPM the nociceptive stimuli are projected to the primary sensory cortex where they are organized somatotopically.

Differently from the information concerning touch and position, pain inputs are also sent to other thalamic nuclei; the medium dorsal thalamic nucleus (that project to the cingulated cortex), the ventromedial nucleus (that is connected to the insular cortex) and the intralaminar nuclei (that project diffusely to all part of the cerebral cortex).

These multiple connections allow our brain to fully represent our perception of pain in the context of other simultaneous perceptions, of our memories and of our present emotional state.

2. Molecular biology of pain

To understand the nature and the molecular mechanisms regulating pain sensation we first have to distinguish among acute, inflammatory and neuropathic pain. In the first case, pain is a signal to warn the organism against a possible tissue injury. It originates in response to a noxious stimulus (mechanical, thermal or chemical) and lasts only while the noxious stimulus is present. Inflammatory pain on the other hand, represents a hypersensitive state due to peripheral tissue inflammation. It is a central response from the CNS and involves a maintained change in responsiveness to noxious stimulation. This

process represents a mechanism to protect and to aid healing of an injured area. Finally, neuropathic pain, that neither support nor protect healing. It represents a hypersensitive state in the absence of noxious stimulation and involves aberrant plastic changes of the somatosensory system caused by a nerve lesion or disease.

2.1. Acute pain

The mechanisms that underlie acute pain are specific for the stimulus that elicits the sensation. There are different peripheral receptors for thermal, mechanical and chemical painful stimulation (Fig. 3).

Heat stimulation: Several lines of evidence support the idea that the receptor for noxious heat stimulation is a member of the transient receptor potential (TRP) channel family, namely the TRPV1. This channel is specifically activated by capsaicin and by temperatures above 43ºC. TRPV1 knockout mice show a slight impairment in their ability to detect and respond to noxious heat (Caterina et al., 2000), suggesting that other members of the family, e.g. TRPV2, 3 and 4, are also involved in the heat response.

Cold stimulation: TRPM8 is sensitive to cold and menthol. Currents through this channel match the electrophysiological characteristics of cold-evoked responses in nerve fibers. TRPM8 knockout mice show a substantial loss of menthol and cold sensitivity. Additional molecules including voltage gated sodium channels (Nav) and potassium channel (Kv4.1 and KCNK2 and 4) cooperate with TRPM8 to fine tune cold threshold or to propagate cold evoked action potentials (Viana et al., 2002; Zimmermann et al., 2007; Noel et al., 2009).

Interestingly TRPV1 and TRPM8 are expressed in non-overlapping nerve fibers. Therefore cold and heat detection is functionally and anatomically organized in two different neuronal populations.

Mechanical stimulation: The molecular basis of the nociceptive response to mechanical stimulation is far from being clarified. It is generally accepted, however, that a core mechanism for such receptor should involve a mechano-sensitive cation channel that is operated by noxious pressure.

Studies in this direction are focused on a possible role for acid sensing ion channels (ASIC) 1, -2 and –3. However, knockout mice for each of these genes did not display any clear impairment in mechano-sensitivity (Price et al., 2000; Price et al., 2001; Page et al., 2004; Roza et al., 2004). Other studies pointed out that TRPA1 could be important in modulating the response to mechanical stimulation (Kwan et al., 2009). Finally, it has been proposed that the KCNK18 potassium channel could be a critical modulator of the

excitability of neurons involved in innocuous and noxious touch sensation (Bautista et al., 2008).

Chemical stimulation: The TRP channels play a prominent role as receptors for noxious chemicals (see the above mentioned TRPV1 and TRPM8 that respond to capsaicin and menthol). Moreover, TRPA1 has emerged as a particularly interesting chemoreceptor. This channel in fact responds to structurally diverse compounds that are able to form covalent adducts with thiol groups (Hinman et al., 2006; Macpherson et al., 2007).

It is important to stress that chemical irritants are also produced endogenously in response to tissue damage with the effect of sensitizing nociceptors to thermal and mechanical stimulation. Thus, chemo-nociception represents an important interface between acute and persistent pain, especially in the context of peripheral tissue injury and inflammation.

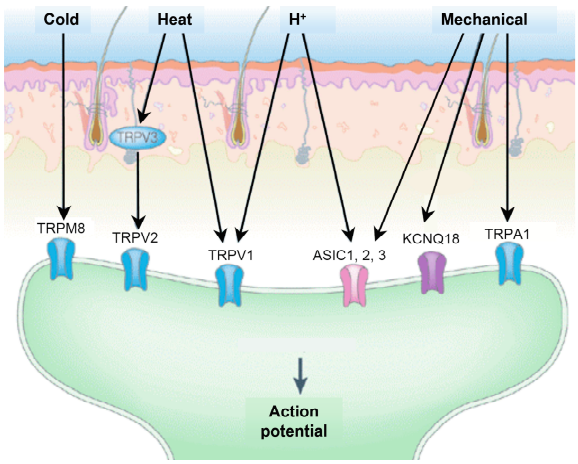

Figure 3. Acute pain. Representation of the molecular mechanisms that underlie the response to thermal, mechanical and chemical pain (Adapted from Marchand et al., 2005)

2.2. Inflammatory pain

Inflammatory associated changes in the chemical environment of the nerve fiber result in the sensitization of the peripheral nerve, i.e. the threshold for activation is reduced and membrane excitability is increased.

Tissue damage is accompanied by the accumulation of endogenous factors that are released from nociceptors or non-neuronal cells such as immune cells, platelets, mast cells, endothelial cells, fibroblasts and keratinocytes. These factors, collectively known as "inflammatory soup", represent a wide array of signaling molecules, such as peptides, neurotransmitters, lipids, neurotrophins, cytokines, extracellular proteases and protons.

Some components of the inflammatory soup can alter neuronal excitability directly by interacting with ion channels, whereas others can bind to metabotropic receptors and mediate their effect through second messengers activated signaling cascades (Fig. 4).

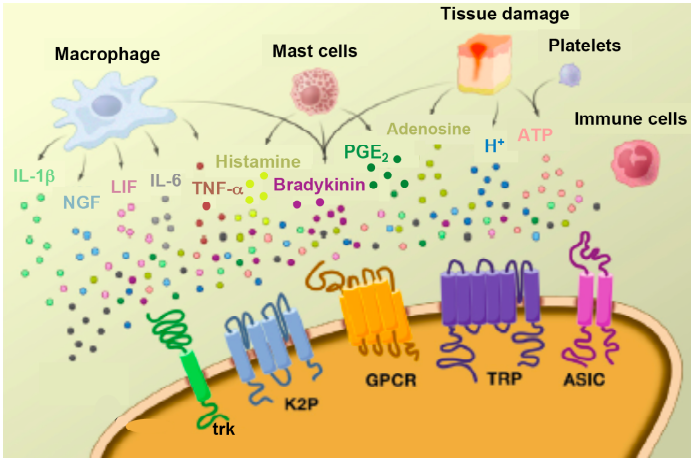

Figure 4. The inflammatory soup. Cartoon showing the different molecules and receptors which compose the inflammatory soup. These molecules alter neuronal excitability and induce hyperalgesia (Adapted from Basbaum et al., 2009)

The main compounds present in the inflammatory soup are:

Bradykinin; signals specifically through BK2 receptors, a GPCR whose activation provokes Ca^{2+} release from intracellular stores and activation of the protein kinase C (PKC) signaling cascade (Premkumar and Ahern, 2000). This results in an immediate depolarization of the neuronal membrane.

Neuronal growth factor (NGF); binds to its specific receptor tyrosine kinase A (TrkA) causing the downstream activation of mitogen activated protein (MAP) kinase and phospholipase C-γ (PLC-γ) (Ganju et al., 1998). The first signaling cascade induces changes in gene expression while the second is responsible for some of the short term posttranslational modifications that underlie thermal hyperalgesia. Moreover NGF can bind, with low affinity, to p75. Binding to this receptor can promote apoptosis through the activation of JNK ot NfkB.

Prostaglandin E2 (PGE2); is the responsible cyclooxygenase enzyme for the conversion of arachidonic acid into PGE2, the main lipid messenger in the inflammatory soup. When PGE2 binds to its specific receptor, belonging to the GPCR family, it induces a rise in cAMP. As a consequence, protein kinase A (PKA) is activated and phosphorylates the tetrodotoxin resistant channels Nav1.8 and Nav1.9 shifting the voltage dependent activation of these channels in the hyperpolarizing direction (Fitzgerald et al., 1999). This

reduces the extent of membrane depolarization needed to initiate an action potential and favors repetitive spiking.

Protons and tissue acidosis; is a hallmark of physiological response to tissue injury (Reeh and Steen, 1996). On one hand protons enhance the response of TRPV1 to both capsaicin and heat (Tominaga et al., 1998), on the other, they activate acid sensitive ASIC channels (Immke and McCleskey, 2001).

Cytokines; injury promotes the release of numerous cytokines, including interleukin 1β (IL-1β), interleukin 6 (IL-6) and tumor necrosis factor α (TNF-α) (Ritner, 2008). Their contribution to the inflammatory response results in increased pain hypersensitivity and production of proalgesic agents

2.3. Neuropathic pain

Neuropathic pain results from lesions in the nervous system caused by mechanical trauma, metabolic disease, neurotoxic chemicals, infection or tumor invasion. Once generated, the sensory hypersensitivity typically persists for a prolonged period, even though the original cause may have long since disappeared. Under these conditions neurons undergo a dramatic change in their activity that is based on a remarkable modification in their transcriptome, the expression of up to 2000 genes has been found altered in neuropathic pain conditions.

Spontaneous pain results from ectopic action potentials generated at multiple sites; the neuroma (the aberrant neuronal growth that takes place at the nerve injury site), the cell body of injured neurons or the neighboring intact fibers. There are different studies trying to depict the modifications that underlie these abnormal electrophysiological features of injured nerve fibers. Voltage gated sodium channels, for example are known to contribute to this ectopic activity (Sheets et al., 2008) even though it is not clear which of these channels is responsible for the abnormal generation of action potentials. Experiments using gene knockdown or selective blockers point to a possible role for Nav1.3 (Hains et al., 2003), Nav1.7 (Hoyt et al., 2007) or Nav1.8 (Roza et al., 2003; Dong et al., 2007). On the other hand single knockout mice for these channels do not show any modification in their neuropathic pain behavior (Nassar et al., 2004; Nassar et al., 2005) probably because of redundancy and gene compensation.

Other studies highlight a possible role for the hyperpolarization-activated cyclic nucleotide-modulated channel (HCN) (Luo et al., 2007), for the KNCQ voltage gated potassium channels (Roza and Lopez-Garcia, 2008) and for the voltage gated calcium channel Cav2.2 (McGivern, 2006).

Another important clue in the understanding of neuropathic pain is the interaction between neurons and the immune system. In the PNS, immune surveillance is performed by macrophages, which account for the initial reaction to nerve damage. Macrophage activation on one side is a central component of the Wallerian degeneration distal to axonal injury and also contributes to pain hypersensitivity with its action at the soma of nerve fibers (Scholz and Woolf, 2007).

In the CNS microglia is massively activated in the dorsal horn of the spinal cord and in the spinal trigeminal nucleus soon after peripheral nerve injury. These particular glial cells share a myeloid lineage and many functional features of macrophages and their activation is a typical hallmark of neuropathic pain (Hu et al., 2007). This process is evoked by a rise in extracellular ATP (Tsuda et al., 2003), which could be actively released from injured primary afferents or increased as these neurons degenerate. Activation of microglia is characterized by the phosphorylation of MAP kinase p38, ERK-1 and -2 and Src-family kinases. It peaks at one week after injury and lasts over several weeks (Jin et al., 2003; Zhuang et al., 2005; Katsura et al., 2006).

Activated microglia releases brain derived neurotrophic factor (BDNF), that provokes an alteration in the concentration of chloride ions, likely downregulating the expression of the potassium chloride co-transporter KCC2. Consequently anion reversal potential is shifted to more positive values than the resting potential. In this condition the effect of GABA receptor activation turns out to be a depolarization (Coull et al., 2005). Moreover microglia secretes IL-1b, IL-6 and TNF-α; a direct modulation of dorsal horn neuron activity by these cytokines may also be part of the development of neuropathic pain (Winkelstein et al., 2001) (Fig. 5).

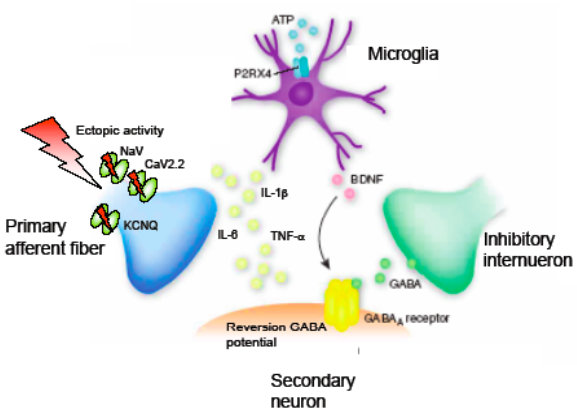

Figure 5. Neuropathic pain. Scheme of the principle mechanisms underlying neuropathic pain; ectopic activity of afferent fibers, microglia activation and reversion of GABA potential in second order neurons (Adapted from Scholz et al., 2008)

3. Pain and synaptic plasticity

Pain sensitivity can be modulated at a peripheral level, as described for inflammatory and neuropathic pain, and at a central level in response to an intense noxious stimulus (Woolf, 1983). The mechanism that underlies the central control of nociceptive transmission relies on synaptic plasticity, a neuronal property that refers to the ability of a synapse to change its strength. In the case of nociception there is a use-dependent facilitation of synaptic transmission in response to strong peripheral stimulation. This phenomenon, known as central sensitization, has been largely characterized in the spinal cord but is also important in the trigeminal nucleus. It leads to a reduction in pain thresholds, amplification in pain responses and spread of pain sensitivity to non-injured areas.

In the spinal cord there are different types of transcription-independent synaptic plasticity that originate in response to different patterns of repetitive noxious stimuli and are generated through specific molecular mechanisms. This can be homosynaptic, which means that the same synapses are activated in the conditioning and in the test inputs, or heterosynaptic, that is the synapses activated by conditioning and test inputs are different.

3.1. Wind-up

Wind-up is a form of homosynaptic activity-dependent plasticity characterized by a progressive increase in action potential output from dorsal horn neurons during a train of repeated low-frequency C-fiber stimuli. Slow inputs (<5 Hz) summation induces a cumulative depolarization. This leads to removal of the voltage dependent Mg^{2+} blockade of the NMDA receptors increasing their sensitivity to glutamate (Thompson et al., 1990). In addition, L-type Ca^{2+} channel current can be recruited, contributing to the establishment of a sustained and progressive depolarization over the course of the stimulation (Morisset and Nagy, 2000). This phenomenon vanishes when the train of stimuli that elicit it is finished.

3.2. Classical central sensitization

Classical central sensitization is a period of facilitated transmission that outlasts the initiating stimulus which is caused by an increased response of the conditioning nociceptors pathway (homosynaptic potentiation) and a recruitment of novel inputs in non-stimulated pathways (heterosynaptic potentiation). In this condition, low threshold

Aβ fibers, which normally signal innocuous sensations, also begin to transmit nociceptive stimuli. Classical central sensitization is evoked by either a synchronized train of repeated inputs, or by asynchronous activation of peripheral terminals of nociceptors (i.e. frank tissue damage).

At the molecular level this increased synaptic strength is evoked after the secretion from the pre-synaptic terminal of BDNF, substance P and glutamate (acting on both ionotropic and metabotropic receptors). This produces an increase in internal Ca^{2+} concentration at the post-synaptic level, which triggers the activation of PKA, PKC and CaMKII. Moreover BDNF induces the phosphorylation of ERK and Src kinases (Yu and Chuang, 1997; Ji et al., 1999). The combined activation of these molecular pathways enhances synaptic strength modulating ion channel and/or receptor activity by a post-translational processing that favors receptor trafficking to the membrane. On one hand, the AMPA receptor is phosphorylated facilitating its membrane expression (Soderling and Derkach, 2000). On the other hand, there is a phosphorylation and a removal of the Mg^{2+} blockade from the NMDA receptor (Guo et al., 2002). In addition, neuronal excitability can also be controlled directly by ERK-dependent phosphorylation of Kv4.2 channels that are the major contributors of A-type K^+ current (Hu and Gereau, 2003). Phosphorylation of these channels reduces de K^+ outward flux and decreases hyperpolarizing current resulting in enhanced neuronal excitability.

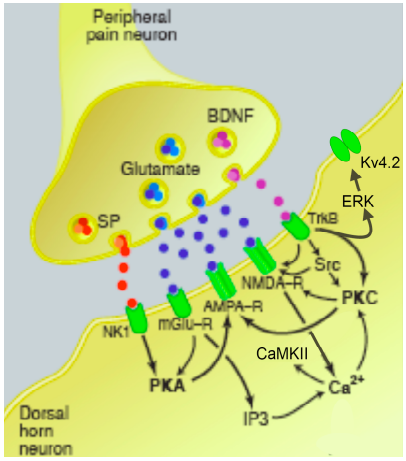

Figure 6. Central sensitization. Schematic representation of the molecular mechanisms which underlie central sensitization. Primary afferent fibers release BDNF, substance P and glutamate that activate specific signaling cascades in dorsal horn neurons. (Adapted from Marx et al., 2004)

3.3. Dorsal horn long term potentiation (LTP)

Although LTP has been most studied in the hippocampus and the cortex, a similar phenomenon can be elicited in the spinal cord, comprising an activity-dependent, long-lasting homosynaptic facilitation. This is known to occur in response to a brief high frequency repetition of trains of stimulation from the nociceptors. This potentiation may last for tens of minutes but varies. It requires an interaction between NMDA receptor and NK1 activation, as well as activation of low threshold T-type Ca^{2+} currents.

3.4. Transcription-dependent central sensitization

Nociceptor activity can produce long-term changes in synaptic activity trough specific changes in gene expression. This is known as late-phase LTP and differently from the above-mentioned forms of synaptic plasticity it is transcription dependent. This phenomenon takes several hours to activate and lasts for prolonged periods.

As said before, intense nociceptor stimulation results in ERK activation. This kinase can enter the nucleus and phosphorylates CREB, stimulating CRE-dependent transcription (Ji et al., 2002). In this way, noxious stimulation increases the expression of the immediate early genes c-fos and COX-2 (Hunt et al., 1987; Samad et al., 2001) as well as late response genes encoding for prodynorphin, NK1 and trkB (Naranjo et al., 1991; Dubner and Ruda, 1992; McCarson and Krause, 1994).

Activity dependent changes in the spinal cord are paralleled by transcriptional changes in primary sensory neurons. Following peripheral inflammation, there is an elevation in the levels of BDNF and substance P, and after peripheral nerve injury there are changes in hundreds of genes that alter primary afferent excitability and synaptic transmission properties. Finally, following both peripheral inflammation and nerve injury, there is a phenotypic switch in some dorsal root ganglion neurons. Large DRG neurons begin to express substance P and BDNF and as a consequence these non-nociceptive afferents gain the capacity to induce central sensitization.

4. BDNF and nociception

Neurotrophins are a family of related proteins including neuronal growth factor (NGF), brain derived neurotrophic factor (BDNF), NT-3 and NT-4/5. All neurotrophins are synthesized as precursor proteins of approximately 30 kDa and are cleaved to a mature form of approximately 13 kDa. All neurotrophins bind with low affinity to the transmembrane receptor p75 and each neurotrophin binds with high affinity to tyrosine

receptor kinase trk family of transmembrane receptors. NGF binds to trkA, BDNF and NT-4/5 to trkB and NT-3 to trkC. Activation of trk receptors leads to dimerization and auto-phosphorylation of different residues that in turn promotes the activation of different signaling pathways, notably the MAPK, PI3K, PLC-γ and PKC cascades. On the other hand, if the p75 receptor is expressed in the absence of trk or if the ratio of p75/trk is high, neurotrophins can activate pathways downstream to this receptor like the JNK or the NF-kB signaling cascades.

During development, neurotrophins support the survival of neuronal subpopulations that express appropriate trk receptors, nonetheless they are also important in adulthood because of their action as modulators of synapic activity. Specifically BDNF promotes the survival of some primary sensory neurons, in particular the mechanoreceptors innervating the Meissner and Pacinian corpuscle (Sedy et al., 2004; Gonzalez-Martinez et al., 2005) and the chemoreceptor innervating the circuvallate papillae (Uchida et al., 2003). In adulthood, BDNF appears to be a central modulator of pain processing both at spinal and supraspinal levels, with a particularly remarkable role in the central sensitization processes that underlie many forms of hyperalgesia.

4.1. BDNF in the nociceptive pathways

Neurotrophic factors can be locally synthesized by neurons and/or endocytosed at somatodendritic domains to be eventually targeted to terminals by anterograde axonal transport (transcytosis) (von Bartheld et al., 2001; von Bartheld, 2004). In the case of BDNF, synthesis and subsequent anterograde transport have been widely documented in neurons as well as in microglia (Coull et al., 2005). Once synthesized, BDNF is stored in dense core vesicles in both central and peripheral neurons (Salio et al., 2007). On the other hand transcytosis of BDNF does not seems to be relevant in vivo.

Sensory ganglia and spinal cord: BDNF is highly expressed in sensory neurons of the DRG and of the trigeminal ganglion (Kashiba et al., 2003; Ichikawa et al., 2006), although it has also been detected in the nodose, petrosal, jugular (Ichikawa et al., 2007) and geniculate ganglia (Farbman et al., 2004). The concentration of this neurotrophin varies in chronic pain condition. Following peripheral inflammation BDNF is increased, while in models of neuropathic pain it is deregulated in different, lesion-specific, ways.

BDNF localization in the spinal dorsal horn is prominent in lamina II, in the terminal of primary afferent fibers, where it is stored together with the sensory neuropeptides substance P and CGRP. There are no second order neurons expressing this neurotrophin in this location.

Supraspinal centers: Among integrative centers, BDNF-expressing neurons are particularly abundant in several layers of the somatosensory cortex as well as in neurons related to the descending pathways that control the supraspinal modulation of pain neurotransmission. It has been suggested that BDNF levels are modulated at supraspinal level in some persistent pain states.

Glial cells: Another important source of BDNF are glial cells, in particular microglia that, once activated, in neuropathic pain condition, can synthesize and secrete this neurotrophin directly into the inner layers of the spinal cord.

4.2. trkB in nociceptive pathways

In the developing and adult CNS alternative splicing generates three different trkB isoforms; the full-length trkB receptor (fl-trkB) and two truncated receptor forms (tr-trkB) (Klein et al., 1990; Middlemas et al., 1991; Barbacid, 1994). All these isoforms share a common extracellular domain, while the truncated ones lack the signal transducing intracellular tyrosine kinase domain. tr-trkB is prevalently expressed in choroids plexus, ependymal cells and astrocytes whereas both fl-trkB and tr-trkB are expressed in neurons. Most sensory ganglia that express BDNF also express trkB, including the DRG, the trigeminal, petrosal and geniculate ganglia. The receptor is also expressed in the second order lamina II neurons of the spinal cord, in the somato-dendritic membranes and in the axon terminals. At the supraspinal level trkB receptor is expressed in virtually all areas related to nociception. This includes the main relay centers, which are the sites of third order neurons (thalamus, reticular formation, hypothalamus), the integrative centers (cortex and amygdala), and neurons in the most important nuclei originating descending pathways.

4.3. The control of BDNF expression

In order to better understand the specific function of BDNF in the context of nociception it is necessary to highlight the molecular mechanisms that finely control the activity-dependent expression of this neurotrophin. The mouse BDNF gene consists of eight 5′ non-coding exons and one 3′ exon that includes the entire open reading frame of the functional protein. Each of the first eight exons has a 5′ promoter region and a splice donor site at the 3′ end. Exon IX contains the only splice acceptor site and two polyadenylation signals. Transcription of the gene results in BDNF transcripts containing one of the eight 5′ exons spliced to the protein coding exon (Aid et al., 2007).

The transcriptional regulation of BDNF is dependent on neuronal activity and relies on the combined action of different factors. The gene is upregulated in response to intracellular rise both in cAMP and in Ca^{2+}. The promoters for BDNF contains within their sequence a CRE element that, binding to CREB, confers the cAMP sensitivity to this gene. Moreover there are several Ca^{2+} responsive regulatory sites that allow the binding to the DNA of transcription factor like DREAM (Mellstrom et al., 2004) or the calcium responsive factor (CaRF) (Tao et al., 2002).

Finally there are growing evidences suggesting that DNA methylation and possibly chromatin remodeling could take part in the activity dependent control of BDNF expression. Methylation of several CpG island in the promoter of BDNF exon IV is activity dependent reduced (Martinowich et al., 2003). The mechanism beneath this phenomenon could be the Ca^{2+} dependent unbinding of the methyl-CpG binding protein 2 from the DNA (Chen et al., 2003).

4.4. Behavioral data suggesting BDNF is a pain modulator

The functional consequences of BDNF-induced plasticity depend on the type of cells affected, their distribution, and the timing of events. In fact, there are evidences that point out that BDNF may serve both pro- and anti-nociceptive roles in different contexts.

BDNF is known to be upregulated in conditions of peripheral inflammation. Sequestering endogenous BDNF reduced pain related behaviors in models of inflammatory pain (Kerr et al., 1999; Thompson et al., 1999). In addition, behavioral studies in neuropathic models report that delivery of antibodies against BDNF at the level of nerve injury reduced pain related behavior in rat (Zhou et al., 2000) and in mouse (Yajima et al., 2005).

Despite these pronociceptive roles, BDNF exhibits antinociceptive properties when delivered pharmacologically in larger amounts in much wider areas of the CNS (i.e. the spinal cord or the midbrain). BDNF intracerebroventricular injection (Cirulli et al., 2000), or grafts of BDNF expressing cells to the spinal cord (Eaton et al., 2002) reduced pain related behavior in neuropathic mice.

5. Downstream Regulatory Element Antagonist Modulator

The downstream regulatory element antagonist modulator (DREAM) belongs to the Neuronal Calcium Sensor (NCS) protein family. DREAM was discovered as the factor in trans able to bind and regulate the promoter region of the prodynorphin gene (Carrion et al., 1999). It is also known as Calsenilin or KChIP3, one of the four members of the

voltage gated Potassium Channel Interacting Protein family. DREAM is expressed throughout the central and peripheral nervous system and in other tissues such as heart, gonads, thyroid and thymus.

The full length DREAM protein consists of 256 amino acids with a predicted molecular mass of around 29 kDa. The DREAM sequence has four EF-hands of which three bind Ca^{2+}, the first one is a non-canonical EF-hand and is not functional. There are also two Leucines, Charged residue-rich Domain (LCD) motifs that permit the establishment of interactions with other proteins.

DREAM is a multifunctional protein that exerts different roles depending on its subcellular localization. In the nucleus it acts as a transcriptional repressor binding to the promoter region of target genes (Carrion et al., 1999). In the cytosol it interacts with different proteins modulating a variety of cellular function.

Recent investigations using mice models for the study of pain processing described the importance of DREAM in regulating nociceptive perception.

5.1. DREAM (calsenilin) and presenilin

Presenilin is a key component of the multi-subunit gamma-secretase complex that account for the proteolytic cleavage of the amyloid precursor protein. Vertebrates have two presenilin genes that encode for presenilin-1 (PS1) and presenilin-2 (PS2). Mutations in presenilin genes are highly associated with most early-onset familial Alzheimer disease cases. Calsenilin was isolated in a two-hybrid screen looking for proteins that could possibly interact with the two presenilins (Buxbaum et al., 1998). It was found that calsenilin binds to the C-terminal part of presenilins at the membrane of the endoplasmic reticulum (ER) and of the Golgi apparatus in a Ca^{2+}-independent way. Transient transfection of calsenilin together with PS1 or PS2 (Lilliehook et al., 2002) results in enhanced apoptosis in response to serum starvation with higher caspase and calpain activity. Moreover, the cotransfection of calsenilin with PS1, but not PS2, results in a reduction of the $[Ca^{2+}]$ in the ER probably due to an increased leakage of Ca^{2+} from the reticulum (Fedrizzi et al., 2008).

5.2. DREAM (KChIP3) and Kv4

In the brain, rapidly inactivating (A-type) voltage gated potassium currents operate at sub-threshold membrane potential to control the excitability of neurons. These currents consist in the outward flux of K^+ ions through a voltage sensitive channel formed by a tetramer of Kv4 pore forming α-subunits.

Electrophysiological studies in heterologous cells (An et al., 2000) demonstrated that the expression of the Kv4 alone is not sufficient to reconstitute the typical features of the A-type currents. In order to recover the characteristics of a native A-type current, cells has to be co-transfected with Kv4 and the Potassium Channel Interacting Protein (KChIP). There are four different genes that encode for KChIP1, KChIP2, KChIP3 (DREAM) and KChIP4, all of which are able to interact with the Kv4 tetramer. The proposed model (Wang, 2008) pictures that a single KChIP molecule binds as a monomer to the N-termini of two adjacent Kv4 fixing the structure of the pore.

The interaction with KChIP promotes Kv4 expression at the plasma membrane and influences the properties of the channel, so that the inactivation kinetic is slowed down and the rate of recovery from the inactive state is increased. The binding of KChIP to Kv4 is independent of Ca^{2+}, whereas the modulation of the A-type current is not. Ca^{2+}-insensitive mutants of KChIP are able to bind to the potassium channel but do not affect the flux through the pore.

5.3. Defining the DREAM interactome

Listing of the DREAM interactome was initiated by putting together results from yeast two-hybrid assays; presenilins and Kv4 channels mentioned above, together with data from the functional analysis of DREAM. Three examples illustrate this second source of information. The first was the interaction with CREM, discovered while trying to understand the regulation by cAMP of the binding of DREAM to DNA (Ledo et al., 2000a). In this study was also described the existence of Leucine, Charged residue-rich domains (LCDs) in DREAM and CREM, which are domains important for the interaction between hormone nuclear receptors and the transcriptional machinery (Le Douarin et al., 1996). Given the high homology between CREM and CREB a similar domain was searched for in the CREB sequence, and an LCD motif was found in the KID domain of CREB that mediates an interaction with DREAM (Ledo et al., 2002). The second example came with the studies trying to understand the function of DREAM in the thyroid gland that could explain its high expression level. It was discovered that DREAM interacts with TTF-1 and Pax-8 regulating the expression of thyroglobulin (Rivas et al., 2004), and with the TSH receptor in folicular thyroid cells (Rivas et al., 2009). Third, while studying the reduction of NMDA-mediated currents in transgenic neurons expressing a Ca^{2+}-insensitive DREAM mutant, the calcium-dependent interaction with PSD-95 was identified and it was shown that this interaction retains PSD-95 from its interaction with src precluding NR2B phosphorylation and NMDA receptor full activity (Wu et al., 2010).

Interestingly, these interactions identified through functional studies turned out to be calcium-dependent in most of the cases, while those discovered using the yeast two-hybrid assays where not sensitive to calcium. Since high calcium concentrations in the yeast cytosol could preclude the interactions sensitive to calcium, a yeast two-hybrid assay was designed, using a calcium-insensitive DREAM mutant with inactivation of each one of the three functional EF-hands. Yeast two-hybrid screening then permitted the identification of new interactions, in all cases independent of the presence of calcium. Three of these interactions have been characterized at the molecular and functional level

The interaction of DREAM with GRK6 or GRK2 kinases phosphorylates DREAM at serine 95. Mutant S95A-DREAM showed reduced capacity for intracellular trafficking from the endoplasmic reticulum to the membrane of different proteins (Ruiz-Gomez et al., 2007).

The interaction with the SUMO-conjugating enzyme Ubc9 led to the identification of two lysine residues where DREAM is sumoylated and that K to R mutants are not sumoylated and do not translocate to the nucleus and lose their repressor properties (Palzcewska et al., submitted).

The interaction with peroxyredoxin-3 (Prx3), an antioxidant enzyme that uses the thioredoxine system as electron donor and protects neurons from oxidative damage. The interaction with Prx3 is functional and showed that DREAM binding to DNA is also regulated by redox signaling. A cysteine to serine mutant acts as a permanently reduced forms and shows greater dimer formation capacity and stronger repressor effect on DRE-dependent transcription (Rivas et al., 2010).

With the exception of one interacting clone that encodes a nucleoprotein, all the positive interactions in this yeast two-hybrid screening correspond to cytosolic and membrane proteins. This may be related to a low representation of nucleoprotein encoding clones or to the fact that these interactions are complex and they are not favored in the yeast environment.

5.4. DREAM as a transcription factor

When DREAM was first isolated (Carrion et al., 1999) it was described as the first known Ca^{2+}-binding protein to function as a DNA-binding transcriptional regulator, and successive studies contributed to shed light on the mechanisms that underlie the activity of DREAM as a transcription factor.

In basal conditions DREAM binds as a tetramer to the Downstream Regulatory Element (DRE) in the promoter of target genes. The DRE site is usually located downstream of the TATA box and the consensus sequence is (Carrion et al., 1998):

5′-Pu N G T C A Pu Pu G-3′

The central core of the sequence is 5′-GTCA-3′, and mutations in any of these four nucleotides strongly affect the binding of DREAM to DNA. Interestingly, the central core sequence functions also in the inverted arrangement.

DREAM binding to the DNA blocks transcription, and upon cellular stimulation the tetramer is released from the DNA so that the target genes can be transcribed. There are two different stimulations able to induce DREAM detachment from the DRE site; the rise in nuclear Ca^{2+} or the interaction with the nucleoproteins α or ε CREM (Ledo et al., 2000b). On one hand, the DREAM tetramer can sense an increase in nuclear Ca^{2+} thanks to the three functional EF-hands present in every single monomer. When all of these EF-hands are bound to Ca^{2+}, the tetramer undergoes a conformational change that strongly decreases its affinity for the DNA. On the other hand, DREAM can interact with α or ε CREM trough the two LCDs that are present in its sequence, as a result of these interactions, DREAM is removed from the DRE site, allowing the transcription of target genes. The phosphorylation of α or ε CREM by PKA can facilitate the interaction between both proteins but is not necessary for CREM mediated derepression at the DRE sites.

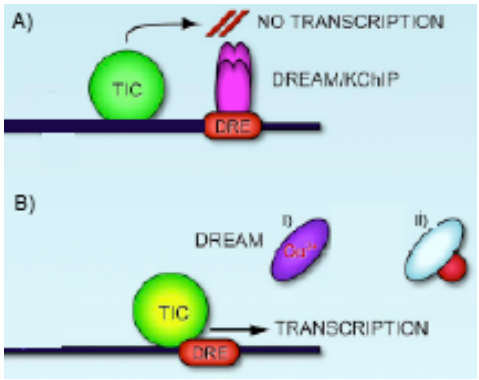

Figure 7. The transcriptional factor DREAM. In basal condition (A) DREAM is bound to the DNA blocking transcription. Upon stimulation (B) trough an increase in nuclear Ca^{2+} (i), or interaction with other nucleoproteins (ii) DREAM is detached from the DNA allowing transcription of target genes. (Adapted from Mellström et al., 2008)

Moreover DREAM represents a point of crosstalk between cAMP and Ca^{2+} signaling pathways in the nucleus, influencing in a Ca^{2+} dependent way the activity of the transcription factor CREB (Ledo et al., 2002). To activate CRE-mediated transcription CREB needs first to be phosphorylated and then to recruit the coactivator CBP. In the absence of Ca^{2+}, DREAM binds to a LCD in CREB located in a region critical for the interaction with CBP, preventing the interaction between these two proteins. Upon calcium stimulation DREAM is detached from CREB allowing transcription.

5.5. Prodynorphin and the endogenous opioid system

The activity of DREAM as a transcription repressor has been demonstrated in vivo for different genes; prodynorphin, fra-2, ICER, AA-NAT, IL-2, IL-4 and NCX3 (Carrion et al., 1999; Link et al., 2004; Gomez-Villafuertes et al., 2005; Savignac et al., 2005). Among these genes, prodynorphin is of particular interest in this study because of its involvement in the control of pain perception. It encodes one of the opioid polypeptides that, together with their receptors, forms part of a crucial system involved in pain modulation, the endogenous opioids.

The group of the opioid receptors is composed of the mu, delta, kappa and nociceptin receptors. They are seven transmembrane domains receptors belonging to the superfamily of G-protein coupled receptors (GPCRs), and they share a 60% homology among them. Their endogenous agonists are the opioid peptides, which originate from the proteolytic processing of four polypeptidic precursors:

Proopiomelanocortin; produces the opioid peptides β-endorphin-1 and –2 and endomorphin-1 and –2. These molecules are selective agonists for the μ opioid receptor and induce a strong analgesic effect (Zadina et al., 1997). β-endorphins are expressed in the hypophysis and in neurons of the arcuate nucleus of the hypothalamus (Bugnon et al., 1979; Sofroniew, 1979). Endomorphins are expressed in the spinal cord and in the thalamus, in nuclei that are related to pain perception.

Proenkephalin; is the precursor of met-enkephalin, leu-enkephalin and the peptides E, F and B, which are agonists for the μ and δ opioide receptors. It is expressed in the limbic system, in the nucleus raphe magnus (RVM), in the periaqueductal gray and in the dorsal horn neurons in the spinal cord. The activity of these peptides induces short-term analgesia.

Pronociceptin; gives rise to nociceptin, which is the agonist of the nociceptin opioid receptor (ORL-1) (Meunier et al., 1995; Reinscheid et al., 1995). The gene is widely expressed throughout the nervous system, its role in pain regulation is still elusive and may differ when acting spinally or supraspinally (Mogil and Pasternak, 2001; Heinricher, 2003).

Prodynorphin; is the precursor, through proteolytic processing, of dynorphin-A and dynorphin-B, two relatively selective agonists for the κ-opioid receptor. This gene is expressed at spinal and supra-spinal levels (Lima et al., 1993) and in sensory nerves. The expression of prodynorphin is upregulated in the spinal cord in cases of chronic pain. The signaling of dynorphins trough the κ-opioid receptor induces a mild analgesia, while on

the other hand the interaction of dynorphin A with bradykinin receptor is fundamental to maintain neuropathic pain states (Lai et al., 2006).

In the promoter region for prodynorphin, apart from DRE, there are five more major regulatory regions; three cAMP responding elements (DynCre-1, -2 and -3) (McMurray et al., 1989), a non-canonical AP-1site (Naranjo et al., 1991) and a fourth CRE site (DynCre-4) located after the transcription start. The concomitant action of these elements results in a tissue specific regulation able to respond to different physiological stimuli.

5.6. DREAM and pain

The evidence that DREAM regulates dynorphin level in the spinal cord suggests that it could regulate pain transmission by controlling the level of κ-receptor activation. To test this hypothesis a knockout mouse for DREAM was generated (Cheng et al., 2002). These mice show a markedly increased basal prodynorphin expression throughout the lumbar spinal cord without presenting any sign of κ-receptor desensitization.

DREAM$^{-/-}$ mice were characterized in a series of behavioral experiment. These mutant mice had essentially normal motor control, spatial learning and anxiety in the open field test. On the other hand, lack of DREAM results in attenuation of pain behavior regardless of the modality of the noxious stimuli (thermal, mechanical or chemical) or the tissue type affected (cutaneous or visceral). In addition, loss of DREAM similarly results in attenuation of both inflammatory and neuropathic pain.

Moreover, a persistent up-regulation of DREAM in the membrane fraction of the dorsal horn of the spinal cord in an inflammatory pain model (Zhang et al., 2007) has been described. These data suggest that DREAM could have other roles in pain modulation apart from its activity as a transcriptional repressor. At the plasma membrane DREAM interacts with the Kv4 channel modulating the A-type K^+ currents, one possible hypothesis is that DREAM is involved in inflammatory pain through its action on this channel. The regulation of A-type currents in the spinal cord plays a central role in the control of pain perception. It is known that knockout mice for the Kv4.2 channel present an impaired pain perception phenotype with enhanced sensibility to mechanical and thermal stimulation (Hu et al., 2006). Intriguingly, these mutated mice show a basal downregulation of the levels of KChIP3 (Menegola and Trimmer, 2006), further high lightening the importance of the fine-tuning of the interaction between these proteins.

OBJECTIVES

OBJECTIVES

The main goal was to study the functional role of DREAM in the control of nociception at the spinal cord/DRG level and at the trigeminal ganglia. In particular we aimed to characterize:

1. The basal response to pain in the spinal cord and DRG in transgenic mice expressing a dominant active mutant of DREAM (daDREAM mice).

2. The response to chronic pain (inflammatory and neuropathic) in daDREAM mice.

3. The transcriptional changes imposed by daDREAM that influence basal nociception.

4. The role of DREAM in the molecular response to chronic inflammatory pain in the spinal cord and DRG.

5. The role of DREAM in the molecular response to trigeminal pain.

6. DREAM target genes that are involved in trigeminal pain perception.

MATERIALS AND METHODS

MATERIALS AND METHODS

1. Transgenic mice

Transgenic mice were previously generated in our laboratory (Savignac et al., 2005). Briefly, the cDNA encoding human DREAM with two amino acid substitutions at EF-hands 2, 3 and 4 and a double amino acid substitution at the N-terminal LCD (line 1) or in the two LCDs (line 16) was inserted downstream of the human CaMK-IIα promoter (Mayford et al., 1996) in a bicistronic expression vector containing an IRES and the LacZ reporter gene. The transgenesis cassette was microinjected into the pronuclei of one-cell embryos (C57BL/6 x CBA F1) using standard techniques. Transgenic progeny was identified by Southern blot and qualitative PCR of tail DNA using specific primers: forward 5′-TTGCAGTGCACGGCAGATACACTTGCTGA-3′ and reverse 5′-CCACTGGTGTGGG CCATAATTCAATTCGC-3′. An amplified fragment of 326 bp indicated the presence of the transgene.

BDNF$^{-/-}$ mice were kindly provided by Dr. J. Alberch (University of Barcelona)

DREAM$^{-/-}$ mice were kindly provided by Dr. M. Vallejo (IIB, CSIC, Madrid)

2. Behavioral experiments

Mice were housed five per cage in a temperature (21 ± 1ºC) and humidity (65 ± 10%) controlled room with a 12/12-light/dark cycle (light from 8 am to 8 pm) with food and water *ad libitum*.

Unless mentioned, adult (3 to 5 months) male mice were used in all experiments. To avoid bias, behavioral experiments were performed blind from 09.00 to 13.00.

2.1. Plantar test

Heat hyperalgesia was assessed using the plantar test (Hargreaves et al., 1988). Mice were habituated for 30 minutes in individual Plexiglas chambers placed on a glass floor. During this time, mice initially exhibited exploratory behavior but subsequently stopped exploring and stood quietly with occasional bouts of grooming. After habituation, a beam of radiant heat (50ºC) was focused to the plantar surface of the hindpaws and the

withdrawal response was measured with a plantar test apparatus (Ugo Basile, Comerio, Italy). The nocifensive withdrawal reflex interrupts the light reflected from the paw onto a photocell and automatically turns off the light and the timer. The latency of the withdrawal response (as an indirect measure of the heat-pain threshold) was thus recorded automatically.

2.2. Von Frey test

Mechanical sensitivity was assessed by von Frey filaments (Stoelting, Wood Dale, IL) in the hind-paw. Mice were placed into a transparent plastic dome with a metal-mesh floor allowing access to the plantar surface of the hindpaws. Mice were placed in the experimental cage for habituation 30 minutes before testing. The filament was pressed perpendicularly to the plantar surface of the hindpaw with sufficient force to cause a slight buckling. A positive response was noted when the hindpaw was sharply withdrawn. Flinching immediately after the removal of the filament was also considered as a positive response. The force (in grams) producing a 50% probability of withdrawal was determined by the "up-down" method (Dixon, 1980). Each trial was repeated twice at 2 minutes intervals, and the mean value represented the paw withdrawal threshold.

2.3. Hindpaw formalin test

Mice were placed in an experimental cage for habituation 30 minutes before testing. The formalin test was performed by injection of 10 μl of 8% formalin subcutaneously into the plantar surface of the right hindpaw. The total time spent in spontaneous nociceptive behavior (licking of the injected paw) was recorded in 5 minutes intervals for 1 hour as previously described (Karim et al., 2001).

2.4. Snoot formalin test

Mice were placed in an experimental cage for habituation 30 minutes before testing. The formalin test was performed by injection of 10 μl of 2% formalin (or 4,5% where indicated) subcutaneously into the vibrissa pad. The total time spent in spontaneous nociceptive behavior (rubbing the injected snoot) was recorded in 3 minutes intervals for 30 minutes as previously described (Clavelou et al., 1989).

3. Chronic pain models

3.1. Inflammatory pain

As inflammatory agent we used Complete Freund's adjuvant (CFA, Sigma-Aldrich, St. Louis, Missouri), a mineral oil suspension of heat inactivated *Mycobacterium tuberculosis* (Chillingworth and Donaldson, 2003).

For inflammation in the hind paws we injected 50 μl of CFA into the plantar surface close to the tibiotarsal joint. The injection was performed in the right paw for behavioral studies, and bilaterally for biochemical studies.

For inflammation in the snoot we injected 10 μl of CFA subcutaneously into the vibrissa pad (Morgan and Gebhart, 2008). The injection was done in the right snoot for behavioral studies, and bilaterally for biochemical studies.

3.2. Chronic constriction injury

Animals were anesthetized with isoflourane inhalation. The sciatic nerve was exposed at the level of the middle of the thigh by blunt dissection through biceps femurs. Proximal to the sciatic trifurcation, about 7 mm of nerve was freed of adhering tissue and 3 ligatures (5.0 chromic gut) were tied loosely around it with about 1 mm spacing. The length of nerve affected was about 3 to 4 mm. Great care was taken to tie the ligatures so that the diameter of the nerve was seen to be barely constricted when viewed with 40 X magnification. The degree of constriction applied retarded, but did not arrest, circulation through the superficial epineurial vasculature and sometimes produced a small, brief twitch in the muscle surrounding the exposure. The incision was closed in layers. In sham-operated mice, an identical dissection was performed except that the sciatic nerve was not ligated.

4. Biochemical and biomolecular techniques

4.1. RNA extraction and reverse transcription

RNA was extracted from whole tissues using TRIzol (Invitrogen Life Technologies, Carlsbad, California) following the manufacturer's protocol. To avoid contamination with genomic DNA the total RNA was then treated with DNAse (Ambion, Austin, Texas) for 30 minutes at 37ºC. The reaction was repeated two times to ensure the purity of samples. The reaction was stopped using DNAse Inactivation Reagent (Ambion).

One μg of the RNA was resuspended in 70 μl RNAse-free distilled water. Six μl of 50 μM random hexamers were added and the mixture was incubated for 10 minutes at room temperature. After the incubation, 39 μl of the following reverse transcriptase buffer were added to the each sample: 23 μl 5X RT buffer (Invitrogen, Life Technologies); 4 μl DTT 0,1 M; 4 μl dNTPs 10 μM (dNTPs, set PCR grade, Invitrogen Life Technologies), 0,5 μl RNAsine (Superase In, Ambion) 1 μl Moloney Murine Leukemia Virus retro-transcriptase. (Invitrogen Life Technologies). The reaction was kept for 90 minutes at 37ºC. The retro-transcriptase was heat-inactivated for 10 minutes at 70ºC

4.2. Real-Time PCR

We quantified transcript levels by quantitative real-time PCR (Q-PCR). Q-PCR for endogenous and mutated DREAM was performed using a pair of primers able to amplify both transcripts: forward 5'-CACCTATGCACACTTCCTCTTCA-3' and reverse 5'-ACCACAAAGTCCTCAAAGTGGAT-3' and two TaqMan MGB probes (Applied Biosystems, Foster City, California): FAM-5'-TGCCTTCGATGCTGAT-3'-MGB and VIC-5'-CGCCTTTGCTGCGGC-3'-MGB, specific for wild type and mutant DREAM, respectively. Primers and probes for quantification of other genes are described below:

BDNF (Sybr Green)	FORWARD: 5′-CGAGTGGGTCACAGCGGCAGA-3′ REVERSE: 5′-CGAACATACGATTGGGTAGTT-3′
TrkB	Commercial kit: Applied Biosystems cod.: Mm00435422_m1
Prodynorphin	FORWARD: 5′-CGTGATGCCCTCTAATGTTATGG-3′ REVERSE: 5′-AGTCTCCTCACCCTCTGTA-3′ PROBE: FAM-5′-TCAACCCCCTGATTTG-3′-MGB
Proenkephalin	Commercial kit: Applied Biosystems cod.: Mm01212875_m1
Prepronociceptin	Commercial kit: Applied Biosystems cod.: Mm00803087_m1
Proopiomelanocortin	Commercial kit: Applied Biosystems cod.: Mm00435074_m1
Mu opioid receptor	Commercial kit: Applied Biosystems cod.: Mm00440568_m1
Delta opioid receptor	Commercial kit: Applied Biosystems cod.: Mm00443063_m1
Kappa opioid receptor	Commercial kit: Applied Biosystems cod.: Mm00440561_m1
Nociceptin receptor	Commercial kit: Applied Biosystems cod.: Mm00440563_m1
Kv4.1	Commercial kit: Applied Biosystems cod.: Mm00492796_m1
Kv4.2	Commercial kit: Applied Biosystems cod.: Mm00498065_m1
Kv4.3 (Sybr Green)	FORWARD: 5′-TGGATATGGAGACATGGTGC-3′

	REVERSE: 5′-GAGCCAAATATCTTCCCTGCG-3′
SV2c	Commercial kit: Applied Biosystems cod.: Mm01282630_m1
MGLL	Commercial kit: Applied Biosystems cod.: Mm00449274_m1
DBNDD2	Commercial kit: Applied Biosystems cod.: Mm00458743_m1
CTSL	Commercial kit: Applied Biosystems cod.: Mm00515597_m1
DTNBP1	Commercial kit: Applied Biosystems cod.: Mm00458743_m1
GABAAα1	Commercial kit: Applied Biosystems cod.: Mm00439040_m1
GABAAα2 (Sybr Green)	FORWARD: 5′-AAGACAAAATTGAGCACATGCA-3′ REVERSE: 5′-TGGGTCCCACACCAGAAGA-3′
GABAAα3	Commercial kit: Applied Biosystems cod.: Mm0043440_m1
GABAAβ3 (Sybr Green)	FORWARD: 5′-CCTTCTGGATCAATTACGATGCA-3′ REVERSE: 5′-TGAGTGTTGATGGTTGTCATGGT-3′
GABAAγ2 (Sybr Green)	FORWARD: 5′-CACAGAAAATGACGCTGTGGAT-3′ REVERSE: 5′-TCATCTGACTTTTGGCTTGTGAA-3′

The results were normalized by quantification of HPRT or GAPDH mRNA, where indicated. HPRT was quantified using the specific primers; forward 5'-TTGGATACAGGCCAGACTTTGTT-3' and reverse 5'-CTGAAGTACTCATTATAGTCAAGGGCATA-3', and the probe FAM-5'-TTGAAATTCCAGACAAGTTT-3'-MGB; GAPDH was quantified using a commercial kit from Applied Biosystems (cod.: 4352339E).

Each experiment was done with a minimum number of 6 mice/line/condition and repeated at least two times with samples collected from independent experiments.

4.4. Protein extraction and Western Blot

4.4.1 Dissection of tissue samples

The dorsal lamina of the spinal cord of wild type and line 1 mice were dissected viewed with a 40X magnification to isolate only the outer laminae. Where indicated, mice were treated with intraplantar CFA or formalin and the dissection took place at different time point after the injection (30 minutes and 6 hours for CFA; 45 minutes for formalin).

Where indicated mice were pretreated with an intraperitoneal injection of bicuculline (Sigma-Aldrich) 1,5 mg/kg, (dissolved in 0,1N HCl and adjusted to pH 5 with 0,1N NaOH) 30 minutes before the beginning of the experimental procedures

4.4.2 Sample processing

Tissue samples were lysed by mild sonication in lysis buffer [50 mM Tris-Hcl, pH 7.5; 150 mM NaCl; 1% Nonidet P-40; EDTA-free protease inhibitor cocktail (Roche Applied Science, Bassel, Swiss); phosphatase inhibitors (Phosphatase inhibitor set II. Calbiochem)]. The lysis was performed rotating the samples at 4ºC for 30 minutes. The lysates were cleared by centrifugation for 10 minutes at 14000 rpm.

After protein quantification by the Bradford method, 10 to 30 μg of total protein were separated in 10% SDS-polyacrylamide gels. After electrophoresis, separated proteins were transferred in semi-dry conditions to PVDF membranes (Millipore). Membranes were blocked with 5% non-fat dry milk in TBS-T [20 mM Tris pH 7,6; 137 mM NaCl; 0,1% Tween-20 (Sigma-Aldrich)] and incubated overnight at 4ºC with the indicated antibodies. Immunolabeling was detected by enhanced chemiluminiscence (ECL Advance. GE Healthcare)

When necessary, membranes were stripped in a stripping buffer containing 100 mM 2-mercaptoethanol; 62,5 Tris-HCl, pH 6,8; 2% SDS for 30 minutes at 50ºC.

The following primary antibodies were used following the manufacturer's instructions:

Anti Phospho-ERK	Monoclonal anti-MAP kinase, activated (Sigma-Aldrich)
Anti ERK	Polyclonal anti-ERK 2 (C14) (Santa Cruz Biotechnology)

5. Affymetrix microarray

5.1- Samples preparation

Total RNA from the trigeminal ganglion of wild type and line 16 mice was prepared as described previously. The RNA was purified using a commercial kit following the manufacturer's instructions (RNeasy mini kit. Quiagen). Samples were pooled in groups of three to finally obtain 3 pools for line 16 mice and 4 pools for wild type mice. The RNA samples were analyzed for purity and integrity using Agilent 2100 Bioanalyzer (Agilent technologies).

5.2. Amplified RNA (aRNA) preparation and fragmentation

Four μg of the different pools of total RNA were used in this process. Total RNA was reverse transcribed to synthesize first-strand cDNA. This reaction was primed using T7 oligo(dT) that contains a T7 promoter sequence. To prepare the second strand of cDNA, DNA polymerase and RNase H were used to simultaneously degrade the RNA and synthesize second-strand cDNA. Synthesis of the aRNA was performed by in vitro transcription. In this step biotin-conjugated nucleotides were added to the reaction, which are incorporated into the newly synthesized aRNA. The quality of the aRNA obtained was controlled with the Agilent 2100 Bioanalyzer. Thereafter, 15 μg of aRNA were heat-fragmented for 35 minutes at 95ºC obtaining aRNA fragments ranging in length between 35 and 200 base pairs.

5.3. Microchip hybridization

Five ug of the fragmented aRNA were used for preliminary control hybridization with TestChip (Affymetrix). In case of positive results 10 μg are hybridized with the MOE 430 2.0 chip (Affymetrix). This chip includes 45000 different probe sets that analyze the expression level of more than 39000 transcripts and variants from 34000 well-characterized mouse genes. Hybridization buffer [100 mM 2-(N-morpholino)ethanesulphonic acid; 1 M NaCl; 20 mM EDTA; 0,01% Tween-20 (Sigma-Aldrich)] was added to each of the samples to a final RNA concentration of 0,05 μg/ml and 200 μl of each sample were incubated with each chip for 16 hours at 45ºC.

The microarrays were stained with streptavidin-phycoerythrin in the Fluidic Station 450 (Affymetrix) and scanned with the GeneChip Scanner 3700 7G System (Affymetrix) with a resolution of 11 μM. Data analysis was carried out using GeneChip Operating System (Affymetrix).

5.4. Statistical analysis

Data normalization and statistical analysis were performed using the R/Bioconductor LIMMA package. Data were normalized through robust multi-array averaging. Linear methods were used to determine differently expressed genes obtaining an estimation of moderated t-statistics p values. The Benjamini-Hochberg correction (Reiner et al., 2003) for multiple comparisons (False Discovery Rate) was applied to these *p* values.

6. Data analysis

Each experiment was repeated at least two times independently and the data are expressed as mean ± SEM. Statistical analysis and curve fitting were performed using Prism 4.0 (Graphpad). Statistical significance of the differences between experimental groups was analyzed using Student's *t*-test unless otherwise stated. * $p < 0,05$; ** $p < 0,01$ and *** $p < 0,001$.

RESULTS

RESULTS

A. FUNCTIONAL ANALYSIS OF DREAM IN PAIN MECHANISMS AT THE SPINAL CORD/DRG LEVEL

A.1. Characterization of daDREAM transgenic lines for the study of spinal cord mechanisms of pain

Regulation of gene expression by DREAM has been associated with changes in the response to noxious stimuli (Cheng et al., 2002; Lilliehook et al., 2003). To specifically analyze the role of DREAM in the molecular pathways that control the response to pain we used transgenic mice that express a dominant active mutant of DREAM (daDREAM) (Gomez-Villafuertes et al., 2005; Savignac et al., 2005). The transgene is mutated in the three functional EF-hands and in the first LCD. As a result, the mutant DREAM is unable to bind Ca^{2+} and to interact with CREB (Carrion et al., 1999; Ledo et al., 2002).

A.1.1. Analysis of daDREAM expression levels

Previous data in our laboratory described the pattern of expression of daDREAM mutant in the lumbar spinal cord of the different available transgenic lines. This screening showed expression of the transgene in the spinal cord of mice from line 1 (L1).

To carry out a detailed characterization of transgene expression in sensory areas associated with spinal pain we performed quantitative real-time PCR (Q-PCR) analysis of of endogenous and daDREAM expression in the lumbar spinal cord and in the DRG from wild type and L1 mice (Fig. 8).

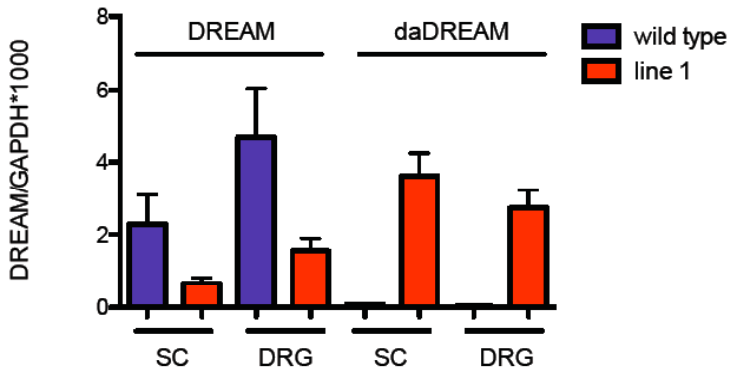

Figure 8. Q-PCR analysis of DREAM and daDREAM expression. DREAM and daDREAM expression was quantified by Q-PCR in the spinal cord (SC) and dorsal root ganglion (DRG) of wild type (n= 12) and line 1 (n= 12) mice. Values are normalized by the content of GAPDH.

A first important result from this analysis was that, both in SC and DRG, the expression level of daDREAM is comparable with the expression of endogenous DREAM (Fig. 8). Based on previous work (Savignac et al., 2005) the ratios of daDREAM versus endogenous DREAM obtained are sufficient for the transgene to display its activity as a dominant active mutant on the functioning of endogenous DREAM/KChIP proteins in the nucleus. Confirming this, and further supporting the idea that DREAM regulates its own transcription, expression of endogenous DREAM mRNA was significantly reduced in line 1 mice, compared to wild type controls, both in the spinal cord (SC) and in dorsal root ganglia (DRG) (Fig. 8). Thus, expression level of daDREAM in SC and DRG ensures that DREAM target genes are constitutively repressed in our transgenic mice giving us the opportunity to study the effect of the transgene expression *in vivo* at the SC/DRG level.

A.1.2. Analysis of nociceptive thresholds in daDREAM mice

Previous experiments showed that DREAM transgenic mice are hyperalgesic when tested both for visceral pain (writhing test) and thermal sensitivity (tail flick test). To further define the basal nociceptive phenotype of daDREAM expressing mice we carried out a complete set of behavioral experiments, including the assessment of pain thresholds to different thermal test and mechanical stimulation as well as the responses to inflammatory and neuropathic chronic pain.

Response to thermal noxious stimulation were measured in wild type and transgenic mice using the plantar test (Hargreaves et al., 1988) to measure the thresholds for foot withdrawal latency.

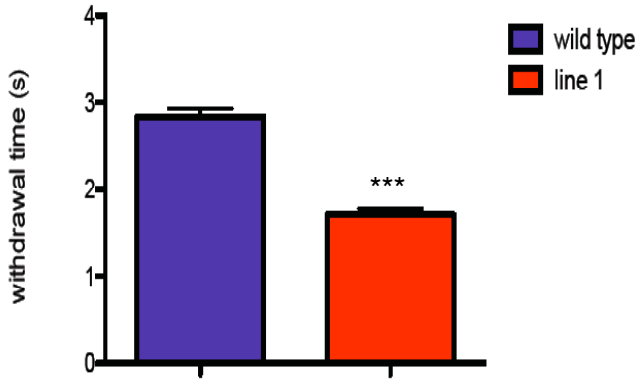

Figure 9. Basal thermal threshold. Basal thermal threshold was evaluated with a plantar test assay in wtild type (n= 19) and line 1 (n= 23) mice.

Transgenic mice showed a hyperalgesic phenotype (Fig. 9) with a mean latency of foot withdrawal of 1,70 ± 0,06 seconds, while for wild type mice it was 2,83 ± 0,09 seconds. These results confirmed previous observations using the tail flick test.

To identify the response to punctuate low threshold mechanical stimulation we used von Frey hairs (Levin et al., 1978).

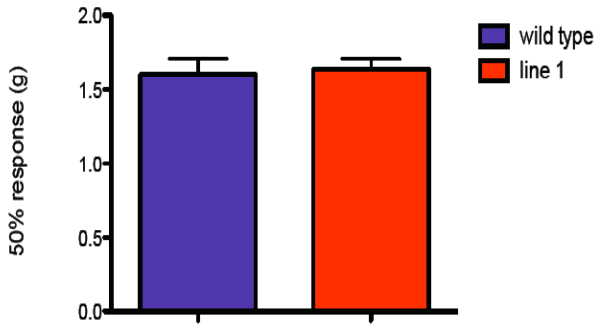

Figure 10. Basal mechanical threshold. Basal mechanical threshold was evaluated using von Frey's hair in wild type (n= 19) and line 1 (n= 23) mice.

Transgenic mice and wild type mice showed the same mechanical sensitivity to a punctate stimulation in the hindpaw (Fig. 10). The 50% response was evoked by a force of 1,60 ± 0,10 grams in the wild type mice, while in transgenic mice it was 1,64 ± 0,06 grams. These results indicate that transgene expression does not affect nociceptive responses to mechanical stimulation, suggesting that endogenous DREAM may not be involved in mechanical noxious perception.

Next, we tested transgenic mice for their response to tonic pain using the formalin test, a model for pain studies commonly used in rodents. Intraplantar injection of formalin activates nociceptors and results in a typical biphasic nociceptive response (Karim et al., 2001). The first phase of nocifensive behavior involves direct activation of nociceptors, whereas the second phase is evoked by mechanisms of peripheral and central sensitization (Puig and Sorkin, 1996).

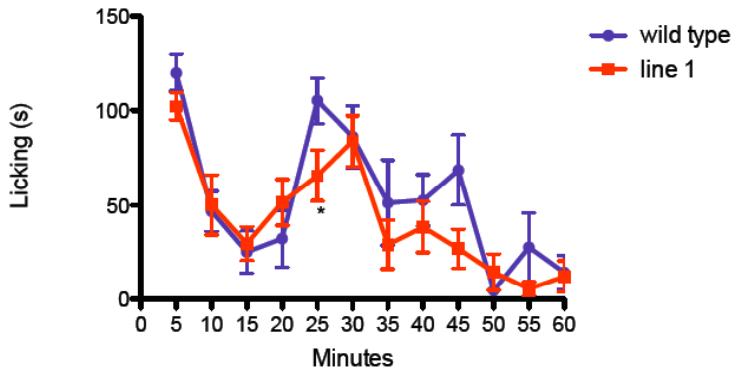

Figure 11. Formalin test. Wild type (n= 8) and line1 (n=8) mice were tested for their licking response after intraplantar injection of formalin. The response was evaluated in blocks of 5 minutes during one hour after the injection.

In the first phase of the formalin test, from 0 to 15 minutes after injection, we did not observe differences between wt and transgenic mice. In the second phase, from 15 to 60 minutes, we recorded a slightly less pronounced response in transgenic mice (Fig. 11). Quantification of the area under the curve for wt and daDREAM expressing mice still did not show a statistically significant decrease in the total licking behavior (Fig. 12). This tendency of a lower response during the second phase of the formalin test could be indicative of a slight impairment of sensitization mechanisms in transgenic mice.

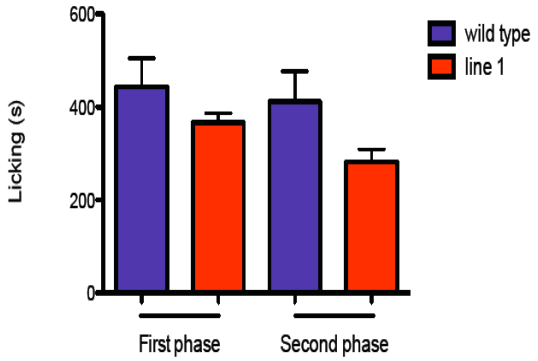

Figure 12. Total nocifensive response to formalin. The nocifensive response to formalin was evaluated measuring the area under the curve in the first phase (0 to 15 minutes) and in the second phase (15 to 60 minutes)) of the formalin test in wild type (n= 8) and line 1 (n= 8) mice.

A.1.3. Transcriptional basis for basal hyperalgesia in daDREAM mice

Earlier transcriptomic analysis of the changes imposed by the expression of daDREAM in the lumbar spinal cord of DREAM transgenic mice identified the μ opioid receptor as a transcriptional target for DREAM repression. In this work we have quantified by real-time PCR some known DREAM target genes as well as DREAM interacting proteins that have been related to nociception. Among target genes, we focused on the opioid system and on BDNF. Among interacting proteins we analyzed the expression of Kv4 channels.

A.1.3.1. The endogenous opioid system

Scattered pieces of evidence suggest that DREAM has an important role in the control of the endogenous opioid tone. Thus, it has been shown that DREAM regulates the expression of prodynorphin (Carrion et al., 1999) and its main receptor, the κ opioid receptor, (Cheng et al., 2002). Furthermore, the downregulation of the μ opioid receptor in the spinal cord, medulla-pons and periaqueductal grey in daDREAM transgenic mice has also been previously shown. To complete the knowledge about the role of DREAM in

the control of the endogenous opioid system we measured expression levels for all the different opioid ligands and receptors in spinal cord and DRG.

The results from the analysis at the spinal cord level are shown in Table 1 and indicate that the expression of the dominant active mutant of DREAM in the spinal cord produces an overall decrease in the transcription of genes encoding both polipeptidic opioid precursors and opioid receptors. Levels of POMC were below the limit of detection in the spinal cord, suggesting that this precursor is not contributing or has a minor role in endogenous opioid mechanisms in this tissue.

PDYN	downregulated
PENK	downregulated
POMC	not detected
PNOC	downregulated
MOR	downregulated
DOR	downregulated
KOR	downregulated
ORL	downregulated

Table 1. The opioid system in the spinal cord of line 1 mice. The expression level of the different members of the opioid system measured via Q-PCR compared to wild type control mice.

In transgenic DRG, expression of PENK and PNOC was reduced, expression of PDYN was not affected and POMC mRNA was again not detectable (Fig. 13). Furthermore, transcription of μ, δ and κ receptors was reduced, while the expression of the opioid-like receptor was not affected (Fig. 14). These results highlighted the importance of DREAM in the transcriptional control of the opioid system also in DRG.

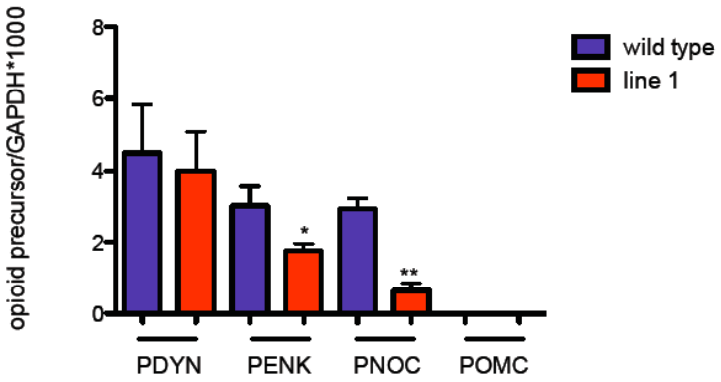

Figure 13. Q-PCR analysis of the polypeptidic opioid precursors expression in the DRG. PDYN, PENK, PNOC and POMC expression was quantified by Q-PCR in the DRG of wild type (n= 14) and line 1 (n= 13) mice. Values are normalized by the content of GAPDH.

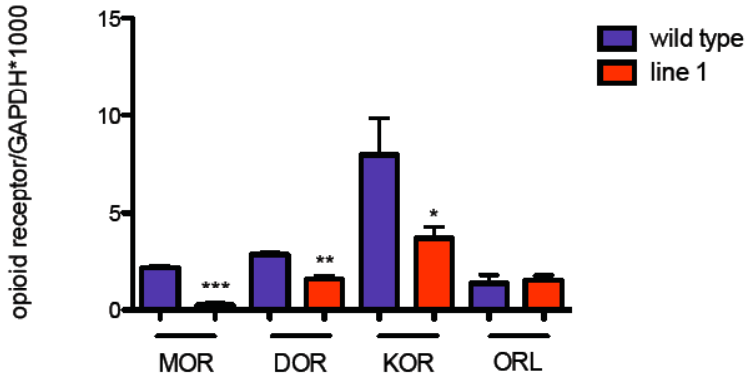

Figure 14. Q-PCR analysis of the expression of opioid receptors in the DRG. MOR, DOR, KOR and ORL expression was quantified by Q-PCR in the DRG of wild type (n= 14) and line 1 (n= 13) mice. Values are normalized by the content of GAPDH.

A.1.3.2. BDNF expression in daDREAM mice

Accumulated evidence during the last 12 years indicates that BDNF plays a critical role in nociception (Kerr et al., 1999; Thompson et al., 1999; Zhou et al., 2000; Yajima et al., 2005). Two aspects were of particular importance for our study i) the role of BDNF in regulation of the response of the second order neurons that transmit pain signal in the dorsal horn of the spinal cord (Pezet and McMahon, 2006) and, ii) the evidence from *in vitro* experiments that DREAM regulates the activity of several BDNF promoters (Mellstrom et al., 2004). Thus, we first measured, by Q-PCR, BDNF expression level in the DRG and in the spinal cord of wt and transgenic mice and found a reduction in both areas (Fig. 15).

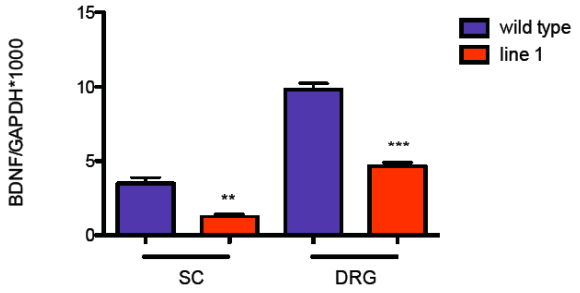

Figure 15. Q-PCR analysis of BDNF expression. BDNF expression was quantified by Q-PCR in the spinal cord (SC) and dorsal root ganglion (DRG) of wild type (n= 12) and line 1 (n= 12) mice. Values are normalized by the content of GAPDH.

Importantly, decreased BDNF expression did not result in a significant change in the expression of its main receptor, the tyrosine kinase receptor trkB, either in spinal cord or in DRG from transgenic mice (Fig. 16).

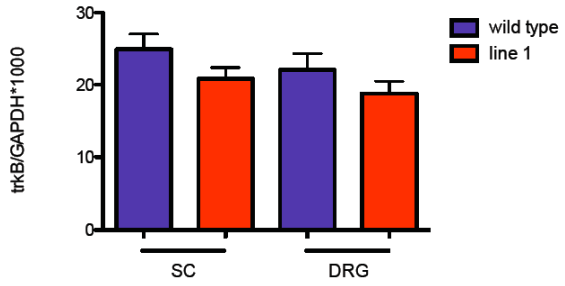

Figure 16. Q-PCR analysis of trkB expression. trkB expression was quantified by Q-PCR in the spinal cord (SC) and dorsal root ganglion (DRG) of wild type (n= 12) and line 1 (n= 12) mice. Values are normalized by the content of GAPDH.

A.1.3.3. Kv4 expression in daDREAM mice

Kv4 channels are the main ion channels responsible for generation of the inhibitory A-type current. These potassium currents have been associated with neuronal plasticity in the hippocampus (Frick et al., 2004) and in the spinal cord (Hu et al., 2006). The calcium insensitive DREAM mutant has been previously shown to affect gating properties of potassium channels *in vitro* (An et al., 2000) and a minor change in A-type currents has been reported in DREAM deficient neurons (Cheng et al., 2002). Moreover, expression of KChIP proteins is altered in genetically modified mice lacking different Kv4 subunits (Menegola and Trimmer, 2006). Because of this, it was important to investigate whether expression of daDREAM modifies Kv4 channels at the transcriptional or functional level.

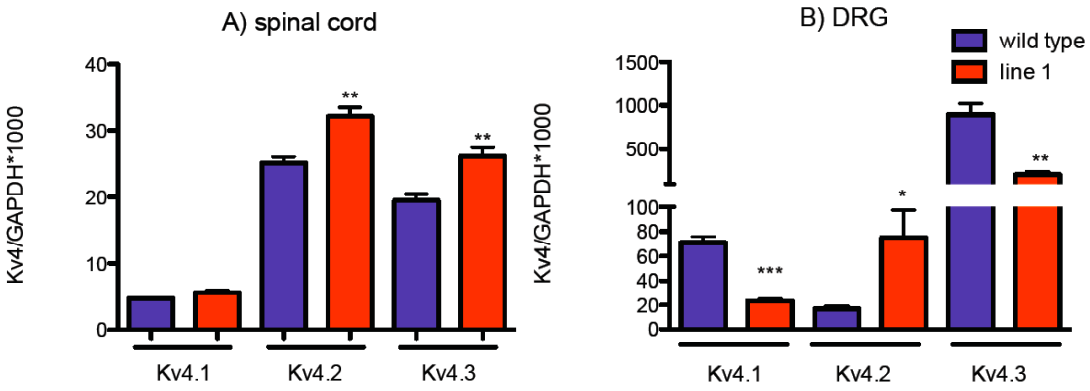

Figure 17. Q-PCR analysis of Kv4 expression in the spinal cord and in the DRG. Kv4.1, Kv4.2 and Kv4.3 expression was quantified by Q-PCR in the spinal cord (A) and in the DRG (B) of wild type (n= 12) and line 1 (n= 12) mice. Values are normalized by the content of GAPDH.

In the spinal cord, quantitative analysis of mRNA levels of the different subunits contributing to A-type currents showed a moderate increase of Kv4.2 and Kv4.3 in daDREAM mice, while Kv4.1 levels were unaffected (Fig. 17 A). Conversely, in the DRG,

expression of the Kv4.1 and Kv4.3 was decreased in transgenic mice while the expression of the Kv4.2 subunit was increased (Fig. 17 B).

Reduced expression of Kv4 subunits has been associated with basal hyperalgesia (Hu et al., 2006; Chien et al., 2007). In our transgenic model, the hyperalgesia is observed in the presence of bidirectional changes in the expression of the Kv4 subunits, both in the spinal cord and in the DRG. To investigate whether these transcriptional changes or the expression of the daDREAM mutant itself have a functional correlate we characterized A-type currents in dorsal horn transgenic neurons. In collaboration with Prof. Lopez-García from Alcalá University, dorsal horn neurons were recorded in voltage-clamp conditions. Interestingly, isolated A-type currents were similar in wild type and transgenic mice and no differences were found in their voltage dependent activation, inactivation (Fig. 18 A) and reactivation (Fig. 18 B). Moreover, neurons from wild type and transgenic mice were recorded in current clamp mode to compare their general state of excitability. We found that the intrinsic excitability of transgenic neurons was essentially unchanged (Fig 18 C).

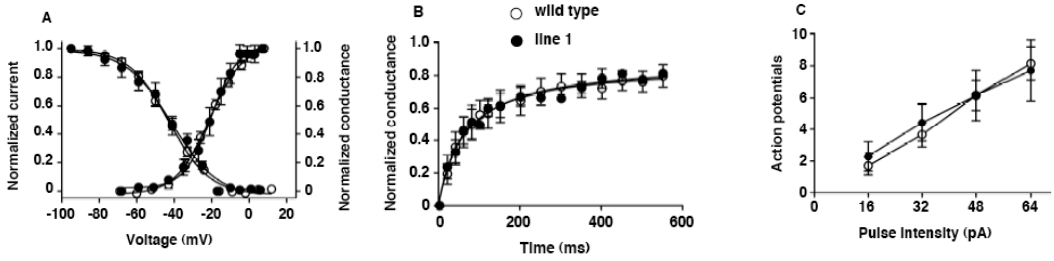

Figure 18. A-type potassium (I_A) currents and neuronal excitability. Comparison between I_A currents observed in dorsal horn neurons from wild type (n= 18) and line 1 (n= 6) mice: activation kinetics (A, right axis), inactivation kinetics (A, left axis) and recovery from inactivation (B) Mean number of action potential obtained in current clamp recordings (C)

These data indicate that daDREAM does not function as a dominant mutant for Kv4 channel activity *in vivo*, and it is therefore unlikely that the basal hyperalgesia observed in transgenic mice is related to changes in A-type currents.

A.2. DREAM and the spinal response to inflammatory pain

The process of central sensitization after chronic pain is defined as the increase in synaptic efficacy in somato-sensory neurons in the dorsal horn of the spinal cord following intense peripheral noxious stimulation. The slightly reduced response of daDREAM transgenic mice in the second phase of the formalin test could be an indication of impaired central sensitization process. To investigate if this was the case and clarify a potential role of DREAM in sensitization processes during chronic pain we

evaluated the response of the transgenic mice in a model of inflammatory pain after intraplantar CFA injection.

A.2.1. Behavioral response to inflammatory pain in daDREAM mice

Inflammatory-induced hyperalgesia after CFA was evaluated in wild type and transgenic mice at different times after treatment, assaying the response to thermal and mechanical stimulation using the plantar test (Fig. 19) and the von Frey hair (Fig. 20), respectively.

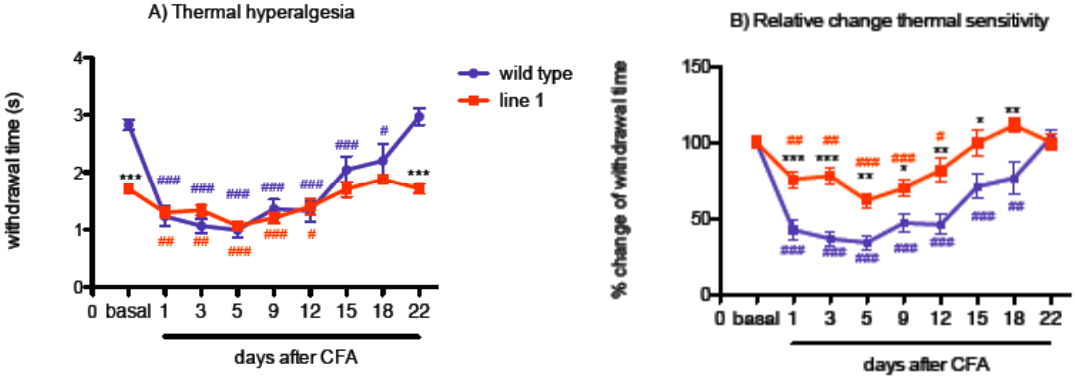

Figure 19. Thermal hyperalgesia after CFA injection. A) Thermal hyperalgesia was evaluated by plantar test in basal condition and at different days after intraplantar CFA injection in wild type (n= 14) and line 1 (n= 14) mice. B) Relative change in thermal sensitivity was calculated with respect to basal levels of wild type and line 1 mice. * = wild type vs line 1 (same day); # and # = basal vs treated for wild type and line 1, respectively.

Injection of CFA produced a similar redness and paw inflammation in wild type and transgenic mice. At 24 hours after CFA, wild type mice developed a pronounced thermal hyperalgesia (withdrawal latency of 1,29 ± 0,02 seconds), which lasted for 18 days (Fig. 19 A). On the contrary, thermal thresholds were only slightly modified in transgenic mice 24 hours after CFA and the hyperalgesic response was observed only up to day 12 after CFA. These differences were better observed when analyzed as relative change to basal thermal sensitivity for each genotype (Fig 19 B). Taken together these data suggest that daDREAM mice displays impaired response to inflammatory pain with milder and shorter-lasting hyperalgesia compared to wild type mice.

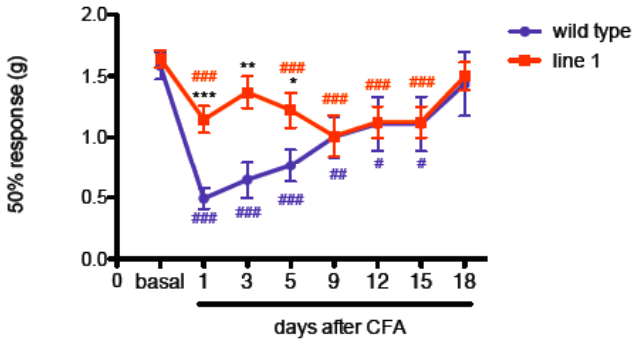

Figure 20. Mechanical hyperalgesia after CFA injection. Mechanical hyperalgesia was evaluated by von Frey's hair in basal condition and at different days after intraplantar CFA in wild type (n= 14) and line 1 (n= 14) mice. *= wild type Vs line 1 (same day). # and # = basal vs treated for wild type and line 1, respectively.

Importantly, similar results were obtained when we tested mechanical sensitivity. Wild type mice display a strong hyperalgesic response starting from day 1 after CFA injection (Fig. 20). Transgenic mice also show enhanced sensitivity to mechanical stimulation after CFA injection, but the hyperalgesia in this case is less pronounced than in wild type mice. These data also sustain the hypothesis of an impaired sensitization in response to a chronic inflammatory stimulus.

A.2.2. Transcriptional basis for modified sensitization in daDREAM mice

To investigate the molecular substrate for the modified sensitization observed in transgenic mice following inflammatory pain, we first characterized the transcriptional response of endogenous DREAM to intraplantar CFA injection (Fig. 21).

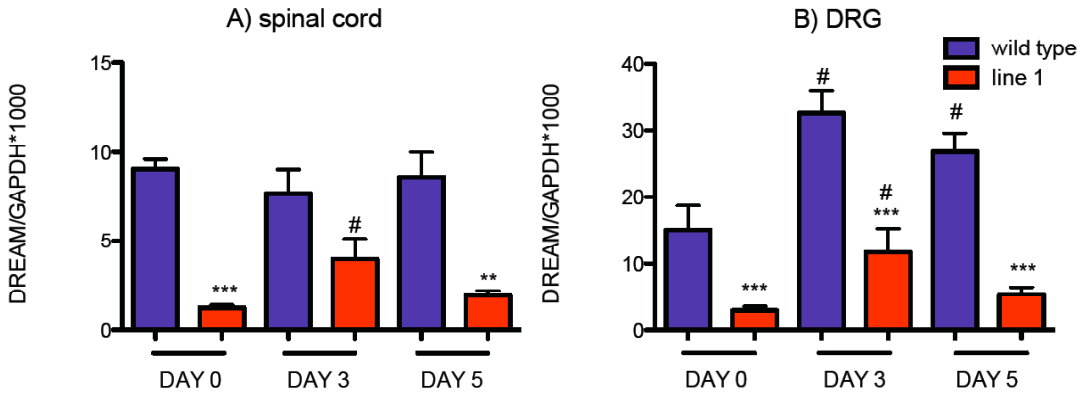

Figure 21. Q-PCR analysis of DREAM expression in the spinal cord and DRG after CFA injection. Endogenous DREAM expression in the spinal cord was quantified by Q-PCR in the spinal cord (A) and DRG (B) of wild type (n=6) and line 1 (n= 6) mice at day 0, 3 and 5 days after intraplantar CFA injection. *= wild type Vs line 1 (same day); #= basal Vs treated (same line). Values are normalized by the content of GAPDH.

In the spinal cord of wt mice the transcription of DREAM was not affected during inflammatory pain (Fig. 21 A). Contrary, in line 1 mice we observed a peak of induction at day 3 and the expression returned to basal levels 5 days after CFA injection.

In the DRG, however, a long lasting increase in DREAM mRNA was observed both in wild type and transgenic mice (Fig. 21 B).

A.2.2.1. The opioid response to inflammatory pain in daDREAM mice

As described earlier, the opioid system is greatly influenced by the expression of daDREAM both in spinal cord and DRG. Thus, we compared the opioid response to inflammatory pain in transgenic versus wt mice.

First we analyzed by Q-PCR the expression level of the polypeptidic precursors for the endogenous opioid peptides in the spinal cord (Fig. 22)

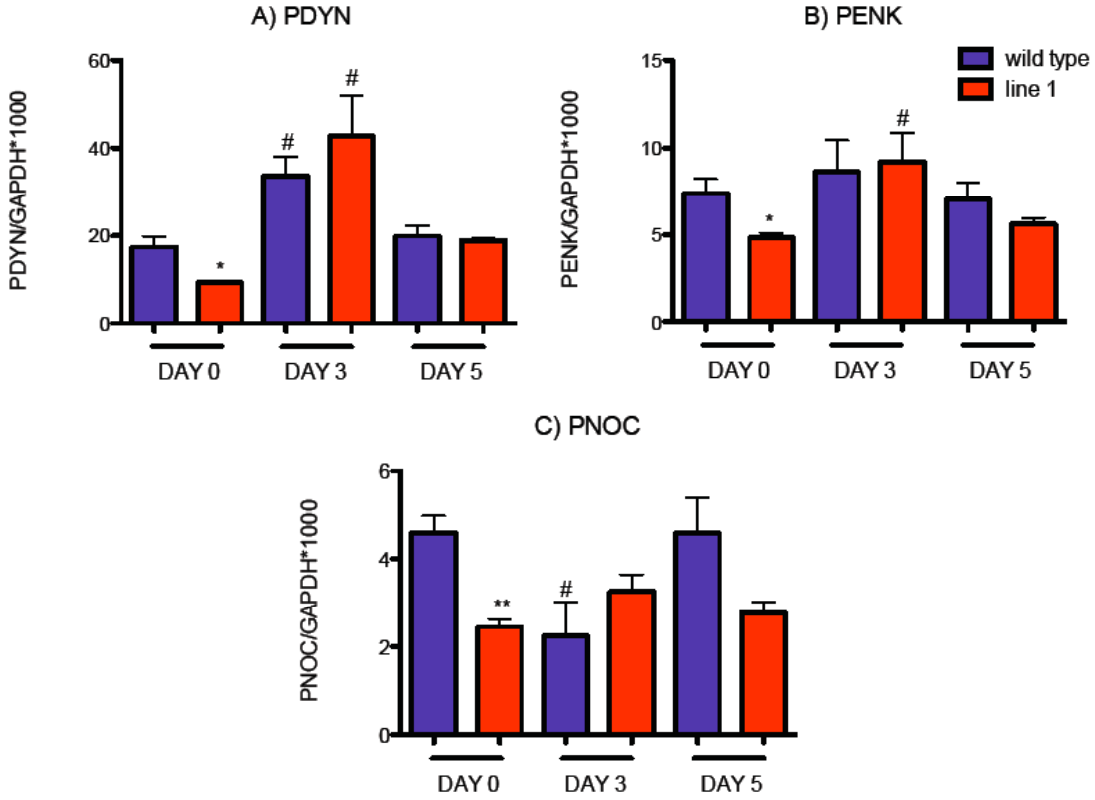

Figure 22. Q-PCR analysis of polypeptidic opioid precursors expression in the spinal cord after CFA injection. PDYN (A), PENK (B) and PNOC (C) expression was quantified by Q-PCR in the spinal cord of wild type (n=6) and line 1 (n= 6) mice at day 0 and 3 and 5 days after intraplantar CFA injection. *= wild type vs line 1 (same day); #= basal vs treated (same line). Values are normalized by the content of GAPDH.

PDYN expression revealed a significant increase at day 3 after the treatment with CFA that disappeared at day 5 in both genotypes (Fig. 22 A). PENK expression revealed no change in wt mice while PENK mRNA was increased in transgenic mice at day 3 and remained elevated 5 days after CFA (Fig. 22 B). PNOC expression was reduced at day 3 and returned to basal level 5 days in wild type mice, on the other hand it was not affected in transgenic mice at any time after CFA (Fig. 22 C).

As for the expression of opioid receptors, i) mu opioid receptor was not affected in wild type mice but was increased two-fold at day 3 in daDREAM mice (Fig. 23 A), ii) delta and kappa opioid receptors were not significantly modified during inflammatory pain in either genotype (Fig. 23 B, C) and iii) expression of ORL was induced at 3 days after CFA in wt but not in transgenic mice (Fig 23 D).

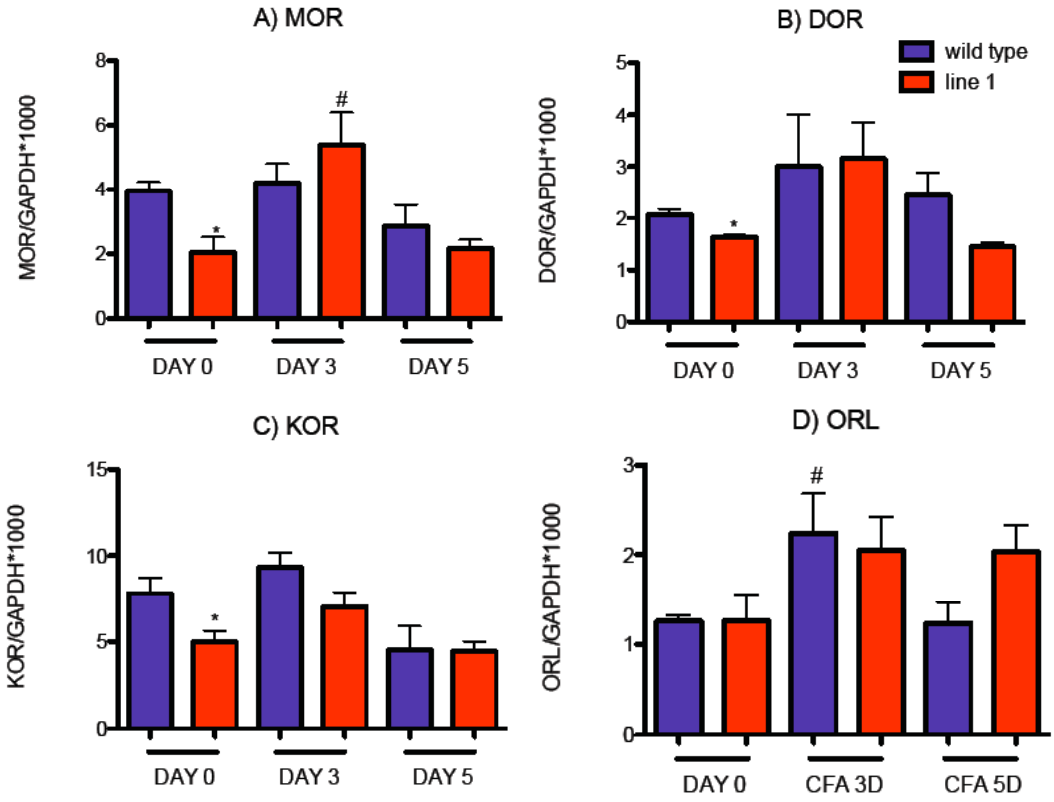

Figure 23. Q-PCR analysis of opioid receptors expression in the spinal cord after CFA injection. MOR (A), DOR (B), KOR (C) and ORL (D) expression was quantified by Q-PCR in the spinal cord of wild type (n=6) and line 1 (n= 6) mice at day 0, 3 and 5 days after intraplantar CFA injection. * = wild type vs line 1 (same day) and #= basal vs treated (same line). Values are normalized by the content of GAPDH.

In the DRG, the response of the opioid system to inflammatory pain was markedly different with respect to the response in the spinal cord (Fig. 24).

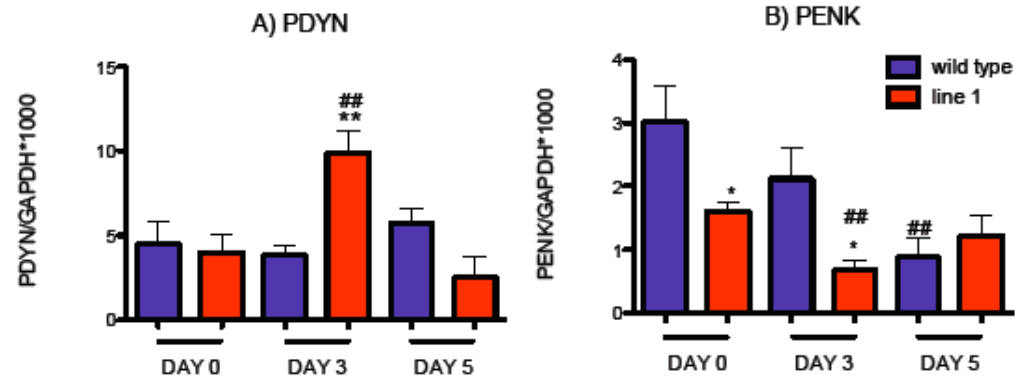

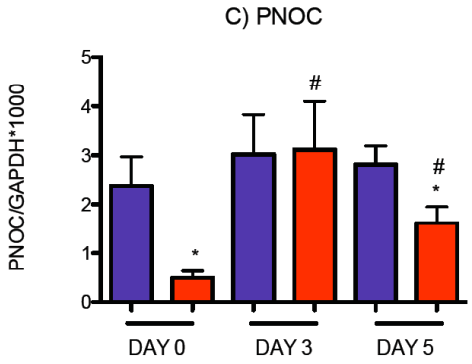

Figure 24. Q-PCR analysis of polypeptidic opioid precursors expression in the DRG after CFA injection. PDYN (A), PENK (B) and PNOC (C) expression was quantified by Q-PCR in the DRG of wild type (n=6) and line 1 (n= 6) mice at day 0 and 3 and 5 days after intraplantar CFA injection. * = wild type vs line 1 (same day) and # = basal vs treated (same line). Values are normalized by the content of GAPDH.

Following CFA injection, expression of i) PDYN and PNOC mRNA was not modified in wt mice but induced at day 3 in transgenic mice (Fig. 24 A, C) and, ii) PENK expression was decreased in both genotypes though with a different time course. In wild type mice the decrease was significant only at day 5 while in transgenic mice the peak of reduction was observed at day 3 (Fig. 24 B).

Inflammatory pain induced very specific changes in opioid receptors expression in the DRG, which were different from the changes observed in the spinal cord:

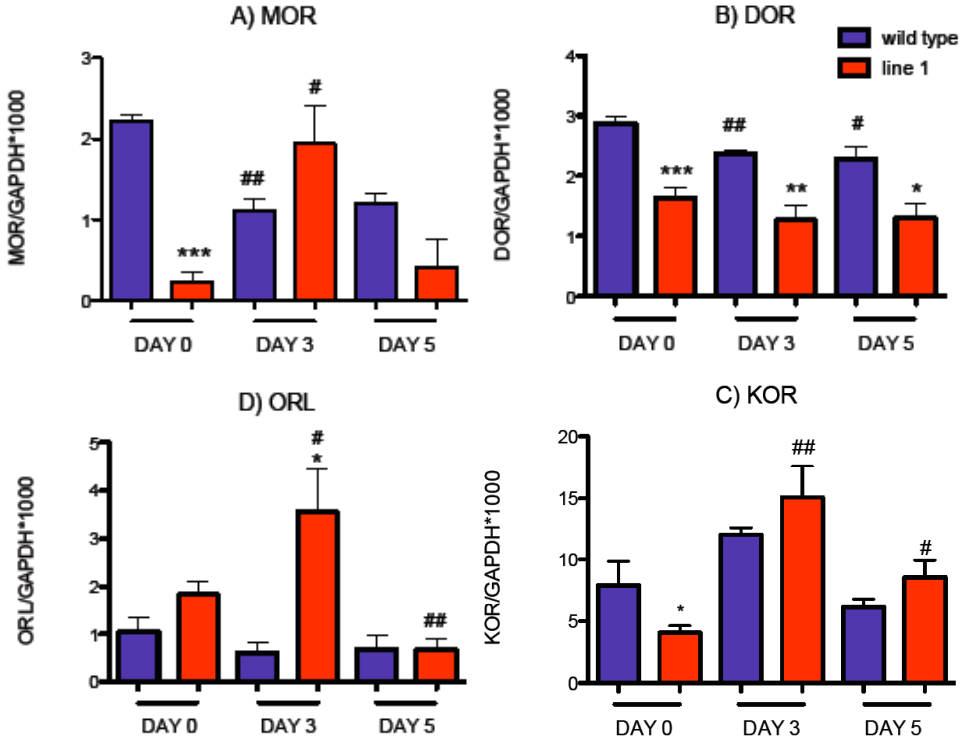

Figure 25. Q-PCR analysis of of the expression of opioid receptors expression in DRG after CFA injection. MOR (A), DOR (B), KOR (C) and ORL (D) expression was quantified via Q-PCR in the DRG of wild type (n=6) and line 1 (n= 6) mice at day 0 and 3 and 5 days after intraplantar CFA injection. *= wild type Vs line 1 (same day); #= basal Vs treated (same line). Values are normalized by the content of GAPDH.

Following CFA injection, levels of MOR and DOR mRNA were stably reduced in wild type mice while a peak of induction at day 3 or no change were observed in transgenic DRG, respectively (Fig. 25 A, B). Expression of KOR and ORL were not affected by the ongoing inflammation in wild type mice, while a 2-fold increase was observed at day 3 in transgenic mice. Elevated KOR mRNA level was still observed at day 5, though to a lower extent, while ORL mRNA was decreased at day 5 in transgenic DRG (Fig. 25 C, D).
In summary we observed that the expression of the dominant active mutant of DREAM in the DRG greatly influenced the endogenous response of the opioid system to inflammation in transgenic mice.

A.2.2.2. The BDNF response to inflammatory pain in daDREAM mice

The neurotrophin BDNF is a key regulator of the sensitization process and previous studies have shown that i) inflammation activates the anterograde transport of BDNF from DRG to synaptic terminals in the spinal cord (Pezet and McMahon, 2006) and ii) BDNF secretion increases neuronal excitability of second-order neurons in external laminae of the dorsal horn (Matayoshi et al., 2005).
Since BDNF is regulated by DREAM in basal conditions, we analyzed the transcriptional response of the BDNF gene to the inflammatory pain induced by CFA injection.

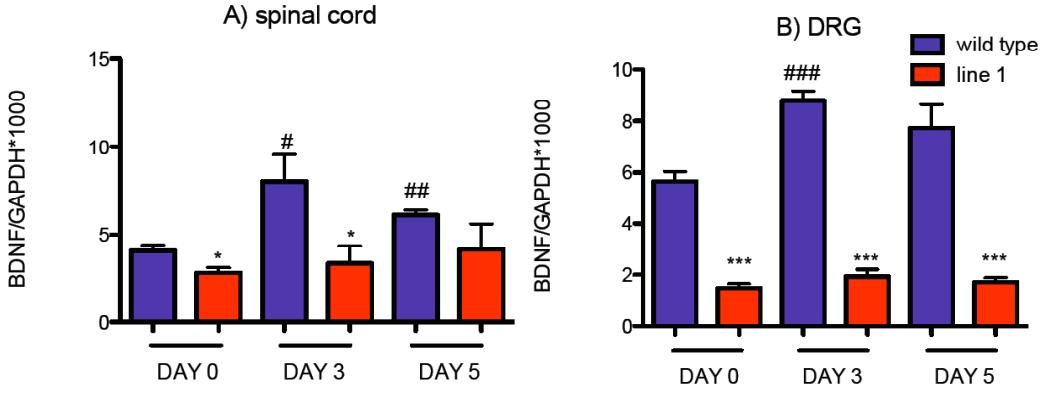

Figure 26. Q-PCR analysis of BDNF expression in the spinal cord and DRG after CFA injection. BDNF expression was quantified via Q-PCR in the spinal cord (A) and DRG (B) of wild type (n=6) and line 1 (n= 6) mice at day 0 and 3 and 5 days after intraplantar CFA injection. = wild type vs line 1 (same day) and # = basal vs treated (same line). Values are normalized by the content of GAPDH.

In DRG from wild type mice, the inflammatory response developed with an increase in BDNF mRNA levels that was maximal at day 3 and remained elevated 5 days after CFA injection (Fig. 26 A). In transgenic mice, however, expression of the daDREAM mutant

blocked the induction of BDNF in response to CFA (Fig. 26 A). At the spinal cord level we found a similar situation; stable induction in BDNF expression in response to chronic inflammatory pain and no change in line 1 mice (Fig. 26 B). These data suggest that the lack of BDNF response in transgenic mice could be responsible for the impairment of spinal sensitization in DREAM transgenic mice during inflammatory pain.

To further sustain our hypothesis of the involvement of BDNF in the abnormal sensitization process in daDREAM mice, we studied changes in the process of spinal facilitation by analyzing dorso-ventral electrophysiological responses in a model of isolated spinal cord *in vitro*. These experiments were performed in collaboration with the laboratory directed by José Antonio López at the University of Alcalá de Henares.

In this experimental model the entire spinal cord was extracted and placed in a recording chamber. Lumbar dorsal roots 4 or 5 were stimulated with a suction electrode to activate afferent fibers and the corresponding ventral root reflexes was recorded. Isolated spinal cord from wild type mice responded with long-term enhancement of dorsal root-ventral root reflexes (DR-VRR) to the application of a conditioning protocol consisting in a prolonged low frequency stimulation of C-fibers (200 μA, 200 μs at 2 Hz). Isolated spinal cord from transgenic mice, however, did not produce the enhancement of DR-VRR after the application of the same protocol (Fig. 27 A). This result parallels the inability of transgenic mice to generate central sensitization.

To confirm the role of reduced BDNF levels in this process, we next analyzed changes in DR-VRR before and after exogenous application of BDNF to the isolated spinal cord from wild type and transgenic mice. Consistent with our results showing that the expression of trkB mRNA is not modified in transgenic mice, exposure to BDNF *in vitro* resulted in a similar facilitation response in isolated spinal cord from wild type and transgenic mice. In both cases, BDNF superfusion produced a significant 2-fold increase in spikes associated with DR-VRR elicited by a wide range of stimulus intensities involving activation of A- and C-fibers (Fig. 27 B, C)

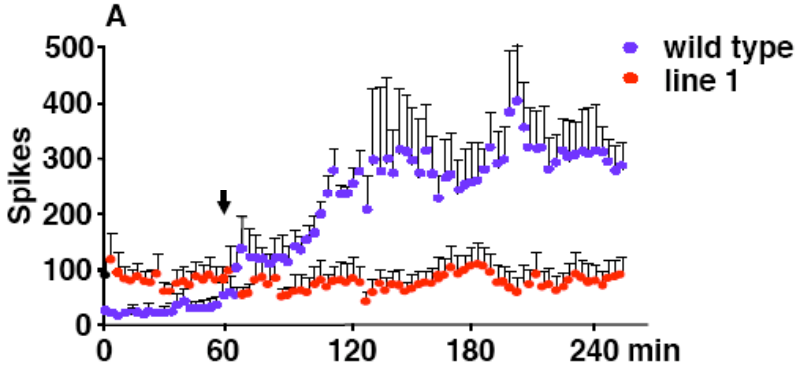

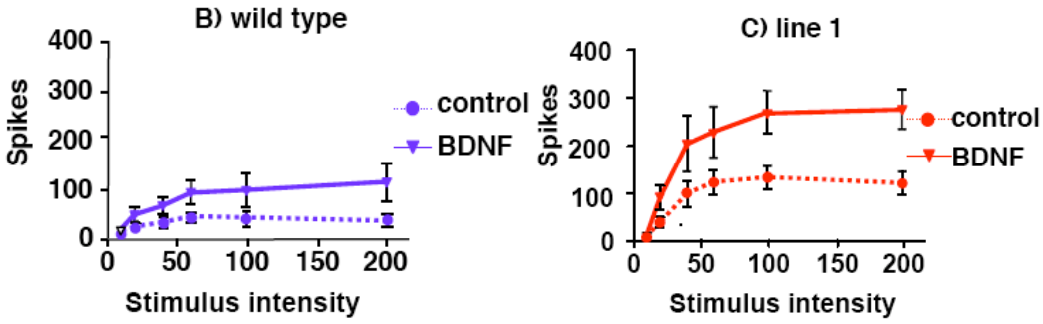

Figure 27. Electrophysiological analysis of the effect of BDNF on spinal sensitization. (A) Number of spikes elicited by A-fiber intensity stimulus before and after administration of a conditioning stimulus (arrow) consisting of 240 shocks (200 μA, 200 μs at 2 Hz). Wild type (n= 6) developed a significant increase (One-way ANOVA, Bonferroni post- test, P<0,01), whereas line 1 (n= 6) mice did not show any change. (B, C) Ventral root responses by graded stimuli before and after prolonged superfusion of exogenous BDNF in wild type (B, n= 5) and line 1 (C, n= 6) mice.

A.2.3. Modified signaling during inflammatory pain in daDREAM mice

ERK phosphorylation is the principal intracellular signaling pathway following trkB receptor activation. To study the activity of this kinase we quantified by Western Blot the level of phosphorylated ERK in wild type and transgenic mice in basal condition and during inflammatory pain (Fig. 28). To specifically analyze the activation of ERK due to BDNF we micro-dissected superficial laminae of the dorsal horn of the lumbar spinal cord, those containing secondary neurons that are directly innervated by nociceptive fibers and are the target of the BDNF secreted by primary afferents.

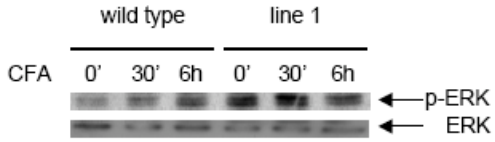

Figure 28. ERK phosphorylation in the dorsal horn neurons after intraplantar CFA injection. ERK phosphorylation was analyzed by Western Blot in the superficial laminae of the lumbar spinal cord in basal condition, 30 minutes and 6 hours after intraplantar injection of CFA.

In wild type mice, induction of ERK phosphorylation was detectable as early as 30 minutes after CFA injection and was maintained for all the six hours of the experiment (Fig. 28). In transgenic mice, by contrast, ERK phosphorylation was enhanced in resting conditions with respect to wild type mice and a mild and short-lasting induction of phospho-ERK could be observed 30 minutes after CFA (Fig. 28). Thus, in transgenic mice the increased basal level of phospho-ERK does not correlate with basal trkB receptor activation.

To understand the modified signaling in transgenic mice we considered an alternative pathway relating ERK activation in dorsal horn neurons and decreased GABAergic tone after administration of the GABAA receptor antagonist bicuculline (Baba et al., 2003). To explore the possibility of reduced basal GABAergic tone in daDREAM spinal cord, we quantified expression levels for the most important GABAA receptor subunits in the lumbar spinal cord from wild type and transgenic mice (Fig. 29)

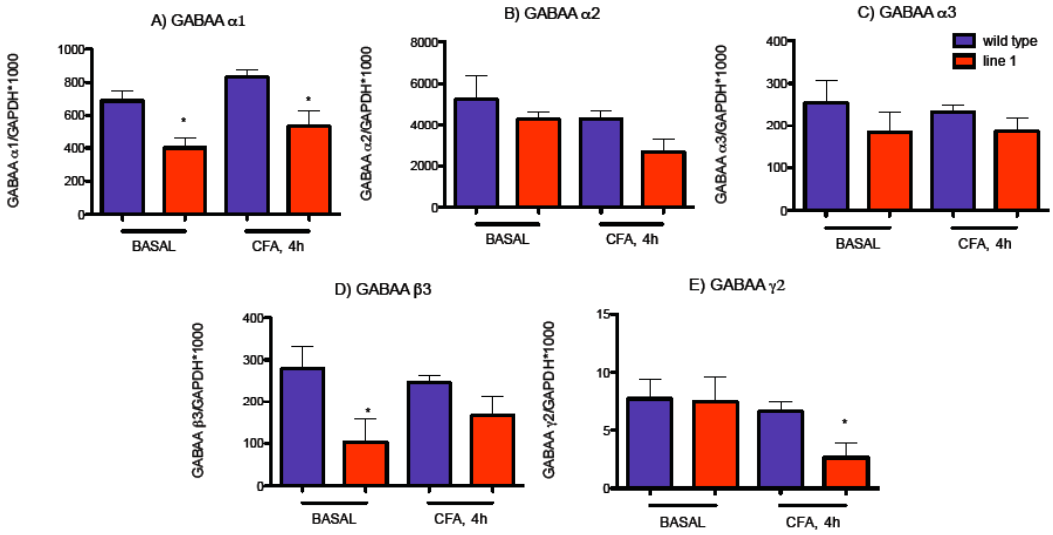

Figure 29. Q-PCR analysis of the expression of GABAA receptors in the spinal cord after CFA injection. GABAA α1 (A), GABAA α2 (B), GABAA α3 (C), GABAA β3 (D) and GABAA γ2 expression was quantified by Q-PCR in the spinal cord of wild type (n=8) and line 1 (n= 8) mice in basal condition and 6 hours after intraplantar CFA injection. * = wild type vs line 1. Values are normalized by the content of GAPDH.

We measured transcript levels of GABAA receptor subunits α1, α2, α3, β3 and γ2 in basal conditions and 4 hours after intraplantar injection of CFA. Importantly, basal expression of the α1 and β3 subunits was significantly reduced in transgenic spinal cord (Fig. 29 A, D). Inflammatory pain, however, did not modify the expression of the different GABAA subunits in wild type spinal cord and had a minor effect on the expression of the γ2 subunit in transgenic spinal cord (Fig. 29 E). Taken together, these results suggest that reduced basal GABAergic tone in transgenic mice might account for the loss of neuronal inhibition that is responsible for the rise in basal ERK phosphorylation and basal hyperalgesia. Nevertheless, expression of different GABAA receptor subunits was not modified during inflammatory pain indicating that alternative signaling may contribute to ERK phosphorylation and the establishment of central sensitization. To further confirm this possibility we quantified the level of ERK phosphorylation in wild type mice before and after systemic treatment with bicuculline via intraperitoneal injection (Fig. 30).

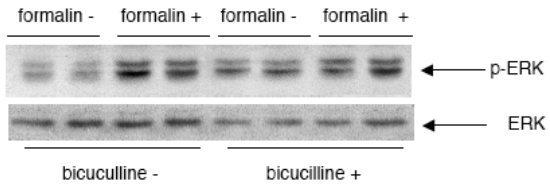

Figure 30. *In vivo* effect of bicuculline on ERK phosphorylation in dorsal horn neurons before and after formalin injection. Western blot of ERK phosphorylation in the superficial laminae of lumbar spinal cord in basal condition and 40 minutes after intraplantar 5% formalin injection. Wild type mice were pretreated with intraperitoneal bicuculline or with saline.

A.3. DREAM and the control of spinal response to neuropathic pain

To further characterize the role of DREAM in the molecular mechanisms that control nociception we studied the response of our transgenic mice after unilateral chronic constriction injury of the sciatic nerve (CCI) (Fig. 31). CCI is a common model of neuropathic pain that consists of a gentle constriction of the sciatic nerve by means of three loose ligatures tied around the nerve (Bennett and Xie, 1988). CCI is known to provoke a long lasting thermal hyperalgesia.

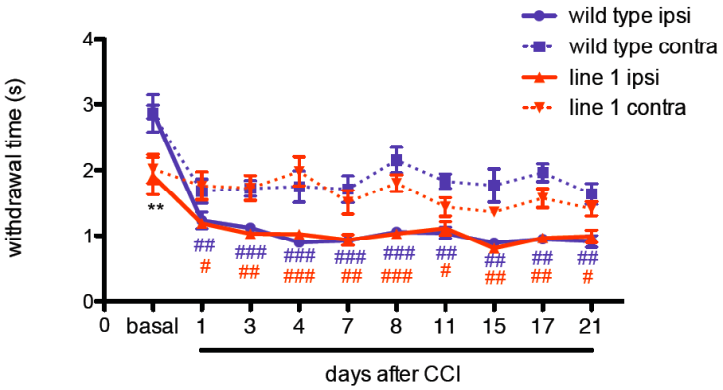

Figure 31. Thermal hyperalgesia after CCI. Thermal hyperalgesia was evaluated by plantar test at day 0 and different days after CCI in wild type (n=6) and line 1 (n= 6) mice in both the ipsilateral and contralateral paw. * = wild type vs line 1 (same day); # = wild type, ipsilateral vs contralateral; # = line 1, ipsilateral vs contralateral.

The analysis of nociceptive thresholds showed that both wild type and transgenic mice developed the same level of hyperalgesia starting from day 1 after surgery. The hyperalgesia of the ipsilateral paw was recorded throughout the 21 days of the experiment with no differences in paw withdrawal latency between wild type and transgenic mice (Fig. 31).

Thus, transgenic mice are not different from wild type mice in their response to neuropathic pain. These results agree with the normal response to neuropathic pain

displayed by mice carrying a conditional deletion of the BDNF gene in nociceptive neurons (Zhao et al., 2006).

Taken together these data suggest that the involvement of DREAM in the regulation of pain perception in neuropathic conditions is minor and much less relevant than its role in inflammatory pain. Our data support the notion that the molecular mechanisms governing these two chronic pain conditions are substantially different.

B. FUNCTIONAL ANALYSIS OF DREAM IN PAIN MECHANISMS IN THE TRIGEMINAL GANGLIA

Studies on the molecular mechanisms of pain perception have traditionally focused on the spinal cord/DRG level, while the trigeminal ganglion has received much less attention. Two reasons could explain this situation, i) there are few behavioral models to study nociception in the area innervated by this nerve (specially in mice) and ii) the difficulty to isolate the trigeminal nucleus, the area where the primary afferents fibers from the trigeminal nerve synapse with the second order neurons. This lack of basic knowledge is unfortunately reflected in the substantial lack of effective treatment for trigeminal pain.

B.1. Characterization of daDREAM transgenic lines for the study of trigeminal pain

B.1.1. Analysis of daDREAM expression levels.

Because of the intrinsic difficulties for the accurate dissection of the trigeminal nucleus, we limited our study to those primary afferent neurons, whose nuclei are grouped in the trigeminal ganglion.

As a first step for this part of the study we screened all transgenic lines available in the laboratory in order to characterize those that express the transgene in the trigeminal ganglion (Fig. 32).

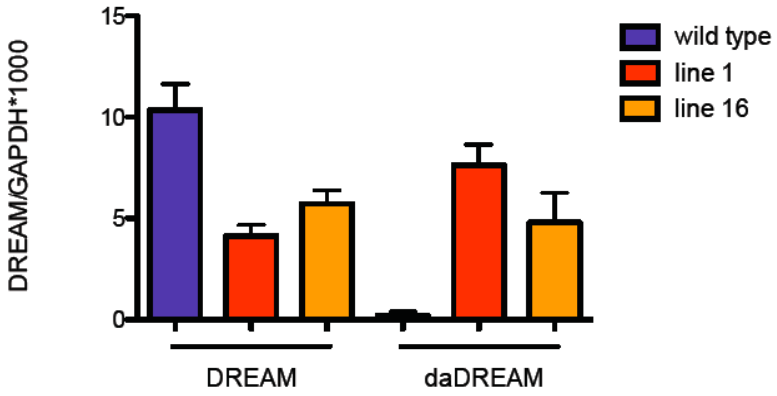

Figure 32. Q-PCR analysis of DREAM and daDREAM expression. DREAM and daDREAM expression was quantified by Q-PCR in the trigeminal ganglion of wild type (n= 10), line 1 (n= 10) and line 16 (n= 10) mice. Values are normalized by the content of GAPDH.

Two lines are positive for daDREAM expression in trigeminal neurons (Fig. 32), line 1, previously used for the spinal cord analysis and line 16 (L16). L16 mice expresses a dominant active DREAM form that in addition to the mutation in the three functional EF-hands and the N-terminal LCD is mutated also in the C-terminal LCD (Ledo et al., 2000b).

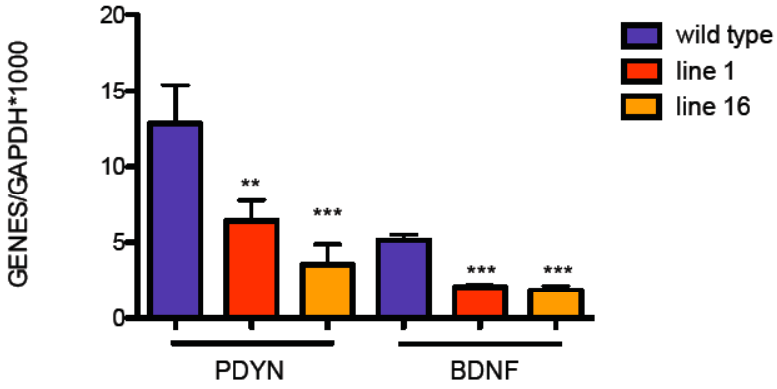

Figure 33 Q-PCR analysis of PDYN and BDNF expression. PDYN and BDNF expression was quantified by Q-PCR in the trigeminal ganglion of wild type (n= 10), line 1 (n= 10) and line 16 (n= 10) mice. Values are normalized by the content of GAPDH.

Importantly, expression of PDYN and BDNF, two *bona fide* target genes for DREAM, was clearly decreased compared to wild type mice in trigeminal neurons from transgenic lines expressing daDREAM (Fig. 33). These results confirmed the relevance of DREAM also in the trigeminal ganglion and validated the use of both lines for the study of trigeminal pain.

B.1.2. Analysis of trigeminal nociceptive thresholds in daDREAM mice

The trigeminal nerve innervates practically the whole facial area. Behavioral testing to assess a nociceptive phenotype in this area is particularly complicated because the stimulus should be applied and the reaction from the animal recorded without restrictions that could induce stress and bias the final output. These difficulties are even more severe when working with mice, due to their extreme susceptibility to stress in experimental conditions.

In this framework, we decided to test the mice using a modification of the formalin test, which involves minimum manipulation (Clavelou et al., 1989). Injection of 5-10 microlitres of 2% formalin in the snoot of the mouse results in a biphasic nociceptive response that is quantified by measuring the time the mice spend rubbing their face in blocks of 3 minutes over a total period of 30 minutes (Fig. 34).

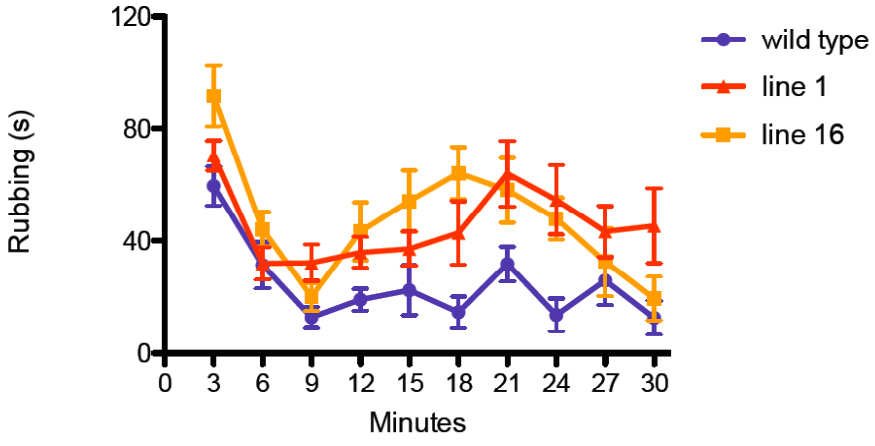

Figigure 34. Formalin test. Wild type (n= 8), line1 (n=8) and line 16 mice were tested for their rubbing response after injection of 2% formalin subcutaneously in the snoot. Transgenic mice showed a statistically significant increased in the nocifensive behavior (One-way ANOVA, Bonferroni post- test, P<0,01). The response was evaluated in blocks of 3 minutes for 30 minutes.

In the first phase of the formalin test (0 to 9 minutes) wild type and L1 mice showed a similar response to formalin. L16 transgenic mice, however, showed a statistically significant increase in the rubbing response (Fig. 34). In the second phase (9 to 30 minutes), we observed a mild response to 2% formalin in wild type mice, while both L1 and L16 displayed a strong secondary response suggesting a clear hyperalgesic phenotype in daDREAM mice (Fig. 34). If compared with the results after formalin injection in the paw (Fig. 11), where no significant differences were observed between wild type and transgenic mice, these results highlighted important differences in the

mechanisms related to pain perception between the trigeminal ganglion and the spinal cord/DRG system.

To further substantiate the role of DREAM in the response to nociceptive stimulation in the trigeminal ganglion we tested DREAM knockout mice in the formalin test. No difference between wild type and knockout mice was observed after 2% formalin injection (Fig. 35 A). To see if a stronger nociceptive stimulus could evoke a different response in these two genotypes we repeated the test using 4,5% formalin (Fig 35 B). Again, the response to 4,5% formalin was the same for wild type and knockout mice in the first phase of the test. In the second phase knockout mice showed a response that, though not statistically different, was constantly smaller than in wild type mice. (Fig. 35 B).

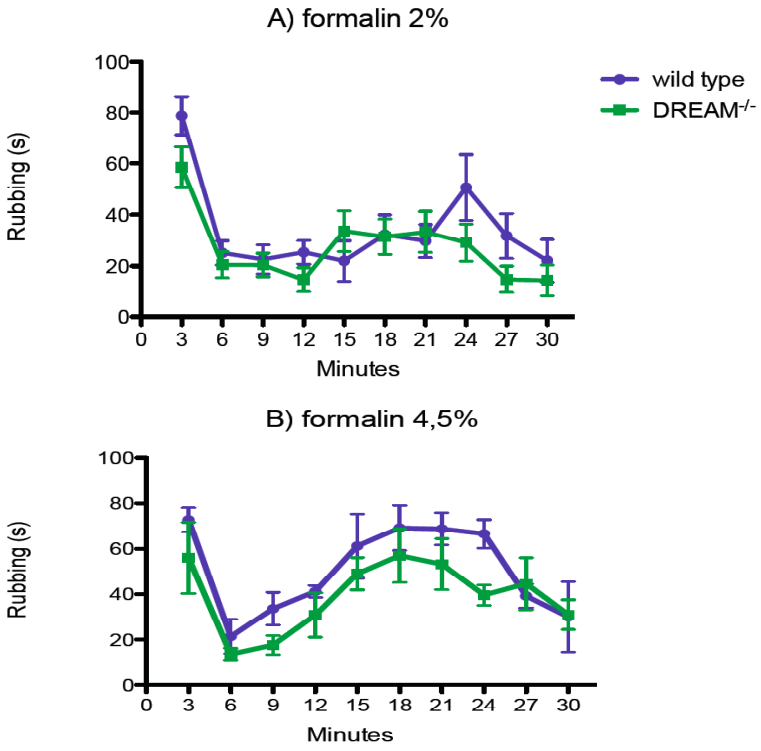

Figure 35. Formalin test. Wild type (n= 8) and DREAM knockout (n=8) mice were tested for their rubbing response after subcutaneous injection of 2% (A) or 4,5% formalin (B) in the snoot. The response was evaluated in block of 3 minutes for 30 minutes.

Analysis of the area under the curve showed that in the second phase of the formalin test the response in knockout mice was significantly smaller than in wild type mice, indicating a hypoalgesic phenotype.

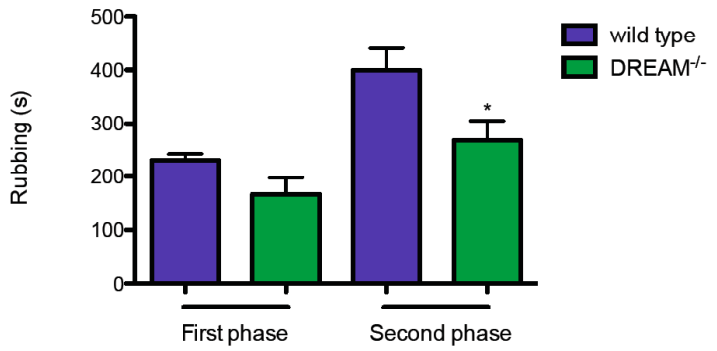

Figure 36. Total nocifensive response to formalin. The nocifensive response to 4,5% formalin was evaluated measuring the area under the curve in the first part (0 to 9 minutes) and in the second part (9 to 30 minutes) of the formalin test in wild type (n= 8) and DREAM knockout (n= 8) mice.

The area under the curve represents an evaluation of the intensity of all the secondary nociceptive responses, thus, this quantification is a tool that allows a more profound characterization of the response. With this analysis we showed that the total time the knockout mice spend rubbing their face during the secondary phase of the formalin test is lower with respect to wild type mice (Fig. 36). This hypoalgesic response of DREAM knockout mice is in agreement with the previously described general hypoalgesic phenotype of these mice (Cheng et al., 2002). Taken together these data suggest that DREAM is of importance in the mechanisms underlying nociception in the trigeminal ganglion.

Since BDNF expression is reduced in trigeminal daDREAM neurons, we next analyzed the behavioral response to formalin injection in the snoot in BDNF knockout mice (Fig. 37). To perform this experiment we used mice heterozygous for the BDNF deletion because the homozygous have strong developmental deficits and die soon after birth (MacQueen et al., 2001). Wild type littermates were used as controls for this experiment.

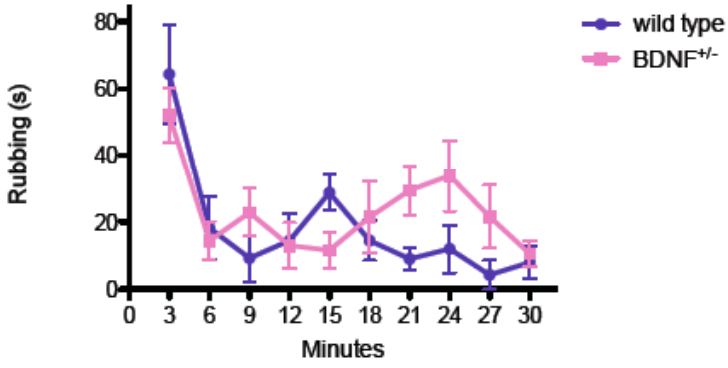

Figure 37. Formalin test. Wild type (n= 10) and BDNF$^{+/-}$ (n=11) mice were tested for their rubbing response after subcutaneous injection of 2% formalin in the snoot. The response was evaluated in block of 3 minutes for 30 minutes.

Wild type and BDNF$^{+/-}$ mice showed the same response in the first phase of the test (Fig. 37). BDNF$^{+/-}$ mice, however, showed a delayed and stronger response in the second phase on the formalin test (9 to 30 minutes). In order to quantify the magnitude of the response in the second phase of the test we calculate the area under the curve (Fig. 38) and found that the response of BDNF$^{+/-}$ mice was increased by 50%. Taken together these data indicate that like daDREAM mice, BDNF$^{+/-}$ mice show a hyperalgesic response to formalin injection in the snoot.

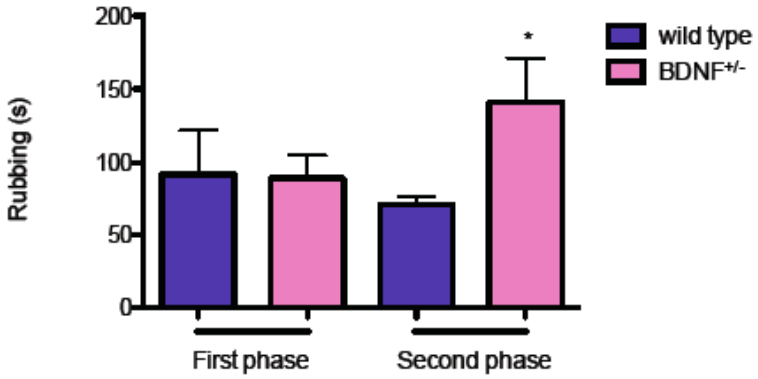

Figure 38. Total nocifensive response to formalin. The nocifensive response to formalin was evaluated measuring the area under the curve in the first phase (0 to 9 minutes) and in the second phase (9 to 30 minutes) of the formalin test in wild type (n= 10) and BDNF$^{+/-}$ (n= 11) mice.

B.1.3. Transcriptomic analysis of the basal trigeminal hyperalgesia in daDREAM mice

Due to a lack of literature on transcriptional responses of trigeminal neurons, we started our study with a genome-wide analysis of daDREAM trigeminal ganglia using the Affymetrix technology. This methodology permits a comprehensive analysis of genome-wide expression on a single microarray. It also includes internal controls to verify the efficiency of the hybridization, that allows the normalization of different data sets and permits an accurate comparison between different conditions.

Since this experiment was meant to define the basic guidelines for our study we compared the transcriptional profiles of wild type and line 16 trigeminal ganglia only in basal conditions in an attempt to isolate the changes imposed by the expression of the dominant active DREAM mutant. The use of only one transgenic line for the transcriptomic analysis was imposed by budget restrictions. The choice of line 16 was

based on two main reasons, i) it showed a stronger hyperalgesic phenotype in the formalin test (see above) and ii) it had a more restricted pattern of transgene expression in the trigeminal ganglion and no expression at the DRG/spinal cord level.

To compare the expression profile of wild type and line 16 mice we carried out seven independent microarray hybridizations, 4 with wild type and 3 with transgenic mice. Each microarray was hybridized with a pool of RNA extracted from the trigeminal ganglions of three different mice. The raw data from these seven hybridizations were grouped and averaged in order to obtain a matrix that described the final results of the analysis.

Results from the hybridizations were considered significant only if they conformed to the following criteria:

Fold change > 1.5 for upregulated gene and < -1.5 for downregualted genes

P value (LIMMA test) < 0,05

FDR value (LIMMA test) < 0,1

A total of 296 downregulated and 295 upregulated genes (see Supplementary data) showed modified expression in L16 respect to wild type trigeminal neurons. To better understand the relevance of these changes we made a functional analysis using Gene Ontology. This protocol categorize the genes of the sub-list in clusters on the basis of three different criteria; cellular compartment, biological processes and molecular function.

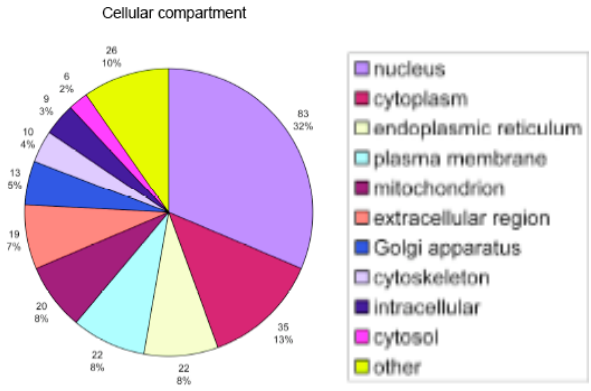

Figure 39. Cellular compartment clustering. Clustering of the genes whose expression is altered il line 16 mice following the Gene Ontology paradigm according to cellular compartment.

According to the first criteria, cellular compartment, a majority of the genes in the sub-list have a nuclear localization (32%) and includes DNA binding proteins, nuclear kinases and a large group of histone-related proteins (Fig. 39).

According to the second criteria, biological processes, genes involved in transcription were the most represented among those influenced by daDREAM expression (19%), while proteins associated with a transport function, including different members of the solute carrier super-family of proteins, constituted the second group in this classification (14%). Proteins involved in metabolic processes and in ion transport were also enriched in the sub-list (Fig. 40).

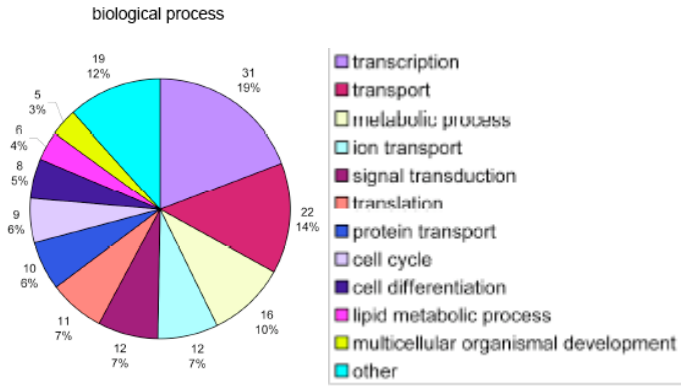

Figure 40. Biological processes clustering. Clustering of the genes whose expression is altered in line 16 mice following the Gene Ontology paradigm according to biological processes.

Finally, clustering of genes with modified expression in daDREAM trigeminal ganglia on the basis of their molecular function highlighted that the vast majority of genes has binding activity, the first three groups of this clustering are in fact involved in protein binding, ion binding and DNA binding (Fig. 41)

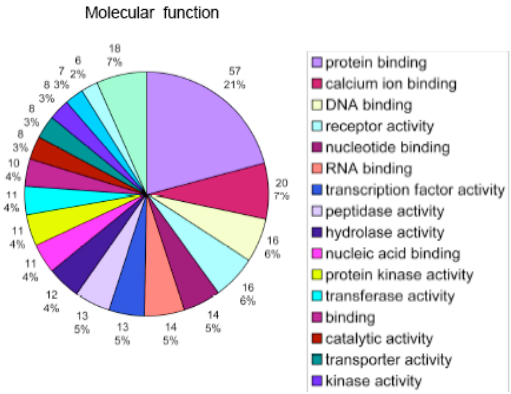

Figure 41. Molecular function clustering. Clustering of the genes whose expression is altered il line 16 mice following the Gene Ontology paradigm according to molecular function.

Overall, the Gene Ontology analysis gave us general guidelines of processes and functions that could be altered in L16 trigeminal neurons. To obtain a more clear idea of the meaning of these changes in terms of a role for DREAM controlling pain mechanisms at the trigeminal level, we searched for direct transcriptional targets for DREAM repression that could mediate the function of DREAM.

We identified 3 genes of potential interest. The shortlist of candidate genes includes; the lipase MGLL, the protease CTSL and DBNDD2, a protein with a dysbindin motif. We then validated the modification of these genes by quantitative real-time PCR and confirmed that indeed they were downregulated in daDREAM trigeminal ganglia (Fig. 42).

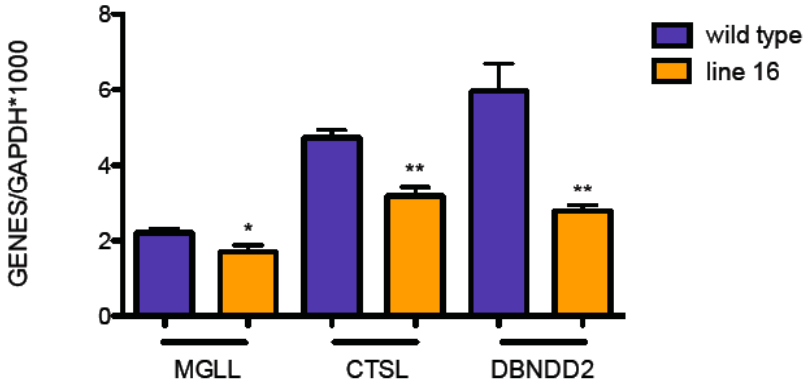

Figure 42. Q-PCR analysis of expression of MGLL CTSL and DBNND2. Alteration in expression level of MGLL CTSL and DBNND2, found in the microarray, was validated by Q-PCR in the trigeminal ganglion of wild type (n= 12), and line 16 (n= 12) mice. Values are normalized by the content of GAPDH.

Moreover, we analyzed the expression level of two other genes of possible interest in the study of the role of DREAM in the control of trigeminal pain. The synaptic vesicle protein SV2c, a recently described drug target in the treatment of trigeminal neuralgia, and DTNBP1, a member of the dysbindin protein family, closely related to DBNDD2, which is involved in nociception. Validation of their reduced expression in daDREAM trigeminal ganglia is shown in Fig. 43.

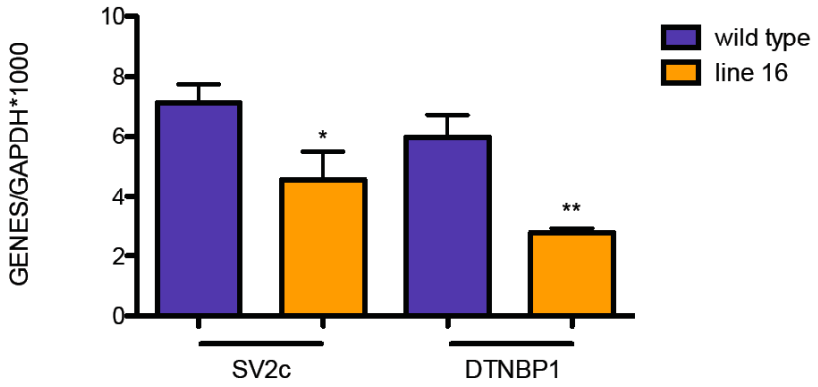

Figure 43. Q-PCR analysis of SV2c, and DTNPB1 expression. Expression level of SV2c and DTNBP1 was measured by Q-PCR in the trigeminal ganglion of wild type (n= 12), and line 16 (n= 12) mice. Values are normalized by the content of GAPDH.

B.2. DREAM and the trigeminal response to inflammatory pain

To further characterize the importance of DREAM in the mechanisms of trigeminal pain, we studied the transcriptional response to inflammatory pain following bilateral injection of CFA into the snoot.

First, we measured transcriptional changes in endogenous DREAM, PDYN and BDNF expression following inflammation.

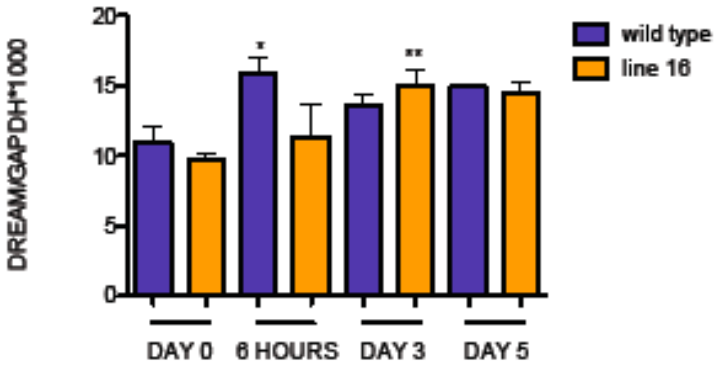

Figure 44. Q-PCR analysis of DREAM expression in trigeminal ganglion after CFA injection. Endogenous DREAM expression was quantified by Q-PCR in the trigeminal ganglion of wild type (n=8) and line 16 (n= 8) mice at day 0 and 6 hours, 3 and 5 days after subcutaneous injection of CFA in the snoot. * = wild type vs line 16 (same day); # = basal vs treated (same line). Values are normalized by the content of GAPDH.

In wild type mice, CFA injection produced a rapid and transient increase in endogenous DREAM mRNA, which was significant only at 6 hours after CFA (Fig. 44). In transgenic mice, however, the peak of expression of endogenous DREAM was delayed and showed statistical significance only 3 days after the treatment (Fig. 44).

Contrary to the effect observed in the SC/DRG, expression of PDYN and BDNF was strongly decreased in wild type mice after CFA (Fig 45 A, B). Expression levels of BDNF returned to basal at day 5 after the injection, while PDYN expression remained decreased all through the time course of the experiment (Fig. 45 A, B). In transgenic mice, PDYN expression was not further reduced after CFA, while BDNF levels were rapidly and transiently downregulated and returned to its basal level already at day 3 after CFA (Fig. 45 A, B).

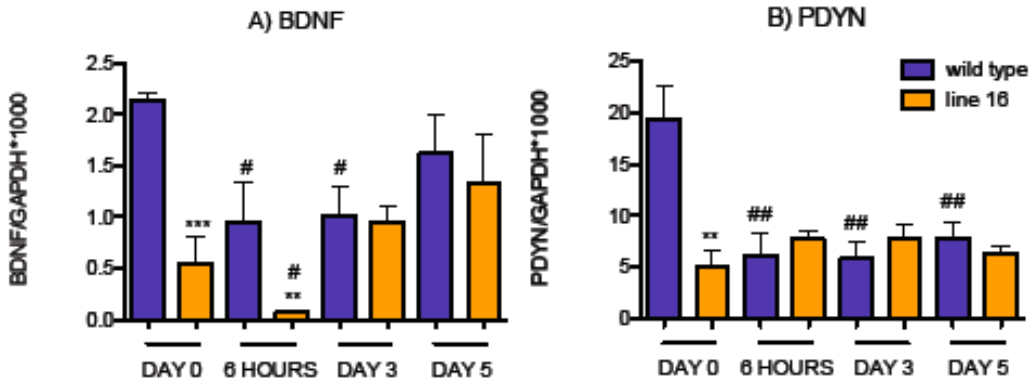

Figure 45. Q-PCR analysis of BDNF and PDYN expression in the trigeminal ganglion after CFA injection. BDNF (A) and PDYN (B) expression was quantified by Q-PCR in the trigeminal ganglion of wild type (n=8) and line 16 (n= 8) mice at day 0 and 6 hours, 3 and 5 days after subcutaneous injection of CFA in the snoot. * = wild type vs line 16 (same day); # = basal vs treated (same line). Values are normalized by the content of GAPDH.

Next, we studied the changes in the opioid system following inflammation (Fig. 46).

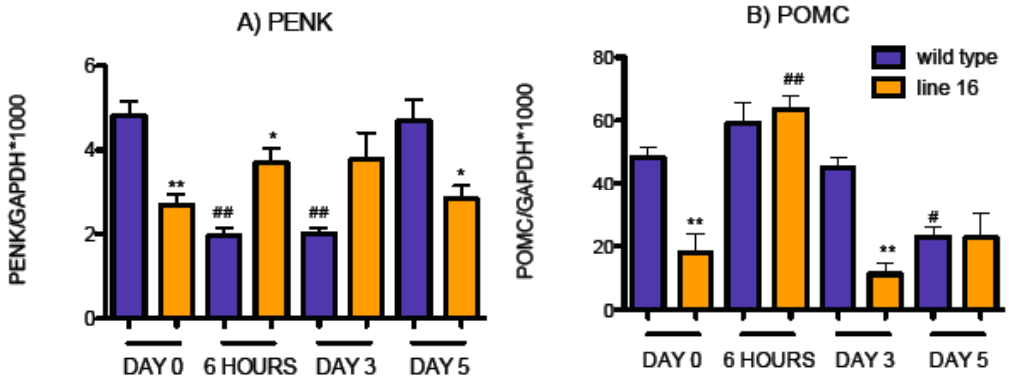

Figure 46. Q-PCR analysis of the expression of polypeptidic opioid precursors in the trigeminal ganglion after CFA injection. PENK (A), POMC (B) expression was quantified by Q-PCR in the trigeminal ganglion of wild type (n=8) and line 16 (n= 8) mice at day 0 and 6 hours, 3 and 5 days after subcutaneous injection of CFA in the snoot. * = wild type vs line 1 (same day); # = basal vs treated (same line). Values are normalized by the content of GAPDH.

Importantly, basal expression levels of opioid precursors were downregulated in line 16 mice, resembling the situation described at the spinal cord and DRG level (Fig. 46). After CFA injection, PENK expression was rapidly reduced and returned to basal 5 days after

the treatment in wild type, while no change was observed in line 16 mice (Fig. 46 A). Expression of POMC was also reduced in response to inflammatory pain. This downregulation is not as rapid as in the case of PENK and it was significant only at 5 days after CFA injection. Curiously, line 16 mice showed an early induction in POMC expression at 6 hours, followed by a reduction at day 3 after the treatment (Fig. 46 B).

PNOC expression in the trigeminal ganglion was below the detection limit.

The basal expression of opioid receptors MOR and DOR was reduced in line 16 mice, while the amount of mRNA for KOR and ORL was not modified (Fig. 47). In summary, as showed in spinal cord and DRG, the basal opioid tone is reduced in transgenic trigeminal ganglion. Following inflammation, MOR expression was not changed in either genotype (Fig. 47 A), DOR levels were reduced at 3 days after CFA injection in wild type but not in line 16 mice (Fig 47 B), KOR expression rapidly increased at 6 hours, stayed high at 3 days and returned to basal at 5 days after CFA in wild type and was not modified at any time in line 16 mice (Fig. 47 C) and ORL levels were rapidly and stably increased after CFA injection in wild type mice but were initially reduced in line 16 to be later increased at 3 and 5 days after CFA (Fig. 47 D).

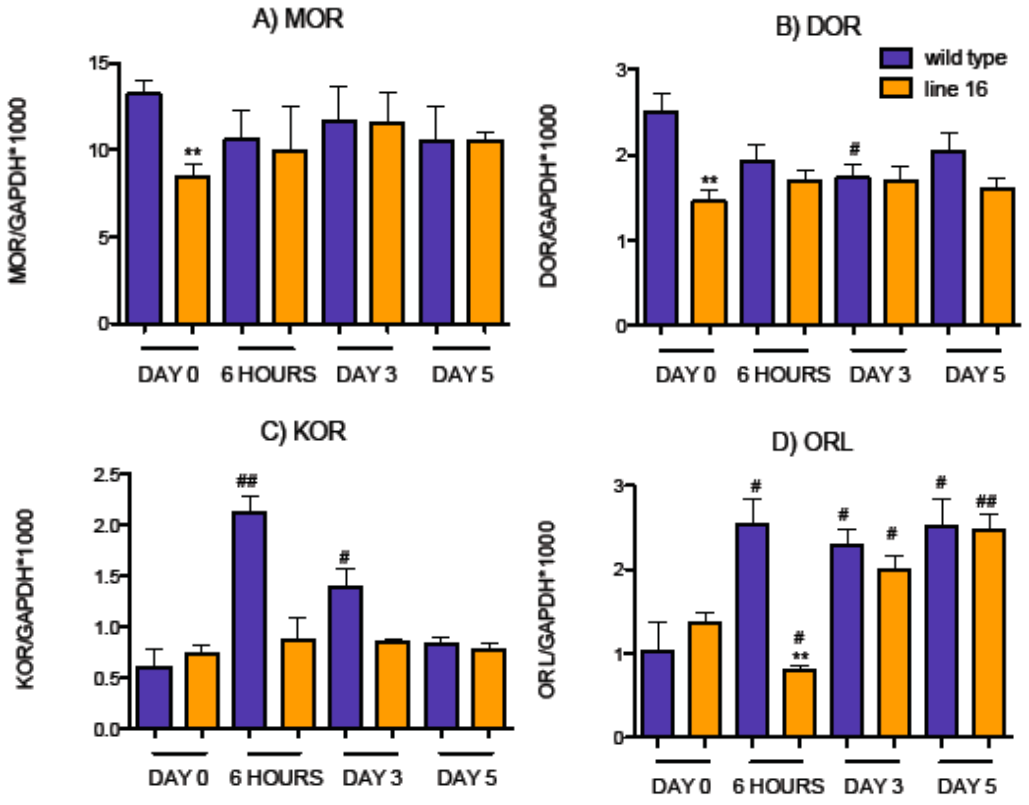

Figure 47. Q-PCR analysis of opioid receptors expression in the trigeminal ganglion after CFA injection. MOR (A), DOR (B), KOR (C) and ORL (D) expression was quantified by Q-PCR

in the trigeminal ganglion of wild type (n=8) and line 16 (n= 8) mice at day 0 and 6 hours, 3 and 5 days after subcutaneous injection of CFA in the snoot. * = wild type vs line 1 (same day); # = basal vs treated (same line). Values are normalized by the content of GAPDH.

Finally we studied the transcriptional response of DREAM target genes identified in the transcriptomic analysis.

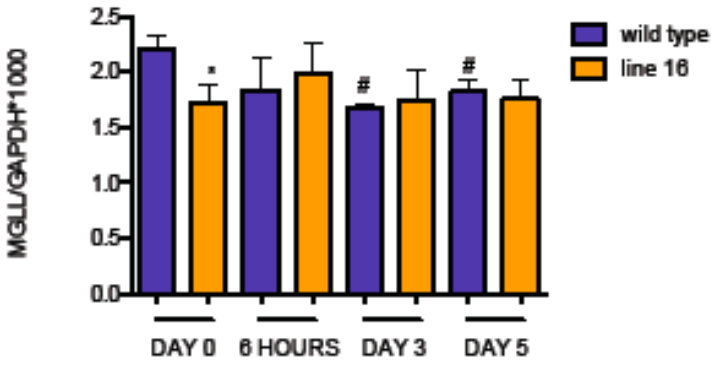

Figure 48. Q-PCR analysis of MGLL expression in the trigeminal ganglion after CFA injection. MGLL expression was quantified by Q-PCR in the trigeminal ganglion of wild type (n=8) and line 16 (n= 8) mice at day 0 and 6 hours, 3 and 5 days after subcutaneous injection of CFA in the snoot. * = wild type vs line 1 (same day); # = basal vs treated (same line). Values are normalized by the content of GAPDH.

MGLL and CTSL expression was reduced at 3 and 5 days after CFA in wild type but was not modified in L16 mice (Fig. 48).

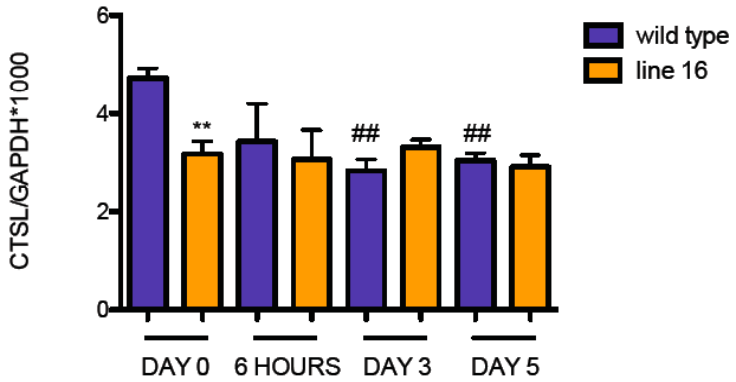

Figure 49. Q-PCR analysis of CTSL expression in the trigeminal ganglion after CFA injection. CTSL expression was quantified by Q-PCR in the trigeminal ganglion of wild type (n=8) and line 16 (n= 8) mice at day 0 and 6 hours, 3 and 5 days after subcutaneous injection of CFA in the snoot. * = wild type vs line 1 (same day); # = basal vs treated (same line). Values are normalized by the content of GAPDH.

The expression level for DBNDD2 was not affected by inflammation produced by CFA injection in wild type or transgenic mice (Fig. 51).

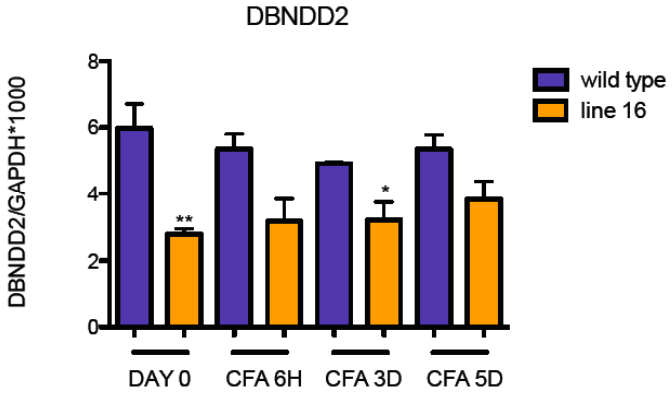

Figure 50. Q-PCR analysis of DBNDD2 expression in the trigeminal ganglion after CFA injection. DBNDD2 expression was quantified by Q-PCR in the trigeminal ganglion of wild type (n=8) and line 16 (n= 8) mice at day 0 and 6 hours, 3 and 5 days after subcutaneous injection of CFA in the snoot. * = wild type vs line 1 (same day); # = basal vs treated (same line). Values are normalized by the content of GAPDH.

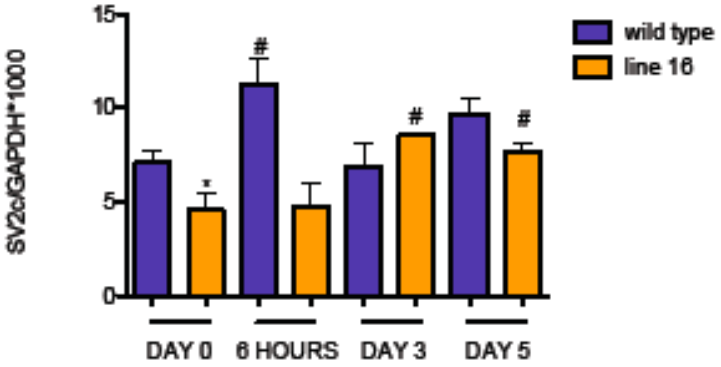

Figure 51. Q-PCR analysis of SV2c expression in the trigeminal ganglion after CFA injection. SV2c expression was quantified by Q-PCR in the trigeminal ganglion of wild type (n=8) and line 16 (n= 8) mice at day 0 and 6 hours, 3 and 5 days after subcutaneous injection of CFA in the snoot. * = wild type vs line 1 (same day); # = basal vs treated (same line). Values are normalized by the content of GAPDH.

In wild type mice SV2c transcription was rapidly and transiently upregulated after CFA injection. The induction peaked at 6 hours and was not present 3 and 5 days after the treatment. In L16 mice, however, SV2c induction was delayed, peaked at 3 days and stays elevated up to 5 days after CFA (Fig. 51)

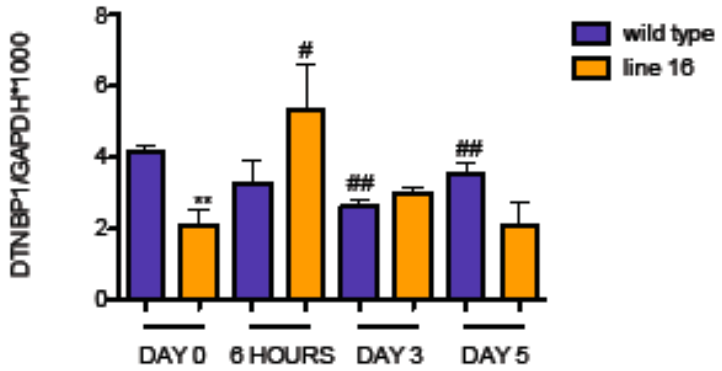

Figure 52. Q-PCR analysis of DTNBP1 expression in the trigeminal ganglion after CFA injection. DBNDD2 expression was quantified by Q-PCR in the trigeminal ganglion of wild type (n=8) and line 16 (n= 8) mice at day 0 and 6 hours, 3 and 5 days after subcutaneous injection of CFA in the snoot. * = wild type vs line 1 (same day); # = basal vs treated (same line). Values are normalized by the content of GAPDH.

In wild type mice the level of expression for DTNBP1 was reduced 3 and 5 days after CFA injection. In line 16 mice, instead, there was an early and transient induction with a peak at 6 hours after CFA (Fig. 52).

DISCUSSION

DISCUSSION

Pain is the alert alarm that our CNS developed to ensure the safety of our body, warning us from possible dangers and focusing our attention to protect the injured area. As important as pain itself, the tonic control of pain is fundamental; the neuronal plasticity that allows the fine-tuning of the intensity of pain perception and that permits the adaptation to different situations and environments. This is the result of the coordinated action of different molecular and cellular mechanisms in the central and peripheral nervous system. The study of this complex network of interactions could ensure a better understanding of this process and could possibly provide the opportunity for improved control of pain perception.

In the field of pain studies, animal models are of capital importance in our effort to picture the mechanisms of nociception in humans. Until the mid nineties the rat was the preferred species for the study of pain. Thanks to the development of technologies for genetic manipulation, however, mice are nowadays the species of choice, as reflected by the 400% growth in studies using mice over the last 15 years (Mogil, 2009).

DREAM was first described as a transcriptional factor controlling the expression of the prodynorphin gene (Carrion et al., 1999) and several studies using DREAM null mice have confirmed the importance of this protein in the control of pain perception showing a hypoalgesic phenotype in DREAM$^{-/-}$ mice (Cheng et al., 2002; Lilliehook et al., 2003).

Here we studied the importance of DREAM in the control of pain perception *in vivo* using a transgenic mouse model that over-expresses a dominant active mutant of DREAM (daDREAM) in pain-related neurons in the spinal cord, DRG and trigeminal ganglia (line 1) or only in the trigeminal neurons (line 16). As previously shown in cerebellar neurons (Gomez-Villafuertes et al., 2005) and in T cells (Savignac et al., 2005), the daDREAM mutant should function in transgenic sensory neurons as a constitutive repressor insensitive to Ca^{2+} and unable to interact with CREB, thus leaving CRE-dependent transcription without the tonic inhibitory control of DREAM.

1. DREAM and the control of nociception in the spinal cord and DRG

DREAM represses transcription binding at specific sites in the DNA as a heterotetramer, and previous studies from our laboratory have shown that expression of daDREAM has a

cross-dominant effect and blocks the function of endogenous KChIP proteins when present in a ratio as low as 1/6 (Savignac et al., 2005). In our transgenic mice the ratio of daDREAM/DREAM mRNA is 1,8 and 6 in the spinal cord and DRG, respectively. This indicates that the expression of the dominant active mutant protein is sufficient to block Ca^{2+} and cAMP dependent derepression by endogenous DREAM/KChIP proteins.

1.1. DREAM and the control of basal pain perception

When tested for a nociceptive phenotype line 1 mice showed a clear hyperalgesia with reduced latencies for thermal sensitivity and greater responses to visceral pain. The responsiveness to mechanical stimulation on the other hand is not altered in our transgenic mice. A phenotype of hyperalgesia in daDREAM mice is in agreement with the hypoalgesia reported in DREAM knockout mice (Cheng et al., 2002) and supports the involvement of transcriptional repressor DREAM in pain modulation.

Since DREAM binds to the promoter of prodynorphin and represses the expression of this gene, an initial and plausible mechanism that could explain its effect on nociception was through the control of endogenous levels of dynorphin peptides. In this work we went one step further and analyzed the expression levels for the different members of the opioid system in the spinal cord and in the DRG of our transgenic mice.

The opioid system is a deeply interrelated network in which secreted peptides interact with multiple receptors to orchestrate a complex set of functions. This strong interplay is shared by the polypeptidic precursors PDYN, PENK and POMC acting on μ, δ and κ opioid receptors. All the opioid peptides arising from these precursors share a common N-terminal motif and all the receptors show a high degree of homology (up to almost 90% in intracellular loops). The ORL receptor on the other hand is peculiar in this scenario, showing no binding affinity for conventional opioid ligands and binds proteolytic products of the PNOC precursor. PNOC has a slightly different N-terminal region from that of the other opioid precursors. The ORL receptor/PNOC system could be considered as a separated system with some sequence identity to the other opioid genes.

In the spinal cord we observed a general repression of the mRNA for polypeptidic opioid precursors as well as for their receptors. We encountered a similar situation in the DRG with the only, but notable, exception of prodynorphin expression that was not downregulated in the DRG of DREAM transgenic mice. Currently, we do not have an explanation for this paradoxical result in the DRG, however, absence of DREAM in the hippocampus of DREAM null mice does not change prodynorphin peptides at this level, but produces a significant increase in dynorphin expression in the spinal cord (Cheng et

al., 2002). Moreover, it has been described that the expression of PDYN gene is controlled by different regulatory elements in its promoter sequence (Naranjo et al., 1991) including four CRE sites, an AP-1 site and the DRE site. Then, one possibility is that, in the DRG, the specific weight of one or several of these other regulatory elements is predominant in controlling the expression of the prodynorphin gene. Nevertheless we observed an overall decrease in the opioid tone in our transgenic mice.

The promoter region of the different opioid receptors had been described and the transcription start site identified (Min et al., 1994; Augustin et al., 1995; Liu et al., 1995; Pan et al., 1996). Interestingly, μ, δ and κ opioid receptor are TATA-less genes, while the ORL receptor, the more distant member of the family, has a TATA box at position -78. Using *in silico* analysis we found DRE sites that are located downstream from the transcriptional start in close proximity to the ATG in these genes. Contrary, all the promoters for polypeptidic precursors for endogenous opioid peptides have a defined TATA box (Kilpatrick et al., 1990; Lamonerie et al., 1996; Mollereau et al., 1996). *In silico* analysis of these promoter regions highlighted the presence of multiple DRE sites. In this work, we did not study the functionality of each one of these regulatory elements but sequence predictions identified them as *bona fide* sites for DREAM binding. As a representative example, the 5' untranslated region of the κ opioid receptor gene, shown in figure 53, contains up to four consensus DRE sites. Of them, three are grouped in tandem, a conformation that confers the most favorable chance to be functionally relevant.

Figure 53. Proximal promoter of the κ opioid receptor. *Bona fide* sites for DREAM binding are indicated (in blue), as well as two alternative transcription start sites (in green), three SP1 binding sites (in red) and the ATG (in orange).

In addition, it has been shown that the repression of some elements of the opioid network triggers the downregulation of the others. Thus, knockout mice for the δ opioid receptor

showed reduced expression of μ opioid receptor (Kitchen et al., 1997) and the contrary is also true (Slowe et al., 1999). Accordingly, direct repression by DREAM of some opioid promoters could produce an unbalanced situation leading to an indirect effect on the expression of other opioid genes. The lack or the poor repressor effect of daDREAM expression on the levels of the most distantly related members of the opioid network, i.e. PNOC and its receptor, could contribute to support this indirect mechanism. In summary, our results suggest that the downregulation of the opioid system could account for the basal state of hyperalgesia observed by the lower withdrawal thresholds to thermal stimuli and the prolonged responses to visceral pain.

Alternatively or in addition to the involvement of the opioid system in basal hyperalgesia, published studies from other laboratories have suggested that changes in the transient A-type potassium current, mediated by Kv4 channels, could also be responsible for hypersensitivity to acute pain stimuli, i) genetic ablation of the Kv4.2 channel that reduces A-type potassium currents increases excitability of dorsal horn neurons and enhances sensitivity to noxious stimuli (Hu et al., 2006), ii) genetic ablation of Kv4 channels results in decreased expression of DREAM/KChIP proteins (Menegola and Trimmer, 2006), suggesting a genetic regulatory loop between this two gene families. Our results, however, do not support this idea, since A-type currents in dorsal horn neurons from line 1 mice were undistinguishable from those of wild type mice in terms of their electrophysiological properties.

1.2. DREAM and the response to inflammatory pain

Modified nociceptive response in transgenic mice is not only restricted to basal nociceptive thresholds in daDREAM mice but is also observed as an impairment of the hyperalgesic response to the inflammatory pain induced by CFA. Given the profound effect of the transgene expression on the basal transcription of the different members of the opioid system we speculated that daDREAM could also influence the transcriptional response of these genes to inflammatory pain

In the spinal cord of wild type mice only prodynorphin expression is increased in response to inflammation. Contrary, in line 1 mice, CFA induced a general increase in transcription for all members of the opioid system. For DOR and KOR, this increase reversed the downregulation that we measured in basal condition. For PDYN, PENK, and MOR it resulted in an increase with respect to the basal level of transcription for these genes in line 1 mice. Considering these experiments it may be possible that the ongoing inflammation could induce the transcription of the opioid system in line 1 mice in order

to revert the effect of the daDREAM mutant as a constitutive repressor. This increase in transcription would adjust the opioid tone in transgenic mice making it similar as in wild type mice.

In transgenic mice the response of the PNOC/ORL receptor system to the ongoing inflammation is completely blocked by the expression of daDREAM. This result confirms the specificity in the regulation of these two members of the opioid system and indicates a major effect of dominant mutant DREAM on their transcription.

In DRG of wild type mice we observed a tendency to a mild decrease in the overall opioid tone with reductions in MOR, DOR and PENK mRNAs and no change in PDYN after CFA. These results are in line with previous data (Obara et al., 2009) that reported little response in the opioid system in the DRG after CFA.

The response of the opioid system in daDREAM expressing mice is more complex. In this case there is an upregulation of the transcription for PDYN, MOR and KOR, DOR is not affected and PENK is downregulated by CFA.

In wild type DRG, the PNOC/ORL system is strongly affected by the treatment with CFA, with a downregulation of the polypeptidic precursor and an upregulation of the receptor. In transgenic mice it seems again that the expression of the daDREAM mutant completely blocks all the changes in the transcription of these two genes.

1.3. DREAM and the central sensitization; the role of BDNF

DREAM transgenic mice showed a tendency to have a smaller secondary response to formalin, as well as a reduced long-standing hyperalgesia during inflammatory pain conditions. Both delayed responses rely on the correct functioning of the central sensitization process, a plastic reaction of the CNS that like the wind-up phenomena has been associated to endogenous BDNF levels (Heppenstall and Lewin, 2001). Since previous in vitro studies from our laboratory showed the regulatory effect of DREAM on BDNF promoter activity (Mellstrom et al., 2004), it was important to analyze BDNF expression in the spinal cord and DRG in line 1 mice in order to understand the abnormal central sensitization process in these mice.

BDNF is expressed in DRG neurons and anterogradely transported to the synaptic terminals that are in contact with the dorsal horn neurons in the spinal cord (Merighi et al., 2004). In the spinal cord, BDNF is secreted in response to sustained activation of peripheral nociceptors and once released BDNF induces a potentiation of the synaptic strength (Pezet and McMahon, 2006).

Our results showed a significant downregulation of BDNF expression *in vivo* both in the spinal cord and in the DRG in line 1 mice. Interestingly, the decreased BDNF production is not counterbalanced by a compensatory upregulation of the transcription of its specific receptor trkB in these two areas. Furthermore, we showed that in response to intraplantar injection of CFA, BDNF levels increased in the DRG and in the spinal cord from wild type mice but not in daDREAM mice, indicating that the transgene is repressing both basal and induced BDNF expression in vivo. Electrophysiology experiments, measuring the long term enhancement of DR-VRRs after low frequency stimulation of primary C-fibers, an in vitro model to simulate central sensitization, confirmed the notion that spinal cord from transgenic mice does not receive enough BDNF from primary afferents. Thus, the decrease of BDNF signaling in the dorsal horn neurons of line 1 mice could be associated with the inability of our transgenic mice to develop long term synaptic plasticity.

Next, we focused on the cascade downstream the activation of trkB receptor. For this reason we studied ERK kinase activity in dorsal horn neurons in basal condition and in response to intraplantar CFA. Complete Freund's adjuvant is known to induce ERK activation in a BDNF-dependent way (Obata et al., 2004). In our transgenic mice basal ERK phosphorylation was higher than in wild type mice and its induction after CFA was less pronounced and of shorter duration. This result is in line with the hypothesis that the inability of line 1 mice to develop full hyperalgesic response to peripheral inflammation and central sensitization may be related to deficient BDNF input in the spinal cord from primary afferents.

Increased basal ERK phosphorylation in line 1 mice could be related to decreased GABAergic tone in neurons since treatment with bicuculline, a GABAA receptor antagonist, results in loss of inhibition in dorsal horn neurons and induces ERK phosphorylation (Baba et al., 2003). Q-PCR analysis of the main GABAA receptor subunits showed a downregulation of GABAA $\alpha 1$ and $\beta 3$ in spinal cord from DREAM transgenic mice supporting the idea that reduced GABAergic tone is directly responsible for the increased basal ERK phosphorylation in line 1 mice.

1.4. DREAM and the response to neuropathic pain

We completed the analysis of the functional role of DREAM on pain perception in the spinal cord/DRG system studying the behavioral response of our transgenic mice to neuropathic pain in a well-established model, the chronic constriction injury (CCI) of the sciatic nerve. As described, CCI induced a potent and long-lasting hyperalgesia that

persisted for all the 21 days of the experiment. Importantly, both wild type and transgenic mice developed a similar strong thermal hyperalgesia in the ipsilateral paw starting from day 1 after the surgery. Thus, contrary to the results in the CFA model of inflammatory pain, transgenic mice did neither show a delay in the development of thermal hyperalgesia, nor weaker hyperalgesia and faster recovery.

Taken together, our results clearly support the idea that molecular mechanisms controlling inflammatory and neuropathic pain are very different, especially in terms of the functional involvement of DREAM.

It is interesting to speculate about how the changes in the basal opioid tone of daDREAM expressing mice do not have repercussion on the behavioral response to neuropathic pain. Nerve injury results in a strong decrease in mRNA for the opioid receptors and for all the polypeptidic precursors, with the exception of prodynorphin (Draisci et al., 1991; Obara et al., 2009). As a matter of fact, this downregulation could possibly account for the reduced effectiveness of locally administrated opioids in neuropathy (Rashid et al., 2004). It is possible that, following CCI, the opioid tone is decreased to the same level in both wild type and line 1 mice compensating the downregulation that we observed in basal conditions. In this scenario the lack of differences in the behavioral response to CCI could be explained by the fact that, after the surgery, both wild type and transgenic mice show the same opioid tone.

2. The effect of DREAM on trigeminal pain

In the second part of this work we studied the role of DREAM in the nociceptive processes controlled by neurons of the trigeminal ganglia. We began our study by characterizing daDREAM expression in the trigeminal ganglion in two different lines, the above described line 1 and line 16, that showed a daDREAM/DREAM ratio of 0,71 to 1 and 1 to 1,1 respectively, and a clear downregulation of PDYN and BDNF mRNAs, showing the *in vivo* functionality of the dominant active mutant in this area. As a consequence, we were able to observe that transgenic mice had a obvious hyperalgesic response to the application of formalin in the snoot, supporting the hypothesis that DREAM participates in the control of pain processing also in the trigeminal ganglion. This hypothesis was further sustained by the reduced nocifensive response of DREAM knockout mice in this same test.

In molecular terms, the trigeminal hyperalgesic phenotype in daDREAM mice could underlie a situation similar to the one we observed at the spinal cord/DRG level where we characterized a downregulation for genes important for nociception. In basal

conditions we measured a reduction of the overall opioid tone in the trigeminal ganglion from transgenic mice, with the only exception of the PNOC/ORL receptor system and of KOR expression. This decrease in the opioid tone is less marked than the one observed in the spinal cord or in the DRG but could still be related to trigeminal hyperalgesia in transgenic mice. Moreover, we observed a strong downregulation of the BDNF gene in both transgenic lines. This situation resembles the scenario in the spinal cord/DRG and could also correlate with the hyperalgesic response to formalin. Interestingly, $BDNF^{+/-}$ mice also showed increased nocifensive response, notably during the last part of the secondary phase of the formalin test. This result at the orofacial level clearly contrast with the strong hypoalgesia shown in $BDNF^{+/-}$ mice after intraplantar injection of formalin (MacQueen et al., 2001) indicating that BDNF is playing different and specific roles in the control of nociception in the trigeminal ganglion and in the spinal cord/DRG.

2.1. Transcriptomic analysis of daDREAM-expressing trigeminal neurons

Expression of endogenous DREAM is high in sensory neurons, where its localization is mainly nuclear. To begin to understand the role of DREAM in sensory neurons in general and in the trigeminal ganglion specifically, we decided to perform a genome-wide expression analysis comparing the expression in trigeminal neurons from wild type and line 16 mice. The selection of line 16 for this analysis was conditioned by the strongest hyperalgesic phenotype in adaptation of the formalin test and because it shows a more restricted expression pattern of daDREAM compared to line 1, which could allow a more precise dissection of DREAM function in trigeminal sensitivity.

The comparison between the transcriptome of wild type and line 16 mice, filtered for the -fold change, the P value and the FDR value generated a sub-list of 296 downregulated genes and 295 upregulated genes.

Functional clustering of these genes using the Gene Ontology program showed a predominance of modified gene expression in genes encoding nuclear proteins (32% of the total) followed by changes in genes encoding proteins with binding ability (21% have protein binding domains, 7% have Ca^{2+} binding domains and 7% have DNA binding domains). Finally, at the cellular level this analysis revealed the importance of changes in the expression of genes encoding proteins involved in the transcription process (19% of the total) and in cellular transport processes (14% of the total).

Since daDREAM functions as a constitutive repressor of DREAM target genes we restricted our validation of the microarray data to 3 downregulated genes MGLL, CTSL and DBNDD2, coding for proteins previously involved in nociception.

The monoglyceride lipase (MGLL), together with the hormone-sensitive lipase (HSL), hydrolyzes intracellular triglycerides (Fredrikson et al., 1986). In addiction, MGLL complements lipoprotein lipase to complete the hydrolysis of monoglycerides resulting from the degradation of lipoproteins. MGLL is expressed in astrocytes and participates in the hydrolysis of 2-arachidonoyl glycerol (2-AG). 2-AG is an endocannabinoid that binds specifically to the CB1 receptor to inhibit presynaptically GABA release (Makara et al., 2005). It has been also shown that 2-AG production is induced in the periaqueductal grey (PAG) in response to stress and induces an opioid independent form of analgesia, the so called stress induced analgesia (SIA). Inhibitors of MGLL enhance SIA when microinjected in the dorsolateral PAG (Hohmann et al., 2005). This is reflected in an increased latency in the tail flick test in rats.

Cathepsin L (CTSL) is part of the catephsin family of lysosomal cysteine proteases, which includes 12 proteases activated by low pH. This protease is involved in the proteolytic processing of prodynorphin in secretory vesicles. Thus, brain levels of the proteolytic peptides dynorphin A, dynorphin B, and α-neoendorphin were decreased by more than 70% in cathepsin L knockout compared to wild type mice (Minokadeh et al., 2009). Moreover, it has recently been reported that a member of this family, namely cathepsin S, is a critical factor for the maintenance of neuropathic pain. After peripheral nerve injury, cathepsin S is expressed in spinal cord microglia in the area of the dorsal horn innervated by damaged fibers. Release of the protease, in turn, cleaves and liberates the membrane-bound chemokine fractalkine (FKN). The released FKN feeds back onto the microglial cells via the CX3CR1 receptor to activate the p38 MAPK pathway (Clark et al., 2007). Activation of this intracellular pathway is thought to contribute to neuropathic pain (Jin et al., 2003). Furthermore, the CTSS inhibitor LHVS attenuates spinal microglia activation and has an anti-hyperalgesic and anti-allodynic effect in neuropathic pain.

Dysbindin domain containing protein 2 (DBNDD2) is a member of a protein family that shares the dysbindin domain, a coiled coil motif involved in protein-protein interactions. So far, DBNDD2 has not been related to pain but DTNBP1, another member of the dysbindin domain protein family, plays an important role in neuronal function. Thus, DTNBP1 is found in muscle cells, as part of the dystrophin associated protein complex, and in neurons, particularly in the synaptic terminals of the mossy fibers in the cerebellum and in the hippocampus. In neurons, DTNBP1 is associated with snapin and

is part of the SNARE protein complex that is involved in the process of synaptic docking and fusion (Benson et al., 2001). Mutations of this gene are associated with cases of schizophrenia (Straub et al., 2002). Sandy mice (sdy) harbor a spontaneous deletion of the DTNBP1 gene and behavioral characterization of these mice highlighted strong cognitive impairment with deficits in spatial and visual memory and emotionally motivated learning and memory. Moreover sdy mice show a hypoalgesic phenotype with an increased paw withdrawal latency when tested for their nociceptive thermal threshold (Bhardwaj et al., 2009). This altered nociception is probably related to impairment in the glutamatergic and dopaminergic systems.

We also added to our list of genes of interest SVc2, a member of the SV2 family of synaptic vesicle proteins, which has a distant relationship with nociception since it has been described in biotechnology protocols as a carrier for the botulinum neurotoxin (BoNT) in the treatment of different forms of pain. SV2 proteins are involved in the regulation of synaptic exocytosis. The two most abundant isoforms, SV2a and SV2b, have a wide distribution throughout the brain. SV2c, on the other hand, has a more restricted pattern of expression (Janz and Sudhof, 1999). SV2 also share homology with mammalian ion and sugar transporters, but transport activity has so far not been demonstrated (Bajjalieh et al., 1992). Botulinum neurotoxin binds to the inner surface of synaptic vesicles, specifically to SV2c, during their exposure to the external medium and is internalized by the subsequent vesicle endocytosis. This mechanism favors internalization in hyperactive nerve terminal (Verderio et al., 2006). BoNT has been thoroughly studied as a treatment for several pain syndromes. In a mouse model of inflammatory pain there are evidence that suggest a role for BoNT in the central control of nociception (Luvisetto et al., 2003). More recently, the clinical effect of subcutaneously injected BoNT in the treatment of idiopathic trigeminal neuralgia has been shown (Zuniga et al., 2008).

The promoter regions of CTSL and MGLL have been extensively studied (Troen et al., 1991; Karlsson et al., 2001) and the transcription start sites have been characterized. In both cases using *in silico* analysis we were able to find *bona fid*e DRE sites located downstream to the start of transcription. On the other hand, we were able to find some *bona fide* DRE sites in the 5' untranslated regions of SV2c, DBNDD2 and DTNBP1 genes with no well characterized transcriptional start site.

2.2. Effect of chronic trigeminal pain on DREAM target genes

Like at the spinal cord/DRG level, expression of endogenous DREAM was rapidly increased in trigeminal ganglia after CFA injection in wild type mice, which supports a

role for DREAM in the development and maintenance of the inflammatory induced hyperalgesia also in trigeminal neurons. Line 16 mice also showed an increase in endogenous DREAM transcription, but this was significant only at 3 days after CFA injection. This could reflect the need for a stronger stimulation to overcome the self-blockade imposed by daDREAM expression on endogenous DREAM in transgenic mice.

Importantly, BDNF expression was rapidly decreased in trigeminal neurons of wild type and transgenic mice after CFA injection. This result is opposite to that observed in spinal cord and DRG. The clear influence of BDNF on nociception in the trigeminal ganglion is far from being clarified but it is interesting to stress that our molecular data parallel our behavioral data in $BDNF^{+/-}$ mice. At the molecular level we saw an opposite response to CFA in the DRG and in the trigeminal ganglion and again we saw a completely different response to formalin injection in the hindpaw and in the snoot. All together these data suggest that BDNF plays a specific role in the control of pain in the trigeminal ganglion. In a recent work it has been described that BDNF expression is upregulated 7 to 14 days after the induction of chronic pain induced by tooth pulp inflammation (Tarsa et al., 2010). Currently, we do not have an explanation for this discrepancy other than the different time course and the different models of inflammation used in these two studies.

Comparison of the transcriptional response of the opioid system in the trigeminal ganglion and in the DRG outlined some similarities but also important differences. In general, the transcriptional response of opioid receptor genes is highly specific in the trigeminal ganglion and differs from what we observed in the DRG with the only exception of DOR, which shows a similar downregulation in both ganglia.

In wild type mice the polypeptidic opioid precursor PENK and PNOC display a similar response in these two ganglia. PDYN expression, however, is strongly downregulated in the trigeminal ganglion, while it is induced in spinal cord and did not change after CFA in the DRG.

In daDREAM trigeminal ganglion the response of the opioid system to inflammation is completely blocked with the only exception of the ORL receptor and POMC, which are upregulated after CFA injection. Again, the different influence of daDREAM on the opioid systems in the DRG and in the trigeminal ganglion highlights the specificities in processing of nociceptive inputs in the different afferent fibers.

The expression of the candidate genes MGLL, CTPL and DTNBP1 in wild type trigeminal ganglia was downregulated in response to inflammatory pain. For MGLL and DTNBP1, both with a pro-algesic function, though through different mechanisms, a downregulation after CFA could be interpreted as a compensatory mechanism to reduce the hyperalgesia

associated with the inflammation. Oddly, expression of DBNDD2 was not modified after CFA in wild type or in transgenic mice and DTNBP1, contrary to the result in wild type, showed an early and transient induction in line 16 mice after CFA. The molecular mechanisms regulating the expression of dysbindin-containing proteins and their functional significance in pain-controlling mechanisms are presently far from being understood. Finally, the down regulation of CTPL, involved in the proteolityc processing of the prodynorphin precursor, could be related to the downregulation of PDYN in trigeminal neurons after CFA and the existence of a putative auto-regulatory loop that controls the expression of these two genes in order to adjust the amount of proteolytic enzyme and substrate.

As a curiosity, perhaps with some biotechnological interest, SV2c expression was upregulated. Since SV2c is involved in the regulation of synaptic exocytosis, the upregulation after CFA injection may be a reflection of the increased synaptic activity induced in primary afferent fibers by the ongoing inflammatory process.

CONCLUSIONS

CONCLUSIONS

1. DREAM participates in the overall control of the opioid tone in primary afferent neurons and in the spinal cord.

2. DREAM regulates spinal sensitization through the control of BDNF gene expression.

3. daDREAM does not function as a dominant mutant for the spinal modulation of Kv4 potassium channel activity *in vivo*.

4. DREAM influences basal ERK phosphorylation *in vivo*, in part through the control of the expression of different GABA receptor subunits in dorsal horn neurons.

5. DREAM plays a different role in the control of inflammatory and neuropathic chronic pain.

6. We have developed a model of orofacial hyperalgesia overexpressing daDREAM in trigeminal neurons.

7. In response to inflammatory pain, the expression of BDNF and PDYN are differently regulated in the spinal cord/DRG system and in the trigeminal ganglion.

8. Genome-wide analysis has identified new DREAM target genes that could be involved in the differential response to inflammatory pain in the trigeminal ganglia.

CONCLUSIONES

1. DREAM participa en el control del tono opioide en las neuronas primarias aferentes y en la medula espinal.

2. DREAM regula la sensibilización espinal a través del control de la expresión génica de BDNF.

3. La sobre-expresión de daDREAM no altera las características electrofisiológicas de la corriente de potasio de tipo A en la medula espinal.

4. DREAM influye en los niveles de fosforilación basal de ERK *in vivo*, reduciendo la expresión génica de diferentes subunidades del receptor GABA en las neuronas del asta dorsal de la medula espinal y con ello el tono inhibitorio.

5. DREAM juega un papel distinto en el control del dolor inflamatorio y neuropático.

6. La sobre-expresión de daDREAM en neuronas de trigémino permite el desarrollo de un modelo de hiperalgesia orofacial.

7. En respuesta a dolor inflamatorio, la expresión de BDNF y PDYN se regula diferentemente en el sistema medula espinal/DRG y en el ganglio trigémino.

8. A través de un análisis genómico hemos identificado nuevos genes diana de DREAM que podrían estar implicados en la respuesta diferencial a dolor inflamatorio en el ganglio trigémino.

REFERENCES

REFERENCES

Aid T, Kazantseva A, Piirsoo M, Palm K, Timmusk T (2007) Mouse and rat BDNF gene structure and expression revisited. J Neurosci Res 85:525-535.

An WF, Bowlby MR, Betty M, Cao J, Ling HP, Mendoza G, Hinson JW, Mattsson KI, Strassle BW, Trimmer JS, Rhodes KJ (2000) Modulation of A-type potassium channels by a family of calcium sensors. Nature 403:553-556.

Augustin LB, Felsheim RF, Min BH, Fuchs SM, Fuchs JA, Loh HH (1995) Genomic structure of the mouse delta opioid receptor gene. Biochem Biophys Res Commun 207:111-119.

Baba H, Ji RR, Kohno T, Moore KA, Ataka T, Wakai A, Okamoto M, Woolf CJ (2003) Removal of GABAergic inhibition facilitates polysynaptic A fiber-mediated excitatory transmission to the superficial spinal dorsal horn. Mol Cell Neurosci 24:818-830.

Bajjalieh SM, Peterson K, Shinghal R, Scheller RH (1992) SV2, a brain synaptic vesicle protein homologous to bacterial transporters. Science 257:1271-1273.

Barbacid M (1994) The Trk family of neurotrophin receptors. J Neurobiol 25:1386-1403.

Basbaum AIaJ, T. M. (2000) Principles of neural Science: McGraw-Hill Companies Inc.

Bautista DM, Sigal YM, Milstein AD, Garrison JL, Zorn JA, Tsuruda PR, Nicoll RA, Julius D (2008) Pungent agents from Szechuan peppers excite sensory neurons by inhibiting two-pore potassium channels. Nat Neurosci 11:772-779.

Bennett GJ, Xie YK (1988) A peripheral mononeuropathy in rat that produces disorders of pain sensation like those seen in man. Pain 33:87-107.

Benson MA, Newey SE, Martin-Rendon E, Hawkes R, Blake DJ (2001) Dysbindin, a novel coiled-coil-containing protein that interacts with the dystrobrevins in muscle and brain. J Biol Chem 276:24232-24241.

Bhardwaj SK, Baharnoori M, Sharif-Askari B, Kamath A, Williams S, Srivastava LK (2009) Behavioral characterization of dysbindin-1 deficient sandy mice. Behav Brain Res 197:435-441.

Bugnon C, Bloch B, Lenys D, Gouget A, Fellmann D (1979) Comparative study of the neuronal populations containing beta-endorphin, corticotropin and dopamine in the arcuate nucleus of the rat hypothalamus. Neurosci Lett 14:43-48.

Buxbaum JD, Choi EK, Luo Y, Lilliehook C, Crowley AC, Merriam DE, Wasco W (1998) Calsenilin: a calcium-binding protein that interacts with the presenilins and regulates the levels of a presenilin fragment. Nat Med 4:1177-1181.

Carrion AM, Mellstrom B, Naranjo JR (1998) Protein kinase A-dependent derepression of the human prodynorphin gene via differential binding to an intragenic silencer element. Mol Cell Biol 18:6921-6929.

Carrion AM, Link WA, Ledo F, Mellstrom B, Naranjo JR (1999) DREAM is a Ca2+-regulated transcriptional repressor. Nature 398:80-84.

Caterina MJ, Leffler A, Malmberg AB, Martin WJ, Trafton J, Petersen-Zeitz KR, Koltzenburg M, Basbaum AI, Julius D (2000) Impaired nociception and pain sensation in mice lacking the capsaicin receptor. Science 288:306-313.

Chen WG, Chang Q, Lin Y, Meissner A, West AE, Griffith EC, Jaenisch R, Greenberg ME (2003) Derepression of BDNF transcription involves calcium-dependent phosphorylation of MeCP2. Science 302:885-889.

Cheng HY, Pitcher GM, Laviolette SR, Whishaw IQ, Tong KI, Kockeritz LK, Wada T, Joza NA, Crackower M, Goncalves J, Sarosi I, Woodgett JR, Oliveira-dos-Santos AJ, Ikura M, van der Kooy D, Salter MW, Penninger JM (2002) DREAM is a critical transcriptional repressor for pain modulation. Cell 108:31-43.

Chien LY, Cheng JK, Chu D, Cheng CF, Tsaur ML (2007) Reduced expression of A-type potassium channels in primary sensory neurons induces mechanical hypersensitivity. J Neurosci 27:9855-9865.

Chillingworth NL, Donaldson LF (2003) Characterisation of a Freund's complete adjuvant-induced model of chronic arthritis in mice. J Neurosci Methods 128:45-52.

Cirulli F, Berry A, Alleva E (2000) Intracerebroventricular administration of brain-derived neurotrophic factor in adult rats affects analgesia and spontaneous behaviour but not memory retention in a Morris Water Maze task. Neurosci Lett 287:207-210.

Clark AK, Yip PK, Grist J, Gentry C, Staniland AA, Marchand F, Dehvari M, Wotherspoon G, Winter J, Ullah J, Bevan S, Malcangio M (2007) Inhibition of spinal microglial cathepsin S for the reversal of neuropathic pain. Proc Natl Acad Sci U S A 104:10655-10660.

Clavelou P, Pajot J, Dallel R, Raboisson P (1989) Application of the formalin test to the study of orofacial pain in the rat. Neurosci Lett 103:349-353.

Coull JA, Beggs S, Boudreau D, Boivin D, Tsuda M, Inoue K, Gravel C, Salter MW, De Koninck Y (2005) BDNF from microglia causes the shift in neuronal anion gradient underlying neuropathic pain. Nature 438:1017-1021.

Dixon WJ (1980) Efficient analysis of experimental observations. Annu Rev Pharmacol Toxicol 20:441-462.

Dong XW, Goregoaker S, Engler H, Zhou X, Mark L, Crona J, Terry R, Hunter J, Priestley T (2007) Small interfering RNA-mediated selective knockdown of Na(V)1.8 tetrodotoxin-resistant sodium channel reverses mechanical allodynia in neuropathic rats. Neuroscience 146:812-821.

Draisci G, Kajander KC, Dubner R, Bennett GJ, Iadarola MJ (1991) Up-regulation of opioid gene expression in spinal cord evoked by experimental nerve injuries and inflammation. Brain Res 560:186-192.

Dubner R, Ruda MA (1992) Activity-dependent neuronal plasticity following tissue injury and inflammation. Trends Neurosci 15:96-103.

Eaton MJ, Blits B, Ruitenberg MJ, Verhaagen J, Oudega M (2002) Amelioration of chronic neuropathic pain after partial nerve injury by adeno-associated viral (AAV) vector-mediated over-expression of BDNF in the rat spinal cord. Gene Ther 9:1387-1395.

Farbman AI, Guagliardo N, Sollars SI, Hill DL (2004) Each sensory nerve arising from the geniculate ganglion expresses a unique fingerprint of neurotrophin and neurotrophin receptor genes. J Neurosci Res 78:659-667.

Fedrizzi L, Lim D, Carafoli E, Brini M (2008) Interplay of the Ca2+-binding protein DREAM with presenilin in neuronal Ca2+ signaling. J Biol Chem 283:27494-27503.

Fitzgerald EM, Okuse K, Wood JN, Dolphin AC, Moss SJ (1999) cAMP-dependent phosphorylation of the tetrodotoxin-resistant voltage-dependent sodium channel SNS. J Physiol 516 (Pt 2):433-446.

Fredrikson G, Tornqvist H, Belfrage P (1986) Hormone-sensitive lipase and monoacylglycerol lipase are both required for complete degradation of adipocyte triacylglycerol. Biochim Biophys Acta 876:288-293.

Frick A, Magee J, Johnston D (2004) LTP is accompanied by an enhanced local excitability of pyramidal neuron dendrites. Nat Neurosci 7:126-135.

Ganju P, O'Bryan JP, Der C, Winter J, James IF (1998) Differential regulation of SHC proteins by nerve growth factor in sensory neurons and PC12 cells. Eur J Neurosci 10:1995-2008.

Gomez-Villafuertes R, Torres B, Barrio J, Savignac M, Gabellini N, Rizzato F, Pintado B, Gutierrez-Adan A, Mellstrom B, Carafoli E, Naranjo JR (2005) Downstream regulatory element antagonist modulator regulates Ca2+ homeostasis and viability in cerebellar neurons. J Neurosci 25:10822-10830.

Gonzalez-Martinez T, Farinas I, Del Valle ME, Feito J, Germana G, Cobo J, Vega JA (2005) BDNF, but not NT-4, is necessary for normal development of Meissner corpuscles. Neurosci Lett 377:12-15.

Guo W, Zou S, Guan Y, Ikeda T, Tal M, Dubner R, Ren K (2002) Tyrosine phosphorylation of the NR2B subunit of the NMDA receptor in the spinal cord during the development and maintenance of inflammatory hyperalgesia. J Neurosci 22:6208-6217.

Hains BC, Klein JP, Saab CY, Craner MJ, Black JA, Waxman SG (2003) Upregulation of sodium channel Nav1.3 and functional involvement in neuronal hyperexcitability associated with central neuropathic pain after spinal cord injury. J Neurosci 23:8881-8892.

Hargreaves K, Dubner R, Brown F, Flores C, Joris J (1988) A new and sensitive method for measuring thermal nociception in cutaneous hyperalgesia. Pain 32:77-88.

Heinricher MM (2003) Orphanin FQ/nociceptin: from neural circuitry to behavior. Life Sci 73:813-822.

Heppenstall PA, Lewin GR (2001) BDNF but not NT-4 is required for normal flexion reflex plasticity and function. Proc Natl Acad Sci U S A 98:8107-8112.

Hinman A, Chuang HH, Bautista DM, Julius D (2006) TRP channel activation by reversible covalent modification. Proc Natl Acad Sci U S A 103:19564-19568.

Hohmann AG, Suplita RL, Bolton NM, Neely MH, Fegley D, Mangieri R, Krey JF, Walker JM, Holmes PV, Crystal JD, Duranti A, Tontini A, Mor M, Tarzia G, Piomelli D (2005) An endocannabinoid mechanism for stress-induced analgesia. Nature 435:1108-1112.

Hoyt SB, London C, Ok H, Gonzalez E, Duffy JL, Abbadie C, Dean B, Felix JP, Garcia ML, Jochnowitz N, Karanam BV, Li X, Lyons KA, McGowan E, Macintyre DE, Martin WJ, Priest BT, Smith MM, Tschirret-Guth R, Warren VA, Williams BS, Kaczorowski GJ, Parsons WH (2007) Benzazepinone Nav1.7 blockers: potential treatments for neuropathic pain. Bioorg Med Chem Lett 17:6172-6177.

Hu HJ, Gereau RWt (2003) ERK integrates PKA and PKC signaling in superficial dorsal horn neurons. II. Modulation of neuronal excitability. J Neurophysiol 90:1680-1688.

Hu HJ, Carrasquillo Y, Karim F, Jung WE, Nerbonne JM, Schwarz TL, Gereau RWt (2006) The kv4.2 potassium channel subunit is required for pain plasticity. Neuron 50:89-100.

Hu P, Bembrick AL, Keay KA, McLachlan EM (2007) Immune cell involvement in dorsal root ganglia and spinal cord after chronic constriction or transection of the rat sciatic nerve. Brain Behav Immun 21:599-616.

Hunt SP, Pini A, Evan G (1987) Induction of c-fos-like protein in spinal cord neurons following sensory stimulation. Nature 328:632-634.

Ichikawa H, Terayama R, Yamaai T, Yan Z, Sugimoto T (2007) Brain-derived neurotrophic factor-immunoreactive neurons in the rat vagal and glossopharyngeal sensory ganglia; co-expression with other neurochemical substances. Brain Res 1155:93-99.

Ichikawa H, Yabuuchi T, Jin HW, Terayama R, Yamaai T, Deguchi T, Kamioka H, Takano-Yamamoto T, Sugimoto T (2006) Brain-derived neurotrophic factor-

immunoreactive primary sensory neurons in the rat trigeminal ganglion and trigeminal sensory nuclei. Brain Res 1081:113-118.

Immke DC, McCleskey EW (2001) ASIC3: a lactic acid sensor for cardiac pain. ScientificWorldJournal 1:510-512.

Janz R, Sudhof TC (1999) SV2C is a synaptic vesicle protein with an unusually restricted localization: anatomy of a synaptic vesicle protein family. Neuroscience 94:1279-1290.

Ji RR, Baba H, Brenner GJ, Woolf CJ (1999) Nociceptive-specific activation of ERK in spinal neurons contributes to pain hypersensitivity. Nat Neurosci 2:1114-1119.

Ji RR, Befort K, Brenner GJ, Woolf CJ (2002) ERK MAP kinase activation in superficial spinal cord neurons induces prodynorphin and NK-1 upregulation and contributes to persistent inflammatory pain hypersensitivity. J Neurosci 22:478-485.

Jin SX, Zhuang ZY, Woolf CJ, Ji RR (2003) p38 mitogen-activated protein kinase is activated after a spinal nerve ligation in spinal cord microglia and dorsal root ganglion neurons and contributes to the generation of neuropathic pain. J Neurosci 23:4017-4022.

Karim F, Wang CC, Gereau RWt (2001) Metabotropic glutamate receptor subtypes 1 and 5 are activators of extracellular signal-regulated kinase signaling required for inflammatory pain in mice. J Neurosci 21:3771-3779.

Karlsson M, Reue K, Xia YR, Lusis AJ, Langin D, Tornqvist H, Holm C (2001) Exon-intron organization and chromosomal localization of the mouse monoglyceride lipase gene. Gene 272:11-18.

Kashiba H, Uchida Y, Senba E (2003) Distribution and colocalization of NGF and GDNF family ligand receptor mRNAs in dorsal root and nodose ganglion neurons of adult rats. Brain Res Mol Brain Res 110:52-62.

Katsura H, Obata K, Mizushima T, Sakurai J, Kobayashi K, Yamanaka H, Dai Y, Fukuoka T, Sakagami M, Noguchi K (2006) Activation of Src-family kinases in spinal microglia contributes to mechanical hypersensitivity after nerve injury. J Neurosci 26:8680-8690.

Kerr BJ, Bradbury EJ, Bennett DL, Trivedi PM, Dassan P, French J, Shelton DB, McMahon SB, Thompson SW (1999) Brain-derived neurotrophic factor modulates nociceptive sensory inputs and NMDA-evoked responses in the rat spinal cord. J Neurosci 19:5138-5148.

Kilpatrick DL, Zinn SA, Fitzgerald M, Higuchi H, Sabol SL, Meyerhardt J (1990) Transcription of the rat and mouse proenkephalin genes is initiated at distinct sites in spermatogenic and somatic cells. Mol Cell Biol 10:3717-3726.

Kitchen I, Slowe SJ, Matthes HW, Kieffer B (1997) Quantitative autoradiographic mapping of mu-, delta- and kappa-opioid receptors in knockout mice lacking the mu-opioid receptor gene. Brain Res 778:73-88.

Klein R, Conway D, Parada LF, Barbacid M (1990) The trkB tyrosine protein kinase gene codes for a second neurogenic receptor that lacks the catalytic kinase domain. Cell 61:647-656.

Kwan KY, Glazer JM, Corey DP, Rice FL, Stucky CL (2009) TRPA1 modulates mechanotransduction in cutaneous sensory neurons. J Neurosci 29:4808-4819.

Lai J, Luo MC, Chen Q, Ma S, Gardell LR, Ossipov MH, Porreca F (2006) Dynorphin A activates bradykinin receptors to maintain neuropathic pain. Nat Neurosci 9:1534-1540.

Lamonerie T, Tremblay JJ, Lanctot C, Therrien M, Gauthier Y, Drouin J (1996) Ptx1, a bicoid-related homeo box transcription factor involved in transcription of the pro-opiomelanocortin gene. Genes Dev 10:1284-1295.

Le Douarin B, vom Baur E, Zechel C, Heery D, Heine M, Vivat V, Gronemeyer H, Losson R, Chambon P (1996) Ligand-dependent interaction of nuclear receptors with potential transcriptional intermediary factors (mediators). Philos Trans R Soc Lond B Biol Sci 351:569-578.

Ledo F, Kremer L, Mellstrom B, Naranjo JR (2002) Ca2+-dependent block of CREB-CBP transcription by repressor DREAM. Embo J 21:4583-4592.

Ledo F, Carrion AM, Link WA, Mellstrom B, Naranjo JR (2000a) DREAM-alphaCREM interaction via leucine-charged domains derepresses downstream regulatory element-dependent transcription. Mol Cell Biol 20:9120-9126.

Ledo F, Link WA, Carrion AM, Echeverria V, Mellstrom B, Naranjo JR (2000b) The DREAM-DRE interaction: key nucleotides and dominant negative mutants. Biochim Biophys Acta 1498:162-168.

Levin S, Pearsall G, Ruderman RJ (1978) Von Frey's method of measuring pressure sensibility in the hand: an engineering analysis of the Weinstein-Semmes pressure aesthesiometer. J Hand Surg Am 3:211-216.

Lilliehook C, Chan S, Choi EK, Zaidi NF, Wasco W, Mattson MP, Buxbaum JD (2002) Calsenilin enhances apoptosis by altering endoplasmic reticulum calcium signaling. Mol Cell Neurosci 19:552-559.

Lilliehook C, Bozdagi O, Yao J, Gomez-Ramirez M, Zaidi NF, Wasco W, Gandy S, Santucci AC, Haroutunian V, Huntley GW, Buxbaum JD (2003) Altered Abeta formation and long-term potentiation in a calsenilin knock-out. J Neurosci 23:9097-9106.

Lima D, Avelino A, Coimbra A (1993) Morphological characterization of marginal (lamina I) neurons immunoreactive for substance P, enkephalin, dynorphin and gamma-aminobutyric acid in the rat spinal cord. J Chem Neuroanat 6:43-52.

Link WA, Ledo F, Torres B, Palczewska M, Madsen TM, Savignac M, Albar JP, Mellstrom B, Naranjo JR (2004) Day-night changes in downstream regulatory element antagonist modulator/potassium channel interacting protein activity contribute to circadian gene expression in pineal gland. J Neurosci 24:5346-5355.

Liu HC, Lu S, Augustin LB, Felsheim RF, Chen HC, Loh HH, Wei LN (1995) Cloning and promoter mapping of mouse kappa opioid receptor gene. Biochem Biophys Res Commun 209:639-647.

Luo L, Chang L, Brown SM, Ao H, Lee DH, Higuera ES, Dubin AE, Chaplan SR (2007) Role of peripheral hyperpolarization-activated cyclic nucleotide-modulated channel pacemaker channels in acute and chronic pain models in the rat. Neuroscience 144:1477-1485.

Luvisetto S, Rossetto O, Montecucco C, Pavone F (2003) Toxicity of botulinum neurotoxins in central nervous system of mice. Toxicon 41:475-481.

Macpherson LJ, Dubin AE, Evans MJ, Marr F, Schultz PG, Cravatt BF, Patapoutian A (2007) Noxious compounds activate TRPA1 ion channels through covalent modification of cysteines. Nature 445:541-545.

MacQueen GM, Ramakrishnan K, Croll SD, Siuciak JA, Yu G, Young LT, Fahnestock M (2001) Performance of heterozygous brain-derived neurotrophic factor knockout mice on behavioral analogues of anxiety, nociception, and depression. Behav Neurosci 115:1145-1153.

Makara JK, Mor M, Fegley D, Szabo SI, Kathuria S, Astarita G, Duranti A, Tontini A, Tarzia G, Rivara S, Freund TF, Piomelli D (2005) Selective inhibition of 2-AG hydrolysis enhances endocannabinoid signaling in hippocampus. Nat Neurosci 8:1139-1141.

Martinowich K, Hattori D, Wu H, Fouse S, He F, Hu Y, Fan G, Sun YE (2003) DNA methylation-related chromatin remodeling in activity-dependent BDNF gene regulation. Science 302:890-893.

Matayoshi S, Jiang N, Katafuchi T, Koga K, Furue H, Yasaka T, Nakatsuka T, Zhou XF, Kawasaki Y, Tanaka N, Yoshimura M (2005) Actions of brain-derived neurotrophic factor on spinal nociceptive transmission during inflammation in the rat. J Physiol 569:685-695.

Mayford M, Baranes D, Podsypanina K, Kandel ER (1996) The 3'-untranslated region of CaMKII alpha is a cis-acting signal for the localization and translation of mRNA in dendrites. Proc Natl Acad Sci U S A 93:13250-13255.

McCarson KE, Krause JE (1994) NK-1 and NK-3 type tachykinin receptor mRNA expression in the rat spinal cord dorsal horn is increased during adjuvant or formalin-induced nociception. J Neurosci 14:712-720.

McGivern JG (2006) Targeting N-type and T-type calcium channels for the treatment of pain. Drug Discov Today 11:245-253.

McMurray CT, Devi L, Calavetta L, Douglass JO (1989) Regulated expression of the prodynorphin gene in the R2C Leydig tumor cell line. Endocrinology 124:49-59.

Mellstrom B, Torres B, Link WA, Naranjo JR (2004) The BDNF gene: exemplifying complexity in Ca2+ -dependent gene expression. Crit Rev Neurobiol 16:43-49.

Menegola M, Trimmer JS (2006) Unanticipated region- and cell-specific downregulation of individual KChIP auxiliary subunit isotypes in Kv4.2 knock-out mouse brain. J Neurosci 26:12137-12142.

Merighi A, Carmignoto G, Gobbo S, Lossi L, Salio C, Vergnano AM, Zonta M (2004) Neurotrophins in spinal cord nociceptive pathways. Prog Brain Res 146:291-321.

Meunier JC, Mollereau C, Toll L, Suaudeau C, Moisand C, Alvinerie P, Butour JL, Guillemot JC, Ferrara P, Monsarrat B, et al. (1995) Isolation and structure of the endogenous agonist of opioid receptor-like ORL1 receptor. Nature 377:532-535.

Middlemas DS, Lindberg RA, Hunter T (1991) trkB, a neural receptor protein-tyrosine kinase: evidence for a full-length and two truncated receptors. Mol Cell Biol 11:143-153.

Min BH, Augustin LB, Felsheim RF, Fuchs JA, Loh HH (1994) Genomic structure analysis of promoter sequence of a mouse mu opioid receptor gene. Proc Natl Acad Sci U S A 91:9081-9085.

Minokadeh A, Funkelstein L, Toneff T, Hwang SR, Beinfeld M, Reinheckel T, Peters C, Zadina J, Hook V (2009) Cathepsin L participates in dynorphin production in brain cortex, illustrated by protease gene knockout and expression. Mol Cell Neurosci 43:98-107.

Mogil JS (2009) Animal models of pain: progress and challenges. Nat Rev Neurosci 10:283-294.

Mogil JS, Pasternak GW (2001) The molecular and behavioral pharmacology of the orphanin FQ/nociceptin peptide and receptor family. Pharmacol Rev 53:381-415.

Mollereau C, Simons MJ, Soularue P, Liners F, Vassart G, Meunier JC, Parmentier M (1996) Structure, tissue distribution, and chromosomal localization of the prepronociceptin gene. Proc Natl Acad Sci U S A 93:8666-8670.

Morgan JR, Gebhart GF (2008) Characterization of a model of chronic orofacial hyperalgesia in the rat: contribution of NA(V) 1.8. J Pain 9:522-531.

Morisset V, Nagy F (2000) Plateau potential-dependent windup of the response to primary afferent stimuli in rat dorsal horn neurons. Eur J Neurosci 12:3087-3095.

Naranjo JR, Mellstrom B, Achaval M, Lucas JJ, Del Rio J, Sassone-Corsi P (1991) Co-induction of jun B and c-fos in a subset of neurons in the spinal cord. Oncogene 6:223-227.

Nassar MA, Levato A, Stirling LC, Wood JN (2005) Neuropathic pain develops normally in mice lacking both Na(v)1.7 and Na(v)1.8. Mol Pain 1:24.

Nassar MA, Stirling LC, Forlani G, Baker MD, Matthews EA, Dickenson AH, Wood JN (2004) Nociceptor-specific gene deletion reveals a major role for Nav1.7 (PN1) in acute and inflammatory pain. Proc Natl Acad Sci U S A 101:12706-12711.

Noel J, Zimmermann K, Busserolles J, Deval E, Alloui A, Diochot S, Guy N, Borsotto M, Reeh P, Eschalier A, Lazdunski M (2009) The mechano-activated K+ channels TRAAK and TREK-1 control both warm and cold perception. Embo J 28:1308-1318.

Obara I, Parkitna JR, Korostynski M, Makuch W, Kaminska D, Przewlocka B, Przewlocki R (2009) Local peripheral opioid effects and expression of opioid genes in the spinal cord and dorsal root ganglia in neuropathic and inflammatory pain. Pain 141:283-291.

Obata K, Yamanaka H, Dai Y, Mizushima T, Fukuoka T, Tokunaga A, Noguchi K (2004) Activation of extracellular signal-regulated protein kinase in the dorsal root ganglion following inflammation near the nerve cell body. Neuroscience 126:1011-1021.

Page AJ, Brierley SM, Martin CM, Martinez-Salgado C, Wemmie JA, Brennan TJ, Symonds E, Omari T, Lewin GR, Welsh MJ, Blackshaw LA (2004) The ion channel ASIC1 contributes to visceral but not cutaneous mechanoreceptor function. Gastroenterology 127:1739-1747.

Pan YX, Xu J, Pasternak GW (1996) Structure and characterization of the gene encoding a mouse kappa3-related opioid receptor. Gene 171:255-260.

Pezet S, McMahon SB (2006) Neurotrophins: mediators and modulators of pain. Annu Rev Neurosci 29:507-538.

Premkumar LS, Ahern GP (2000) Induction of vanilloid receptor channel activity by protein kinase C. Nature 408:985-990.

Price MP, McIlwrath SL, Xie J, Cheng C, Qiao J, Tarr DE, Sluka KA, Brennan TJ, Lewin GR, Welsh MJ (2001) The DRASIC cation channel contributes to the detection of cutaneous touch and acid stimuli in mice. Neuron 32:1071-1083.

Price MP, Lewin GR, McIlwrath SL, Cheng C, Xie J, Heppenstall PA, Stucky CL, Mannsfeldt AG, Brennan TJ, Drummond HA, Qiao J, Benson CJ, Tarr DE, Hrstka RF, Yang B, Williamson RA, Welsh MJ (2000) The mammalian sodium channel BNC1 is required for normal touch sensation. Nature 407:1007-1011.

Puig S, Sorkin LS (1996) Formalin-evoked activity in identified primary afferent fibers: systemic lidocaine suppresses phase-2 activity. Pain 64:345-355.

Rashid MH, Inoue M, Toda K, Ueda H (2004) Loss of peripheral morphine analgesia contributes to the reduced effectiveness of systemic morphine in neuropathic pain. J Pharmacol Exp Ther 309:380-387.

Reeh PW, Steen KH (1996) Tissue acidosis in nociception and pain. Prog Brain Res 113:143-151.

Reiner A, Yekutieli D, Benjamini Y (2003) Identifying differentially expressed genes using false discovery rate controlling procedures. Bioinformatics 19:368-375.

Reinscheid RK, Nothacker HP, Bourson A, Ardati A, Henningsen RA, Bunzow JR, Grandy DK, Langen H, Monsma FJ, Jr., Civelli O (1995) Orphanin FQ: a neuropeptide that activates an opioidlike G protein-coupled receptor. Science 270:792-794.

Rexed B (1952) The cytoarchitectonic organization of the spinal cord in the cat. J Comp Neurol 96:414-495.

Ritner HL, Machelska, H. and Stein, C. (2008) Immune system pain and analgesia. Oxford: Oxford: Academic Press.

Rivas M, Mellstrom B, Naranjo JR, Santisteban P (2004) Transcriptional repressor DREAM interacts with thyroid transcription factor-1 and regulates thyroglobulin gene expression. J Biol Chem 279:33114-33122.

Rivas M, Aurrekoetxea K, Mellstrom B, Naranjo JR (2010) Redox signaling regulates transcriptional activity of the Ca2+-dependent repressor DREAM. Antioxid Redox Signal.

Rivas M, Mellstrom B, Torres B, Cali G, Ferrara AM, Terracciano D, Zannini M, Morreale de Escobar G, Naranjo JR (2009) The DREAM protein is associated with thyroid enlargement and nodular development. Mol Endocrinol 23:862-870.

Roza C, Lopez-Garcia JA (2008) Retigabine, the specific KCNQ channel opener, blocks ectopic discharges in axotomized sensory fibres. Pain 138:537-545.

Roza C, Laird JM, Souslova V, Wood JN, Cervero F (2003) The tetrodotoxin-resistant Na+ channel Nav1.8 is essential for the expression of spontaneous activity in damaged sensory axons of mice. J Physiol 550:921-926.

Roza C, Puel JL, Kress M, Baron A, Diochot S, Lazdunski M, Waldmann R (2004) Knockout of the ASIC2 channel in mice does not impair cutaneous mechanosensation, visceral mechanonociception and hearing. J Physiol 558:659-669.

Ruiz-Gomez A, Mellstrom B, Tornero D, Morato E, Savignac M, Holguin H, Aurrekoetxea K, Gonzalez P, Gonzalez-Garcia C, Cena V, Mayor F, Jr., Naranjo JR (2007) G protein-coupled receptor kinase 2-mediated phosphorylation of downstream regulatory element antagonist modulator regulates membrane trafficking of Kv4.2 potassium channel. J Biol Chem 282:1205-1215.

Salio C, Averill S, Priestley JV, Merighi A (2007) Costorage of BDNF and neuropeptides within individual dense-core vesicles in central and peripheral neurons. Dev Neurobiol 67:326-338.

Samad TA, Moore KA, Sapirstein A, Billet S, Allchorne A, Poole S, Bonventre JV, Woolf CJ (2001) Interleukin-1beta-mediated induction of Cox-2 in the CNS contributes to inflammatory pain hypersensitivity. Nature 410:471-475.

Savignac M, Pintado B, Gutierrez-Adan A, Palczewska M, Mellstrom B, Naranjo JR (2005) Transcriptional repressor DREAM regulates T-lymphocyte proliferation and cytokine gene expression. Embo J 24:3555-3564.

Scholz J, Woolf CJ (2007) The neuropathic pain triad: neurons, immune cells and glia. Nat Neurosci 10:1361-1368.

Sedy J, Szeder V, Walro JM, Ren ZG, Nanka O, Tessarollo L, Sieber-Blum M, Grim M, Kucera J (2004) Pacinian corpuscle development involves multiple Trk signaling pathways. Dev Dyn 231:551-563.

Sheets PL, Heers C, Stoehr T, Cummins TR (2008) Differential block of sensory neuronal voltage-gated sodium channels by lacosamide [(2R)-2-(acetylamino)-N-benzyl-3-methoxypropanamide], lidocaine, and carbamazepine. J Pharmacol Exp Ther 326:89-99.

Sherrington CS (1906) The integrative action of nervous system. New York: Scribner.

Slowe SJ, Simonin F, Kieffer B, Kitchen I (1999) Quantitative autoradiography of mu-,delta- and kappa1 opioid receptors in kappa-opioid receptor knockout mice. Brain Res 818:335-345.

Soderling TR, Derkach VA (2000) Postsynaptic protein phosphorylation and LTP. Trends Neurosci 23:75-80.

Sofroniew MV (1979) Immunoreactive beta-endorphin and ACTH in the same neurons of the hypothalamic arcuate nucleus in the rat. Am J Anat 154:283-289.

Straub RE, Jiang Y, MacLean CJ, Ma Y, Webb BT, Myakishev MV, Harris-Kerr C, Wormley B, Sadek H, Kadambi B, Cesare AJ, Gibberman A, Wang X, O'Neill FA, Walsh D, Kendler KS (2002) Genetic variation in the 6p22.3 gene DTNBP1, the human ortholog of the mouse dysbindin gene, is associated with schizophrenia. Am J Hum Genet 71:337-348.

Tao X, West AE, Chen WG, Corfas G, Greenberg ME (2002) A calcium-responsive transcription factor, CaRF, that regulates neuronal activity-dependent expression of BDNF. Neuron 33:383-395.

Tarsa L, Balkowiec-Iskra E, Kratochvil FJ, 3rd, Jenkins VK, McLean A, Brown AL, Smith JA, Baumgartner JC, Balkowiec A (2010) Tooth pulp inflammation increases brain-derived neurotrophic factor expression in rodent trigeminal ganglion neurons. Neuroscience 167:1205-1215.

Thompson SW, King AE, Woolf CJ (1990) Activity-Dependent Changes in Rat Ventral Horn Neurons in vitro; Summation of Prolonged Afferent Evoked Postsynaptic Depolarizations Produce a d-2-Amino-5-Phosphonovaleric Acid Sensitive Windup. Eur J Neurosci 2:638-649.

Thompson SW, Bennett DL, Kerr BJ, Bradbury EJ, McMahon SB (1999) Brain-derived neurotrophic factor is an endogenous modulator of nociceptive responses in the spinal cord. Proc Natl Acad Sci U S A 96:7714-7718.

Tominaga M, Caterina MJ, Malmberg AB, Rosen TA, Gilbert H, Skinner K, Raumann BE, Basbaum AI, Julius D (1998) The cloned capsaicin receptor integrates multiple pain-producing stimuli. Neuron 21:531-543.

Troen BR, Chauhan SS, Ray D, Gottesman MM (1991) Downstream sequences mediate induction of the mouse cathepsin L promoter by phorbol esters. Cell Growth Differ 2:23-31.

Tsuda M, Shigemoto-Mogami Y, Koizumi S, Mizokoshi A, Kohsaka S, Salter MW, Inoue K (2003) P2X4 receptors induced in spinal microglia gate tactile allodynia after nerve injury. Nature 424:778-783.

Uchida N, Kanazawa M, Suzuki Y, Takeda M (2003) Expression of BDNF and TrkB in mouse taste buds after denervation and in circumvallate papillae during development. Arch Histol Cytol 66:17-25.

Verderio C, Rossetto O, Grumelli C, Frassoni C, Montecucco C, Matteoli M (2006) Entering neurons: botulinum toxins and synaptic vesicle recycling. EMBO Rep 7:995-999.

Viana F, de la Pena E, Belmonte C (2002) Specificity of cold thermotransduction is determined by differential ionic channel expression. Nat Neurosci 5:254-260.

von Bartheld CS (2004) Axonal transport and neuronal transcytosis of trophic factors, tracers, and pathogens. J Neurobiol 58:295-314.

von Bartheld CS, Wang X, Butowt R (2001) Anterograde axonal transport, transcytosis, and recycling of neurotrophic factors: the concept of trophic currencies in neural networks. Mol Neurobiol 24:1-28.

Wang K (2008) Modulation by clamping: Kv4 and KChIP interactions. Neurochem Res 33:1964-1969.

Winkelstein BA, Rutkowski MD, Sweitzer SM, Pahl JL, DeLeo JA (2001) Nerve injury proximal or distal to the DRG induces similar spinal glial activation and selective cytokine expression but differential behavioral responses to pharmacologic treatment. J Comp Neurol 439:127-139.

Woolf CJ (1983) Evidence for a central component of post-injury pain hypersensitivity. Nature 306:686-688.

Wu LJ, Mellstrom B, Wang H, Ren M, Domingo S, Kim SS, Li XY, Chen T, Naranjo JR, Zhuo M (2010) DREAM (Downstream Regulatory Element Antagonist Modulator) contributes to synaptic depression and contextual fear memory. Mol Brain 3:3.

Yajima Y, Narita M, Usui A, Kaneko C, Miyatake M, Narita M, Yamaguchi T, Tamaki H, Wachi H, Seyama Y, Suzuki T (2005) Direct evidence for the involvement of brain-derived neurotrophic factor in the development of a neuropathic pain-like state in mice. J Neurochem 93:584-594.

Yu O, Chuang DM (1997) Neurotrophin protection against toxicity induced by low potassium and nitroprusside in cultured cerebellar granule neurons. J Neurochem 68:68-77.

Zadina JE, Hackler L, Ge LJ, Kastin AJ (1997) A potent and selective endogenous agonist for the mu-opiate receptor. Nature 386:499-502.

Zhang Y, Li Y, Yang YR, Zhu HH, Han JS, Wang Y (2007) Distribution of downstream regulatory element antagonist modulator (DREAM) in rat spinal cord and upregulation of its expression during inflammatory pain. Neurochem Res 32:1592-1599.

Zhao J, Seereeram A, Nassar MA, Levato A, Pezet S, Hathaway G, Morenilla-Palao C, Stirling C, Fitzgerald M, McMahon SB, Rios M, Wood JN (2006) Nociceptor-derived brain-derived neurotrophic factor regulates acute and inflammatory but not neuropathic pain. Mol Cell Neurosci 31:539-548.

Zhou XF, Deng YS, Xian CJ, Zhong JH (2000) Neurotrophins from dorsal root ganglia trigger allodynia after spinal nerve injury in rats. Eur J Neurosci 12:100-105.

Zhuang ZY, Gerner P, Woolf CJ, Ji RR (2005) ERK is sequentially activated in neurons, microglia, and astrocytes by spinal nerve ligation and contributes to mechanical allodynia in this neuropathic pain model. Pain 114:149-159.

Zimmermann K, Leffler A, Babes A, Cendan CM, Carr RW, Kobayashi J, Nau C, Wood JN, Reeh PW (2007) Sensory neuron sodium channel Nav1.8 is essential for pain at low temperatures. Nature 447:855-858.

Zuniga C, Diaz S, Piedimonte F, Micheli F (2008) Beneficial effects of botulinum toxin type A in trigeminal neuralgia. Arq Neuropsiquiatr 66:500-503.

SUPPLEMENTARY DATA

SUPPLEMENTARY DATA

List of downregulated genes

Fold change < -1,5; P value (LIMMA) < 0,05; FDR value (LIMMA) < 0,1

fold change	pval	FDR	probe ID	gene symbol
-2.46	0.00000010	0.00006349	1415694_at	Wars | tryptophanyl-tRNA synthetase
-1.60	0.00152236	0.07297937	1415903_at	Slc38a1 | solute carrier family 38, member 1
-1.52	0.00003902	0.00569589	1416247_at	Dctn3 | dynactin 3
-1.57	0.00049380	0.03400132	1416594_at	Sfrp1 | secreted frizzled-related sequence protein 1
-2.03	0.00000145	0.00049118	1417185_at	Ly6a | lymphocyte antigen 6 complex, locus A
-1.68	0.00007159	0.00885543	1417261_at	Mbtd1 | mbt domain containing 1
-1.94	0.00008924	0.01026761	1417379_at	Iqgap1 | IQ motif containing GTPase activating protein 1
-1.54	0.00020823	0.01904920	1417495_x_at	Cp | ceruloplasmin
-1.67	0.00023745	0.02071556	1417789_at	Ccl11 | small chemokine (C-C motif) ligand 11
-2.20	0.00025426	0.02171862	1417933_at	Igfbp6 | insulin-like growth factor binding protein 6
-1.93	0.00000025	0.00012695	1418172_at	Hebp1 | heme binding protein 1
-2.19	0.00022071	0.01985323	1418174_at	Dbp | D site albumin promoter binding protein
-2.27	0.00001322	0.00250517	1418191_at	Usp18 | ubiquitin specific peptidase 18
-2.10	0.00000271	0.00074025	1418294_at	Epb4.1l4b | erythrocyte protein band 4.1-like 4b
-1.70	0.00017896	0.01675741	1418392_a_at	Gbp3 | guanylate nucleotide binding protein 3
-1.57	0.00010574	0.01171768	1418414_at	Kcnh1 | potassium voltage-gated channel, subfamily H (eag-related), member 1
-1.55	0.00000645	0.00142755	1418472_at	Aspa | aspartoacylase (aminoacylase) 2
-15.46	0.00000000	0.00000019	1418493_a_at	Snca | synuclein, alpha
-1.57	0.00005104	0.00691246	1418580_at	Rtp4 | receptor transporter protein 4
-1.55	0.00055914	0.03653064	1418652_at	Cxcl9 | chemokine (C-X-C motif) ligand 9
-1.73	0.00005830	0.00768343	1418684_at	2310012P17Rik | RIKEN cDNA 2310012P17
-1.51	0.00029114	0.02370181	1418697_at	Inmt | indolethylamine N-methyltransferase
-1.96	0.00000206	0.00062459	1418774_a_at	Atp7a | ATPase, Cu++ transporting, alpha polypeptide
-1.73	0.00195498	0.08389294	1418877_at	Foxd1 | Forkhead box D1
-1.52	0.00002645	0.00430674	1418941_at	Pcdhb22 | protocadherin beta 22
-2.50	0.00000160	0.00052950	1419043_a_at	Iigp1 | interferon inducible GTPase 1
-1.52	0.00067348	0.04115392	1419564_at	Zfp467 | zinc finger protein 467
-1.64	0.00000255	0.00070978	1419672_at	Spock1 | sparc/osteonectin, cwcv and kazal-like domains proteoglycan 1
-1.90	0.00069427	0.04217593	1419903_at	Dbndd2 | Dysbindin (dystrobrevin binding protein 1) domain containing 2
-1.72	0.00017835	0.01675741	1420039_s_at	Cbx7 | chromobox homolog 7
-1.52	0.00224337	0.08971951	1420256_x_at	Prph1 | Peripherin 1
-2.28	0.00011558	0.01244145	1420287_at	--- | Transcribed locus
-2.22	0.00194169	0.08385249	1420357_s_at	Xlr3a | X-linked lymphocyte-regulated 3A /// X-linked lymphocyte-regulated 3B /// predicted gene, EG574437
-1.54	0.00101498	0.05502684	1420861_at	Dctn4 | dynactin 4
-1.78	0.00008400	0.00981469	1420863_at	Dctn4 | dynactin 4
-1.63	0.00039996	0.02952322	1421087_at	Per3 | period homolog 3 (Drosophila)
-1.71	0.00000805	0.00170718	1421139_a_at	Zfp386 | zinc finger protein 386 (Kruppel-like)
-24.33	0.00000000	0.00000019	1421144_at	Rpgrip1 | retinitis pigmentosa GTPase regulator interacting protein 1
-1.96	0.00007042	0.00877357	1421339_at	Extl3 | exostoses (multiple)-like 3
-1.54	0.00034522	0.02616784	1421512_at	Cep250 | centrosomal protein 250
-2.89	0.00000043	0.00019623	1422903_at	Ly86 | lymphocyte antigen 86
-1.64	0.00006259	0.00808867	1423000_a_at	Dgke | diacylglycerol kinase, epsilon
-2.08	0.00000031	0.00015259	1423150_at	Scg5 | secretogranin V

-2.16	0.00000004	0.00003442	1423216_a_at	2510049I19Rik | RIKEN cDNA 2510049I19
-1.71	0.00004459	0.00630365	1423314_s_at	Pde7a | phosphodiesterase 7A
-1.51	0.00021024	0.01907893	1423693_at	Ela1 | elastase 1, pancreatic
-1.62	0.00274559	0.09993060	1424101_at	Hnrpl | heterogeneous nuclear ribonucleoprotein L
-2.15	0.00007256	0.00887786	1424176_a_at	Anxa4 | annexin A4
-2.95	0.00000171	0.00054382	1424836_a_at	Clasp2 | CLIP associating protein 2
-3.75	0.00000002	0.00001912	1424893_at	Ndel1 | nuclear distribution gene E-like homolog 1 (A. nidulans)
-1.54	0.00192232	0.08352466	1424987_at	5430435G22Rik | RIKEN cDNA 5430435G22
-1.62	0.00038254	0.02870728	1425191_at	Ocel1 | occludin/ELL domain containing 1
-2.25	0.00000611	0.00136526	1425385_a_at	Igh-6 | Immunoglobulin heavy chain 6 (heavy chain of IgM)
-1.72	0.00002433	0.00406487	1425856_at	Cib1 | Calcium and integrin binding 1 (calmyrin)
-1.51	0.00060691	0.03867460	1425879_at	Zfp352 | zinc finger protein 352
-5.39	0.00000000	0.00000089	1426289_at	Qrich1 | glutamine-rich 1
-1.52	0.00003822	0.00563335	1426441_at	Slc11a2 | solute carrier family 11 (proton-coupled divalent metal ion transporters), member 2
-1.59	0.00023255	0.02040540	1426785_s_at	Mgll | monoglyceride lipase
-1.73	0.00001064	0.00211329	1427246_at	Magi1 | membrane associated guanylate kinase, WW and PDZ domain containing 1
-4.19	0.00000003	0.00002456	1427328_a_at	Clasp2 | CLIP associating protein 2
-2.01	0.00034204	0.02610226	1427329_a_at	Igh-6 | immunoglobulin heavy chain 6 (heavy chain of IgM)
-2.36	0.00000025	0.00012695	1427351_s_at	Igh-6 | immunoglobulin heavy chain 6 (heavy chain of IgM)
-2.16	0.00064773	0.04029441	1428055_at	Rian | RNA imprinted and accumulated in nucleus
-2.47	0.00000296	0.00080016	1428692_at	Hddc3 | HD domain containing 3
-1.66	0.00011273	0.01225490	1428851_at	1300014I06Rik | RIKEN cDNA 1300014I06 gene
-1.55	0.00029673	0.02406987	1428921_at	2810021B07Rik | RIKEN cDNA 2810021B07 gene
-1.58	0.00013145	0.01366027	1429040_at	2610005L07Rik | RIKEN cDNA 2610005L07
-2.30	0.00000022	0.00011671	1429215_at	2310058N22Rik | RIKEN cDNA 2310058N22
-1.52	0.00016796	0.01618657	1429219_at	1200009F10Rik | RIKEN cDNA 1200009F10
-1.57	0.00026506	0.02244810	1429247_at	Anxa6 | annexin A6
-2.02	0.00000052	0.00022062	1429335_at	Snapc1 | small nuclear RNA activating complex, polypeptide 1
-1.54	0.00016111	0.01579653	1429688_at	Arntl2 | aryl hydrocarbon receptor nuclear translocator-like 2
-1.52	0.00268826	0.09891671	1429725_at	Atbf1 | AT motif binding factor 1
-1.58	0.00006207	0.00804396	1429785_at	5830458C19Rik | RIKEN cDNA 5830458C19
-3.78	0.00000002	0.00002078	1429870_at	C630040K21Rik | RIKEN cDNA C630040K21
-2.34	0.00011676	0.01250870	1429882_at	2610005L07Rik | RIKEN cDNA 2610005L07
-16.60	0.00000000	0.00000089	1429951_at	Ssbp2 | single-stranded DNA binding protein 2
-2.03	0.00000423	0.00103625	1430047_at	Brctd1 | BRCT domain containing 1
-2.21	0.00001205	0.00232315	1430196_at	8430408J09Rik | RIKEN cDNA 8430408J09
-1.68	0.00045456	0.03243868	1430529_at	Csnk1a1 | casein kinase 1, alpha 1
-1.66	0.00051820	0.03488270	1430556_at	Spag9 | sperm associated antigen 9
-1.89	0.00014651	0.01474983	1430829_s_at	Fto | fatso
-4.60	0.00000000	0.00000019	1430979_a_at	Prdx2 | peroxiredoxin 2
-1.79	0.00001378	0.00258220	1431006_at	--- | ---
-1.74	0.00050883	0.03459179	1431044_at	Thoc1 | THO complex 1
-1.79	0.00050236	0.03432881	1431406_at	Agxt2l1 | alanine-glyoxylate aminotransferase 2-like 1
-1.54	0.00068021	0.04140077	1431700_at	Grin2b | glutamate receptor, ionotropic, NMDA2B (epsilon 2)
-1.80	0.00000225	0.00065785	1432606_at	2610012C04Rik | RIKEN cDNA 2610012C04 gene
-5.40	0.00000002	0.00001768	1432646_a_at	EG640370 | predicted gene, EG640370 /// predicted gene, EG667653 /// hypothetical protein LOC672953
-1.54	0.00048820	0.03377012	1433557_at	Cbx7 | chromobox homolog 7
-1.68	0.00016019	0.01577423	1433623_at	Zfp367 | zinc finger protein 367
-1.98	0.00000058	0.00023850	1433685_a_at	C330011F01Rik | RIKEN cDNA C330011F01 gene /// RIKEN cDNA 6430706D22 gene
-1.82	0.00003772	0.00562049	1434045_at	Cdkn1b | cyclin-dependent kinase inhibitor 1B
-5.53	0.00000000	0.00000070	1434171_at	C330011K17Rik | RIKEN cDNA C330011K17
-1.56	0.00006094	0.00792073	1434329_s_at	Adipor2 | adiponectin receptor 2

-7.22	0.00000000	0.00000019	1434340_at	1110020P15Rik | RIKEN cDNA 1110020P15
-2.65	0.00000041	0.00019284	1434341_x_at	1110020P15Rik | RIKEN cDNA 1110020P15
-2.31	0.00000190	0.00059321	1434441_at	1110018J18Rik | RIKEN cDNA 1110018J18
-1.58	0.00007187	0.00885656	1434632_at	--- | Transcribed locus
-2.72	0.00000036	0.00017075	1435129_at	Ptp4a2 | Protein tyrosine phosphatase 4a2
-1.55	0.00016678	0.01610693	1435267_at	A430108E01Rik | RIKEN cDNA A430108E01
-1.53	0.00012764	0.01339458	1435459_at	Fmo2 | flavin containing monooxygenase 2
-3.31	0.00001775	0.00317712	1435521_at	Msi2 | Musashi homolog 2 (Drosophila)
-6.40	0.00000000	0.00000288	1435579_at	4933409K07Rik | RIKEN cDNA 4933409K07
-1.61	0.00005272	0.00705596	1435618_at	Pnma2 | paraneoplastic antigen MA2
-1.84	0.00026505	0.02244810	1435906_x_at	Gbp2 | guanylate nucleotide binding protein 2
-1.57	0.00002708	0.00436178	1436319_at	Sulf1 | sulfatase 1
-2.11	0.00000520	0.00119051	1436356_at	Lgals7 | lectin, galactose binding, soluble 7
-9.51	0.00000000	0.00000002	1436520_at	AI450948 | expressed sequence AI450948
-1.67	0.00069626	0.04220704	1436713_s_at	Gtl2 | GTL2, imprinted maternally expressed untranslated mRNA
-23.45	0.00000000	0.00000140	1436853_a_at	Snca | synuclein, alpha
-1.55	0.00088362	0.05019167	1437142_a_at	Pigo | phosphatidylinositol glycan anchor biosynthesis, class O
-1.61	0.00174730	0.07935159	1437214_at	Lrrtm4 | leucine rich repeat transmembrane neuronal 4
-1.76	0.00000221	0.00065038	1437297_at	Chd8 | chromodomain helicase DNA binding protein 8
-1.55	0.00178900	0.08060530	1437612_at	Nup62 | Nucleoporin 62
-1.56	0.00007266	0.00887786	1437710_x_at	1700021P22Rik | RIKEN cDNA 1700021P22 gene
-1.63	0.00019680	0.01815144	1437717_x_at	2610005L07Rik | RIKEN cDNA 2610005L07 gene /// RIKEN cDNA A430108E01 gene /// similar to p47 protein isoform a
-1.84	0.00003466	0.00529936	1437767_s_at	Fts | fused toes
-1.55	0.00039538	0.02932894	1437878_s_at	Ttc14 | tetratricopeptide repeat domain 14
-1.64	0.00027747	0.02303030	1437892_at	Zfp306 | zinc finger protein 306
-1.79	0.00154506	0.07373929	1437932_a_at	Cldn1 | claudin 1
-1.86	0.00002546	0.00417480	1438041_at	--- | ---
-1.87	0.00000044	0.00019623	1438049_at	A430108E01Rik | RIKEN cDNA A430108E01
-1.88	0.00092514	0.05168821	1438112_at	9430021M05Rik | RIKEN cDNA 9430021M05
-3.74	0.00000001	0.00000697	1438130_at	Taf15 | TAF15 RNA polymerase II, TATA box binding protein (TBP)-associated factor
-2.25	0.00013007	0.01357972	1438211_s_at	Dbp | D site albumin promoter binding protein
-1.90	0.00000393	0.00097383	1438398_at	Rbm39 | RNA binding motif protein 39
-1.61	0.00001124	0.00219733	1438466_at	Dnahc7c | dynein, axonemal, heavy chain 7c /// dynein, axonemal, heavy chain 7b /// dynein heavy chain-related
-3.03	0.00000496	0.00116425	1438528_at	Pcm1 | Pericentriolar material 1
-6.60	0.00000001	0.00000648	1438754_at	--- | ---
-1.60	0.00016445	0.01595031	1438772_at	Zfp367 | zinc finger protein 367
-6.43	0.00000000	0.00000346	1438936_s_at	Ang1 | angiogenin, ribonuclease A family, member 1
-2.88	0.00000377	0.00095086	1438937_x_at	Ang1 | angiogenin, ribonuclease A family, member 1
-10.10	0.00000000	0.00000019	1439059_at	BC031748 | CDNA sequence BC031748
-3.33	0.00000786	0.00168059	1439195_at	--- | ---
-1.53	0.00001486	0.00275812	1439249_at	Wac | WW domain containing adaptor with coiled-coil
-4.01	0.00000004	0.00003269	1439279_at	3110007F17Rik | RIKEN cDNA 3110007F17
-2.28	0.00002375	0.00401822	1439300_at	--- | ---
-1.83	0.00017705	0.01667043	1439406_x_at	Fars2 | phenylalanine-tRNA synthetase 2 (mitochondrial)
-1.76	0.00017479	0.01653714	1439614_at	--- | Transcribed locus
-2.33	0.00005126	0.00692243	1439655_at	Ube2d2 | Ubiquitin-conjugating enzyme E2D 2
-2.64	0.00000240	0.00068030	1439712_at	Ints10 | integrator complex subunit 10
-1.61	0.00213149	0.08723451	1439968_x_at	Dbndd2 | dysbindin (dystrobrevin binding protein 1) domain containing 2
-2.60	0.00001380	0.00258220	1440046_at	BC031748 | cDNA sequence BC031748
-1.57	0.00005175	0.00696687	1440223_at	Rbm6 | RNA binding motif protein 6
-1.58	0.00130192	0.06575361	1440416_at	Usp46 | Ubiquitin specific peptidase 46
-2.06	0.00000386	0.00096272	1440636_at	Mrpl3 | Mitochondrial ribosomal protein L3
-2.53	0.00000068	0.00027664	1440651_at	Dusp16 | Dual specificity phosphatase 16
-2.34	0.00054674	0.03615646	1440771_at	Zkscan1 | zinc finger with KRAB and SCAN domains 1
-1.87	0.00000930	0.00190307	1440781_at	B830007D08Rik | RIKEN cDNA B830007D08

-1.59	0.00001901	0.00336759	1440871_at	Magi1 | membrane associated guanylate kinase, WW and PDZ domain containing 1
-1.67	0.00268890	0.09891671	1440893_at	--- | ---
-2.46	0.00000165	0.00053813	1441100_at	Mbtd1 | mbt domain containing 1
-1.90	0.00001276	0.00243780	1441142_at	2700081L22Rik | RIKEN cDNA 2700081L22 gene
-1.65	0.00023046	0.02030116	1441238_at	9030416H16Rik | RIKEN cDNA 9030416H16 gene
-1.54	0.00032559	0.02552795	1441293_at	EG635504 | Predicted gene, EG635504
-3.32	0.00000043	0.00019623	1441373_at	Msi2 | Musashi homolog 2 (Drosophila)
-3.14	0.00000087	0.00033423	1441404_at	Pafah1b1 | Platelet-activating factor acetylhydrolase, isoform 1b, beta1 subunit
-1.96	0.00000310	0.00082826	1441576_at	2410002O22Rik | RIKEN cDNA 2410002O22 gene
-2.80	0.00000009	0.00006037	1441580_at	Sgpp2 | Sphingosine-1-phosphate phosphotase 2
-1.68	0.00052667	0.03530768	1441604_at	Esd | Esterase D/formylglutathione hydrolase
-2.56	0.00001471	0.00274216	1441643_at	March3 | membrane-associated ring finger (C3HC4) 3
-2.25	0.00002469	0.00409469	1441683_at	1110033M05Rik | RIKEN cDNA 1110033M05 gene
-1.70	0.00004598	0.00646015	1441746_at	--- | ---
-1.51	0.00264661	0.09824273	1441862_at	Ppox | protoporphyrinogen oxidase
-1.61	0.00007567	0.00912504	1441975_at	Acpp | acid phosphatase, prostate
-1.80	0.00002112	0.00366379	1442017_at	Nfs1 | nitrogen fixation gene 1 (S. cerevisiae)
-2.03	0.00000069	0.00027716	1442024_at	Ppp1r3e | Protein phosphatase 1, regulatory (inhibitor) subunit 3E
-1.83	0.00004568	0.00643768	1442188_at	--- | 0 day neonate cerebellum cDNA, RIKEN full-length enriched library, clone:C230031C13 product:unclassifiable, full insert sequence
-1.84	0.00004929	0.00677723	1442201_at	--- | Transcribed locus
-3.97	0.00000015	0.00008819	1442213_at	LOC552908 | hypothetical LOC552908
-1.86	0.00006813	0.00855857	1442279_at	Epc1 | Enhancer of polycomb homolog 1 (Drosophila)
-2.59	0.00000880	0.00183697	1442384_at	--- | Transcribed locus
-2.05	0.00000193	0.00059640	1442447_at	Znrf3 | Zinc and ring finger 3
-3.55	0.00000000	0.00000133	1442742_at	Atp2c1 | ATPase, Ca++-sequestering
-2.52	0.00000005	0.00004066	1442824_at	8030497I03Rik | RIKEN cDNA 8030497I03 gene
-4.43	0.00000002	0.00001816	1442886_at	Tra2a | transformer 2 alpha homolog (Drosophila)
-2.41	0.00000005	0.00003564	1443095_at	--- | ---
-7.41	0.00000000	0.00000315	1443153_at	Trip11 | Thyroid hormone receptor interactor 11
-1.66	0.00007167	0.00885543	1443239_at	Mtap2 | Microtubule-associated protein 2
-1.67	0.00014463	0.01460463	1443256_at	Clca6 | Chloride channel calcium activated 6
-1.63	0.00142430	0.06956862	1443741_x_at	Whsc1 | Wolf-Hirschhorn syndrome candidate 1 (human) /// similar to Wolf-Hirschhorn syndrome candidate 1 protein isoform 1
-1.58	0.00027805	0.02303030	1443778_at	LOC672274 | similar to Transcription factor SOX-4
-1.70	0.00000690	0.00151013	1443858_at	LOC552905 | Hypothetical LOC552905
-1.63	0.00005491	0.00728402	1443876_at	Camk2a | Calcium/calmodulin-dependent protein kinase II alpha
-1.52	0.00009785	0.01108871	1444486_at	Klhl5 | kelch-like 5 (Drosophila)
-2.38	0.00003633	0.00549862	1444517_at	--- | ---
-2.31	0.00000919	0.00189360	1444878_at	Dock10 | Dedicator of cytokinesis 10
-1.64	0.00001942	0.00340833	1444971_at	Rbm5 | RNA binding motif protein 5
-3.22	0.00000369	0.00094457	1445307_at	Auts2 | Autism susceptibility candidate 2
-1.59	0.00067720	0.04127339	1445428_at	--- | ---
-1.53	0.00051815	0.03488270	1445680_x_at	F2rl2 | coagulation factor II (thrombin) receptor-like 2
-1.75	0.00000122	0.00042981	1445724_at	Iqgap1 | IQ motif containing GTPase activating protein 1
-1.52	0.00022098	0.01985323	1445892_at	Per2 | Period homolog 2 (Drosophila)
-1.57	0.00230990	0.09154532	1445957_at	Evl | Ena-vasodilator stimulated phosphoprotein
-1.96	0.00028967	0.02369808	1446102_at	D9Ertd292e | DNA segment, Chr 9, ERATO Doi 292, expressed
-2.57	0.00000360	0.00092904	1446140_at	Pcm1 | Pericentriolar material 1
-3.82	0.00000444	0.00107611	1446144_at	Pex2 | peroxin 2
-1.52	0.00038216	0.02870728	1446220_at	Gm484 | gene model 484, (NCBI)
-1.66	0.00002947	0.00467149	1446391_at	Snca | Synuclein, alpha
-1.82	0.00005080	0.00691246	1446406_at	Paqr8 | Progestin and adipoQ receptor family member VIII

-1.68	0.00007211	0.00886133	1446514_at	Dpp10 | Dipeptidylpeptidase 10
-1.82	0.00000088	0.00033423	1446648_at	Stxbp4 | Syntaxin binding protein 4
-1.54	0.00048086	0.03360991	1446951_at	--- | ---
-1.57	0.00088851	0.05040580	1447147_at	Atg7 | Autophagy-related 7 (yeast)
-1.80	0.00247713	0.09483952	1447176_at	A930008G19Rik | RIKEN cDNA A930008G19
-3.09	0.00000008	0.00005768	1447723_at	--- | 16 days neonate cerebellum cDNA, RIKEN full-length enriched library, clone:9630018J10 product:unclassifiable, full insert sequence
-1.51	0.00027150	0.02280286	1447937_a_at	4933409K07Rik | RIKEN cDNA 4933409K07 gene /// similar to 4933409K07Rik protein /// similar to 4933409K07Rik protein /// hypothetical protein LOC622738 /// similar to similar to 4933409K07Rik protein /// hypothetical protein LOC665845
-1.59	0.00016953	0.01623366	1448293_at	--- | ---
-1.84	0.00000235	0.00067062	1448395_at	Sfrp1 | secreted frizzled-related sequence protein 1
-1.84	0.00027587	0.02300792	1449025_at	Ifit3 | interferon-induced protein with tetratricopeptide repeats 3
-3.72	0.00007474	0.00903709	1449347_a_at	Xlr4b | X-linked lymphocyte-regulated 4B /// X-linked lymphocyte-regulated 4A /// X-linked lymphocyte-regulated 4E
-4.17	0.00000013	0.00007612	1449603_at	AI594671 | expressed sequence AI594671
-2.05	0.00000519	0.00119051	1449874_at	Ly96 | lymphocyte antigen 96
-2.05	0.00000166	0.00053813	1450154_at	Folh1 | folate hydrolase
-3.51	0.00001518	0.00280500	1450170_x_at	H2-K1 | Histocompatibility 2, K1, K region
-1.53	0.00021213	0.01917322	1450391_a_at	Mgll | monoglyceride lipase
-1.63	0.00011062	0.01209404	1450702_at	Hfe | hemochromatosis
-2.27	0.00005196	0.00697436	1450783_at	Ifit1 | interferon-induced protein with tetratricopeptide repeats 1
-3.42	0.00000012	0.00007507	1450933_at	Pde7a | phosphodiesterase 7A
-1.72	0.00005434	0.00722969	1451022_at	Lrp6 | low density lipoprotein receptor-related protein 6
-2.06	0.00000016	0.00009301	1451146_at	Zfp386 | zinc finger protein 386 (Kruppel-like) /// similar to zinc finger protein 386 (Kruppel-like) isoform a
-3.88	0.00000000	0.00000353	1451411_at	Gprc5b | G protein-coupled receptor, family C, group 5, member B
-1.67	0.00017318	0.01651064	1451478_at	Angptl7 | angiopoietin-like 7
-1.62	0.00000978	0.00197885	1451555_at	Nln | neurolysin (metallopeptidase M3 family)
-1.69	0.00011978	0.01277144	1451777_at	BC013672 | cDNA sequence BC013672
-1.76	0.00000482	0.00114258	1451993_at	9130404D08Rik | RIKEN cDNA 9130404D08 gene
-1.51	0.00269683	0.09912789	1452401_at	Wtap | Wilms tumour 1-associating protein
-1.80	0.00005606	0.00741472	1452439_s_at	Sfrs2 | splicing factor, arginine/serine-rich 2 (SC-35)
-1.68	0.00000986	0.00198611	1452442_at	Usp13 | Ubiquitin specific peptidase 13 (isopeptidase T-3)
-1.68	0.00003589	0.00544991	1452640_at	3110007F17Rik | RIKEN cDNA 3110007F17 gene /// predicted gene, EG546368 /// predicted gene, EG625591
-1.99	0.00000169	0.00054346	1452730_at	1110033J19Rik | RIKEN cDNA 1110033J19
-8.19	0.00000000	0.00000288	1452907_at	Galc | galactosylceramidase
-1.79	0.00000709	0.00153674	1452997_at	2610005L07Rik | RIKEN cDNA 2610005L07
-1.63	0.00000386	0.00096272	1453196_a_at	Oasl2 | 2-5 oligoadenylate synthetase-like 2
-1.95	0.00000213	0.00063714	1453332_at	2410002O22Rik | RIKEN cDNA 2410002O22
-1.68	0.00002204	0.00377611	1453377_at	Sh2d4a | SH2 domain containing 4ª
-1.54	0.00005093	0.00691246	1453589_a_at	2610005L07Rik | RIKEN cDNA 2610005L07
-1.69	0.00006290	0.00810550	1453836_a_at	Mgll | monoglyceride lipase
-1.67	0.00022553	0.02005773	1453841_at	2310050P20Rik | RIKEN cDNA 2310050P20
-1.66	0.00045878	0.03263642	1454232_at	9430027B09Rik | RIKEN cDNA 9430027B09
-2.04	0.00000020	0.00010826	1454686_at	C330011F01Rik | RIKEN cDNA C330011F01 gene /// RIKEN cDNA 6430706D22 gene
-1.52	0.00054998	0.03631698	1454904_at	Mtm1 | X-linked myotubular myopathy gene 1
-2.16	0.00000275	0.00074603	1455213_at	4930488E11Rik | RIKEN cDNA 4930488E11
-1.53	0.00024217	0.02096414	1455647_at	Ar | androgen receptor
-1.61	0.00000549	0.00124431	1455649_at	Ttc9 | tetratricopeptide repeat domain 9
-1.65	0.00003095	0.00486389	1455657_at	2610207I05Rik | RIKEN cDNA 2610207I05
-6.92	0.00000000	0.00000144	1455715_at	2610044O15Rik | RIKEN cDNA 2610044O15
-1.59	0.00004407	0.00628986	1455849_at	--- | ---
-1.84	0.00002210	0.00377611	1455933_at	Tra2a | transformer 2 alpha homolog (Drosophila)

-1.62	0.00030307	0.02436654	1456288_at	Slfn5 | schlafen 5
-1.82	0.00001669	0.00301035	1456351_at	Brd8 | bromodomain containing 8
-2.15	0.00000096	0.00034677	1456386_at	Rbm39 | RNA binding motif protein 39
-1.65	0.00003873	0.00568645	1456430_at	Ttc14 | tetratricopeptide repeat domain 14
-2.11	0.00026529	0.02244810	1456532_at	Pdgfd | Platelet-derived growth factor, D polypeptide
-1.87	0.00000944	0.00191800	1456570_at	Epb4.1l4b | Erythrocyte protein band 4.1-like 4b
-1.55	0.00008459	0.00985826	1456596_at	6430550H21Rik | RIKEN cDNA 6430550H21
-1.51	0.00004977	0.00682324	1456748_a_at	Nipsnap1 | 4-nitrophenylphosphatase domain and non-neuronal SNAP25-like protein homolog 1 (C. elegans)
-1.93	0.00016902	0.01623366	1456775_at	Ints8 | integrator complex subunit 8
-3.42	0.00000198	0.00060711	1456781_at	--- | 10 days neonate cortex cDNA, RIKEN full-length enriched library, clone:A830044L07 product:unclassifiable, full insert sequence
-1.68	0.00002660	0.00431545	1456807_at	Ppp1r3e | protein phosphatase 1, regulatory (inhibitor) subunit 3E
-2.79	0.00000004	0.00003269	1456911_at	Clasp2 | CLIP associating protein 2
-1.51	0.00186902	0.08270928	1456943_a_at	Dbndd2 | dysbindin (dystrobrevin binding protein 1) domain containing 2
-1.85	0.00002706	0.00436178	1456947_at	Pafah1b1 | Platelet-activating factor acetylhydrolase, isoform 1b, beta1 subunit
-2.81	0.00000006	0.00004204	1457231_at	Hif1a | Hypoxia inducible factor 1, alpha subunit
-2.18	0.00000025	0.00012695	1457259_at	--- | Transcribed locus
-2.04	0.00000107	0.00038189	1457262_at	2610207I05Rik | RIKEN cDNA 2610207I05
-2.66	0.00000170	0.00054382	1457324_at	4933409K07Rik | RIKEN cDNA 4933409K07 gene
-1.68	0.00076865	0.04555450	1457350_at	Per2 | period homolog 2 (Drosophila)
-1.56	0.00004054	0.00589794	1457483_at	Arid5b | AT rich interactive domain 5B (Mrf1 like)
-1.84	0.00046484	0.03270661	1457551_at	Acvr1 | Activin A receptor, type 1
-1.65	0.00039721	0.02936812	1457658_x_at	Anxa4 | annexin A4
-2.75	0.00000084	0.00032889	1457724_at	Ctsl | cathepsin L
-1.76	0.00051005	0.03459179	1457839_at	Dhx40 | DEAH (Asp-Glu-Ala-His) box polypeptide 40
-1.52	0.00039395	0.02932894	1457934_at	Rbm12 | RNA binding motif protein 12
-2.09	0.00004440	0.00629722	1457969_at	Rabif | RAB interacting factor
-2.26	0.00000609	0.00136526	1458003_at	Zfp398 | zinc finger protein 398
-1.94	0.00008642	0.00996881	1458123_at	9630002A11Rik | RIKEN cDNA 9630002A11
-1.76	0.00205917	0.08588374	1458147_at	Mamdc1 | MAM domain containing 1
-2.17	0.00000073	0.00029013	1458188_at	Dpysl2 | Dihydropyrimidinase-like 2
-1.52	0.00015240	0.01520706	1458220_at	Dlc1 | deleted in liver cancer 1
-1.69	0.00006770	0.00852942	1458317_at	Eml1 | Echinoderm microtubule associated protein like 1
-1.54	0.00005863	0.00768729	1458400_at	9630050P21Rik | RIKEN cDNA 9630050P21 gene
-1.66	0.00017946	0.01675741	1458586_at	--- | ---
-1.72	0.00013905	0.01431286	1458669_at	--- | Transcribed locus
-1.72	0.00084453	0.04902061	1458684_at	Ss18 | synovial sarcoma translocation, Chromosome 18
-1.87	0.00202840	0.08549783	1458719_at	--- | Transcribed locus
-1.87	0.00056083	0.03655202	1458892_at	9430047G12Rik | RIKEN cDNA 9430047G12 gene
-1.99	0.00123162	0.06329239	1459224_at	Ppp1r13b | Protein phosphatase 1, regulatory (inhibitor) subunit 13B
-2.05	0.00010399	0.01160912	1459450_at	Chd9 | Chromodomain helicase DNA binding protein 9
-1.66	0.00030667	0.02461036	1459475_at	D10Ertd761e | DNA segment, Chr 10, ERATO Doi 761, expressed
-2.01	0.00002175	0.00374490	1459710_at	--- | Transcribed locus
-14.93	0.00000000	0.00000033	1459747_at	--- | ---
-1.93	0.00010740	0.01184366	1460045_at	Cdh7 | cadherin 7, type 2
-1.58	0.00002389	0.00401822	1460330_at	Anxa3 | annexin A3
-2.48	0.00000044	0.00019623	1460587_at	B230215L15Rik | RIKEN cDNA B230215L15

List of upregulated genes

Fold change < 1,5; P value (LIMMA) < 0,05; FDR value (LIMMA) < 0,1

fold change	pval	FDR	probe ID	gene symbol
+1.51	0.00022398	0.02000378	1460592_at	Epb4.1l1 | erythrocyte protein band 4.1-like 1
+2.12	0.00000023	0.00011709	1460466_at	1700047I17Rik | RIKEN cDNA 1700047I17 gene /// similar to signal recognition particle 54
+2.45	0.00026182	0.02228006	1460187_at	Sfrp1 | secreted frizzled-related sequence protein 1
+1.88	0.00000541	0.00123185	1460167_at	Aldh7a1 | aldehyde dehydrogenase family 7, member A1
+1.74	0.00013263	0.01371920	1460113_at	B930093H17Rik | RIKEN cDNA B930093H17 gene
+1.73	0.00000266	0.00073183	1460102_at	Clasp1 | CLIP associating protein 1
+2.81	0.00003801	0.00562049	1460092_at	Lsamp | Limbic system-associated membrane protein
+2.40	0.00000008	0.00005632	1459698_at	EG622320 | Predicted gene, EG622320
+1.62	0.00015573	0.01547042	1459609_at	Arhgap10 | Rho GTPase activating protein 10
+8.86	0.00000000	0.00000168	1459253_at	Arrdc3 | Arrestin domain containing 3
+1.58	0.00125590	0.06407507	1459197_at	--- | ---
+2.71	0.00000300	0.00080438	1458886_at	--- | ---
+1.65	0.00212140	0.08713776	1458693_at	Scn8a | Sodium channel, voltage-gated, type VIII, alpha
+4.87	0.00000000	0.00000027	1458585_at	--- | Transcribed locus
+2.18	0.00007933	0.00943823	1458541_at	Dctn4 | dynactin 4
+2.19	0.00000463	0.00111054	1458324_x_at	--- | 16 days embryo head cDNA, RIKEN full-length enriched library, clone:C130051K14 product:unclassifiable, full insert sequence
+7.90	0.00000000	0.00000006	1458240_at	Magi1 | Membrane associated guanylate kinase, WW and PDZ domain containing 1
+1.81	0.00154870	0.07383503	1458203_at	Spire1 | Spire homolog 1 (Drosophila)
+1.97	0.00023423	0.02051227	1458128_at	1110028C15Rik | RIKEN cDNA 1110028C15
+2.00	0.00000253	0.00070875	1457751_at	4832420A03Rik | RIKEN cDNA 4832420A03
+1.69	0.00002145	0.00370663	1457712_at	Chd8 | chromodomain helicase DNA binding protein 8
+1.57	0.00060292	0.03857259	1457651_x_at	Rem2 | rad and gem related GTP binding protein 2
+1.87	0.00000767	0.00165525	1457338_at	Ppp1r12b | Protein phosphatase 1, regulatory (inhibitor) subunit 12B
+2.07	0.00000219	0.00064926	1457306_at	--- | Transcribed locus
+1.53	0.00002849	0.00454056	1457270_at	B230343A10Rik | RIKEN cDNA B230343A10
+2.37	0.00006952	0.00870910	1457257_x_at	--- | 0 day neonate lung cDNA, RIKEN full-length enriched library, clone:E030046E07 product:unclassifiable, full insert sequence
+1.59	0.00004880	0.00673116	1457140_s_at	4632411J06Rik | RIKEN cDNA 4632411J06 gene
+1.59	0.00013936	0.01431286	1457040_at	Lgi2 | leucine-rich repeat LGI family, member 2
+1.54	0.00008492	0.00986517	1456981_at	Tmc7 | transmembrane channel-like gene family 7
+2.20	0.00014941	0.01497497	1456663_x_at	Tm2d2 | TM2 domain containing 2
+1.96	0.00000115	0.00040892	1456449_at	Supt16h | Suppressor of Ty 16 homolog (S. cerevisiae)
+1.53	0.00001110	0.00219581	1456293_s_at	Ccnh | cyclin H /// similar to cyclin H
+2.05	0.00025064	0.02149082	1456187_at	Slc7a14 | solute carrier family 7 (cationic amino acid transporter, y+ system), member 14
+1.54	0.00181973	0.08150112	1456084_x_at	Fmod | fibromodulin
+1.53	0.00004426	0.00629704	1455806_x_at	Ndufa12 | NADH dehydrogenase (ubiquinone) 1 alpha subcomplex, 12 /// similar to 13kDa differentiation-associated protein
+3.16	0.00000200	0.00060926	1455773_at	--- | ---
+3.60	0.00000211	0.00063413	1455600_at	Rps3 | ribosomal protein S3
+2.04	0.00000090	0.00033860	1455452_x_at	AI449310 | expressed sequence AI449310
+1.92	0.00001629	0.00297366	1455444_at	Gabra2 | gamma-aminobutyric acid (GABA-A) receptor, subunit alpha 2
+2.92	0.00003250	0.00503695	1455380_at	Pcyox1l | prenylcysteine oxidase 1 like
+1.61	0.00216099	0.08788354	1455277_at	Hhip | Hedgehog-interacting protein
+1.66	0.00002048	0.00357958	1455012_s_at	Trim37 | tripartite motif protein 37

+1.93	0.00000646	0.00142755	1454950_at	B930006L02Rik | RIKEN cDNA B930006L02
+1.58	0.00015637	0.01549946	1454924_at	Fut10 | fucosyltransferase 10
+2.09	0.00016220	0.01586875	1454817_at	Utp18 | UTP18, small subunit (SSU) processome component, homolog (yeast)
+1.62	0.00041498	0.03038302	1454159_a_at	Igfbp2 | insulin-like growth factor binding protein 2
+1.82	0.00050949	0.03459179	1454040_at	5730591J02Rik | RIKEN cDNA 5730591J02
+2.31	0.00000012	0.00007507	1453791_at	2810449C10Rik | RIKEN cDNA 2810449C10 gene
+1.93	0.00000484	0.00114258	1453755_at	Lsm11 | U7 snRNP-specific Sm-like protein LSM11
+1.56	0.00056715	0.03682474	1453744_a_at	Ankrd40 | ankyrin repeat domain 40
+3.16	0.00000003	0.00002901	1453715_at	Sv2c | synaptic vesicle glycoprotein 2c
+1.86	0.00000995	0.00199370	1453698_at	6030451C04Rik | RIKEN cDNA 6030451C04
+1.53	0.00014433	0.01460463	1453550_a_at	Mlstd2 | male sterility domain containing 2
+1.57	0.00034422	0.02613560	1453540_at	5430404G13Rik | RIKEN cDNA 5430404G13
+1.53	0.00021105	0.01911366	1453485_s_at	1110005A03Rik | RIKEN cDNA 1110005A03
+1.51	0.00008339	0.00977157	1453179_at	Phca | phytoceramidase, alkaline
+1.66	0.00003787	0.00562049	1452947_at	Gprc5c | G protein-coupled receptor, family C, group 5, member C
+1.67	0.00009235	0.01054441	1452754_at	Creld2 | cysteine-rich with EGF-like domains 2
+1.96	0.00000806	0.00170718	1452590_a_at	Plac9 | placenta specific 9
+1.51	0.00071815	0.04324332	1452462_a_at	Banp | Btg3 associated nuclear protein
+5.23	0.00000001	0.00001259	1452406_x_at	Erdr1 | erythroid differentiation regulator 1
+1.76	0.00005909	0.00771968	1452366_at	4732435N03Rik | RIKEN cDNA 4732435N03
+1.72	0.00001167	0.00226883	1452365_at	4732435N03Rik | RIKEN cDNA 4732435N03 gene
+1.54	0.00001227	0.00235575	1452258_at	Phf20 | PHD finger protein 20
+2.39	0.00000053	0.00022142	1451602_at	Snx6 | sorting nexin 6
+1.51	0.00141050	0.06929719	1451542_at	Ssbp2 | single-stranded DNA binding protein 2
+2.96	0.00000095	0.00034569	1451513_x_at	Serpina1a | serine (or cysteine) peptidase inhibitor, clade A, member 1a /// serine (or cysteine) preptidase inhibitor, clade A, member 1b
+2.77	0.00000009	0.00006242	1451447_at	Cuedc1 | CUE domain containing 1
+1.57	0.00042758	0.03100384	1451336_at	Lgals4 | lectin, galactose binding, soluble 4
+2.03	0.00000815	0.00171275	1451319_at	Senp1 | SUMO1/sentrin specific peptidase 1
+1.62	0.00053438	0.03570524	1451198_at	Gatad2a | GATA zinc finger domain containing 2A
+1.55	0.00098614	0.05377974	1450852_s_at	F2r | coagulation factor II (thrombin) receptor
+1.85	0.00034045	0.02610226	1450843_a_at	Serpinh1 | serine (or cysteine) peptidase inhibitor, clade H, member 1
+1.81	0.00001120	0.00219733	1450523_at	Cntn2 | contactin 2
+2.01	0.00044723	0.03206776	1450483_at	Gja12 | gap junction membrane channel protein alpha 12
+2.14	0.00000035	0.00016787	1450470_at	--- | ---
+2.24	0.00007110	0.00883346	1450208_a_at	Elmo1 | engulfment and cell motility 1, ced-12 homolog (C. elegans)
+1.56	0.00057020	0.03686671	1450089_a_at	Srprb | signal recognition particle receptor, B subunit
+1.53	0.00209496	0.08659531	1449936_at	8430419L09Rik | RIKEN cDNA 8430419L09
+1.65	0.00191694	0.08343713	1449866_at	Syt2 | synaptotagmin II
+5.00	0.00000003	0.00002441	1449578_at	Supt16h | suppressor of Ty 16 homolog (S. cerevisiae)
+2.69	0.00000050	0.00021592	1449491_at	Card10 | caspase recruitment domain family, member 10
+1.60	0.00002500	0.00411548	1449148_a_at	Phtf1 | putative homeodomain transcription factor 1
+1.53	0.00062801	0.03933900	1449135_at	Sox18 | SRY-box containing gene 18
+1.74	0.00001873	0.00333907	1448908_at	Ppap2b | phosphatidic acid phosphatase type 2B
+2.00	0.00024137	0.02093483	1448756_at	S100a9 | S100 calcium binding protein A9 (calgranulin B)
+1.53	0.00019526	0.01804617	1448698_at	Ccnd1 | cyclin D1
+2.59	0.00004354	0.00623339	1448680_at	Serpina1c | serine (or cysteine) peptidase inhibitor, clade A, member 1c
+1.55	0.00202118	0.08535341	1448397_at	Gjb6 | gap junction membrane channel protein beta 6
+1.60	0.00204771	0.08588374	1448229_s_at	Ccnd2 | cyclin D2
+1.65	0.00007694	0.00922639	1448140_at	Ciapin1 | cytokine induced apoptosis inhibitor 1
+25.93	0.00000000	0.00000019	1447831_s_at	Mtmr7 | myotubularin related protein 7
+1.87	0.00003781	0.00562049	1447808_s_at	Slc15a2 | solute carrier family 15 (H+/peptide transporter), member 2
+1.60	0.00033820	0.02599164	1447745_at	Aqp4 | aquaporin 4

+1.96	0.00000226	0.00065802	1447396_at	LOC545253 | Hypothetical protein LOC545253
+1.52	0.00034328	0.02611784	1446981_at	A830010M20Rik | RIKEN cDNA A830010M20
+1.62	0.00066817	0.04088909	1446598_at	Prkca | Protein kinase C, alpha
+1.93	0.00000266	0.00073183	1446445_at	--- | 12 days embryo spinal ganglion cDNA, RIKEN full-length enriched library, clone:D130018F08 product:unclassifiable, full insert sequence
+1.57	0.00012289	0.01304156	1446357_at	BC020402 | cDNA sequence BC020402
+2.25	0.00003727	0.00562049	1446332_at	Pcdhgc3 | Protocadherin gamma subfamily C, 3
+1.69	0.00010717	0.01184366	1446155_at	--- | 11 days embryo head cDNA, RIKEN full-length enriched library, clone:6230415F21 product:unclassifiable, full insert sequence
+2.41	0.00000091	0.00033860	1446148_x_at	C79248 | expressed sequence C79248
+2.72	0.00000048	0.00021249	1446147_at	C79248 | expressed sequence C79248
+3.44	0.00000004	0.00003180	1446130_at	Pctk2 | PCTAIRE-motif protein kinase 2
+2.32	0.00002397	0.00401822	1445710_x_at	1110051B16Rik | RIKEN cDNA 1110051B16
+1.60	0.00092655	0.05168821	1445618_at	--- | ---
+2.50	0.00000371	0.00094559	1445281_a_at	B230311B06Rik | RIKEN cDNA B230311B06
+2.08	0.00002497	0.00411548	1445235_at	Ythdf3 | YTH domain family 3
+1.51	0.00232765	0.09192574	1445104_at	E230029C05Rik | RIKEN cDNA E230029C05
+1.61	0.00008146	0.00961716	1444801_at	2900041M22Rik | RIKEN cDNA 2900041M22
+1.63	0.00001615	0.00296171	1444714_at	LOC667452 | Similar to Doublecortin domain-containing protein 2
+3.57	0.00000019	0.00010090	1444260_at	--- | Transcribed locus
+2.50	0.00001285	0.00244503	1444198_at	--- | ---
+2.15	0.00000191	0.00059321	1444195_at	Rmnd5a | Required for meiotic nuclear division 5 homolog A (S. cerevisiae)
+6.41	0.00000000	0.00000011	1444128_at	Pip5k2b | Phosphatidylinositol-4-phosphate 5-kinase, type II, beta
+2.93	0.00000050	0.00021592	1444037_at	Lman1 | lectin, mannose-binding, 1
+1.87	0.00004669	0.00651934	1443922_at	Rcor3 | REST corepressor 3
+2.51	0.00000003	0.00002901	1443904_at	Fads6 | fatty acid desaturase domain family, member 6
+1.53	0.00050235	0.03432881	1443882_at	--- | Transcribed locus
+2.24	0.00000057	0.00023850	1443865_at	Gabra2 | gamma-aminobutyric acid (GABA-A) receptor, subunit alpha 2
+1.88	0.00000152	0.00050708	1443799_at	--- | ---
+2.38	0.00000141	0.00048182	1443212_at	Large | Like-glycosyltransferase
+1.63	0.00242385	0.09398547	1443127_at	9630021D06Rik | RIKEN cDNA 9630021D06
+1.65	0.00001723	0.00309657	1443087_at	Cdc23 | CDC23 (cell division cycle 23, yeast, homolog)
+2.99	0.00000002	0.00002180	1443020_at	Hmbox1 | Homeobox containing 1
+3.54	0.00000000	0.00000140	1442916_at	Psd3 | Pleckstrin and Sec7 domain containing 3
+1.58	0.00008509	0.00986517	1442725_at	--- | ---
+2.32	0.00000017	0.00009328	1442654_at	A530054K11Rik | RIKEN cDNA A530054K11
+1.53	0.00003741	0.00562049	1442624_at	C920008N22Rik | RIKEN cDNA C920008N22
+1.60	0.00020688	0.01900314	1442256_at	Prkcd | protein kinase C, delta
+2.66	0.00001035	0.00206562	1442019_at	Rcvrn | Recoverin
+1.79	0.00210687	0.08676338	1441978_at	Aqp6 | aquaporin 6
+2.86	0.00000011	0.00006930	1441493_at	Erc1 | ELKS/RAB6-interacting/CAST family member 1
+1.75	0.00000148	0.00049927	1440989_at	--- | ---
+2.61	0.00000005	0.00003725	1440699_at	--- | ---
+1.75	0.00085601	0.04943268	1440342_at	G530011O06Rik | RIKEN cDNA G530011O06
+8.59	0.00000000	0.00000017	1440142_s_at	Gfap | glial fibrillary acidic protein
+2.30	0.00041382	0.03034765	1440139_at	Nedd4l | Neural precursor cell expressed, developmentally down-regulated gene 4-like
+3.03	0.00000004	0.00003269	1440125_at	A530054K11Rik | RIKEN cDNA A530054K11
+1.51	0.00006327	0.00812959	1440081_at	Cep192 | centrosomal protein 192
+1.52	0.00003290	0.00506585	1440071_at	Magi1 | membrane associated guanylate kinase, WW and PDZ domain containing 1
+2.07	0.00000918	0.00189360	1439998_at	Jmjd1c | jumonji domain containing 1C
+2.60	0.00000050	0.00021592	1439843_at	Camk4 | calcium/calmodulin-dependent protein kinase IV
+1.60	0.00000455	0.00109817	1439578_at	Lsm11 | U7 snRNP-specific Sm-like protein LSM11
+3.60	0.00000000	0.00000181	1439538_at	Ccdc127 | coiled-coil domain containing 127
+1.68	0.00154463	0.07373929	1439422_a_at	C1qdc2 | C1q domain containing 2
+2.11	0.00076287	0.04527111	1439364_a_at	Mmp2 | matrix metallopeptidase 2
+2.65	0.00000030	0.00014968	1439336_at	Tcf4 | Transcription factor 4

+2.09	0.00000374	0.00094681	1439272_at	Lcorl | ligand dependent nuclear receptor corepressor-like
+1.86	0.00002396	0.00401822	1439241_x_at	Srd5a2l | steroid 5 alpha-reductase 2-like
+6.02	0.00000000	0.00000089	1439200_x_at	--- | ---
+4.72	0.00000019	0.00010370	1439170_at	--- | ---
+2.22	0.00003213	0.00501412	1439138_at	2310035C23Rik | RIKEN cDNA 2310035C23
+1.56	0.00008558	0.00989666	1438980_x_at	4732466D17Rik | RIKEN cDNA 4732466D17
+2.97	0.00000251	0.00070859	1438862_at	A630005I04Rik | RIKEN cDNA A630005I04
+1.82	0.00000346	0.00089641	1438756_at	Ankrd29 | ankyrin repeat domain 29
+1.71	0.00032761	0.02560742	1438730_at	BC028801 | cDNA sequence BC028801
+1.77	0.00010532	0.01169911	1438642_at	--- | ---
+1.54	0.00240993	0.09386038	1438590_at	Rapgef3 | Rap guanine nucleotide Exchange factor (GEF) 3
+2.31	0.00000087	0.00033423	1438543_at	Spata13 | Spermatogenesis associated 13
+1.64	0.00001933	0.00340609	1438491_x_at	A530054K11Rik | RIKEN cDNA A530054K11
+1.71	0.00000816	0.00171275	1438444_at	Spink10 | serine peptidase inhibitor, Kazal type 10
+4.22	0.00000001	0.00000648	1438435_at	Phca | phytoceramidase, alkaline
+1.66	0.00002788	0.00447468	1438418_at	4932432K03Rik | RIKEN cDNA 4932432K03
+1.53	0.00074210	0.04433069	1438188_x_at	Slc25a29 | solute carrier family 25 (mitochondrial carrier, palmitoylcarnitine transporter), member 29
+2.05	0.00000131	0.00045528	1438187_at	Slc25a29 | solute carrier family 25 (mitochondrial carrier, palmitoylcarnitine transporter), member 29
+1.63	0.00018640	0.01733402	1438183_x_at	Sord | sorbitol dehydrogenase
+1.76	0.00008341	0.00977157	1438123_at	--- | ---
+2.10	0.00000344	0.00089641	1437923_at	AI314760 | expressed sequence AI314760
+1.99	0.00000067	0.00027488	1437432_a_at	Trim12 | tripartite motif protein 12
+1.84	0.00000503	0.00116944	1437388_at	Fut10 | fucosyltransferase 10
+1.68	0.00002570	0.00420036	1437308_s_at	F2r | coagulation factor II (thrombin) receptor
+2.42	0.00002365	0.00401822	1437126_at	Immt | Inner membrane protein, mitochondrial
+1.52	0.00014475	0.01460463	1437018_at	Pnma2 | paraneoplastic antigen MA2
+3.63	0.00000436	0.00106271	1436734_at	E130309F12Rik | RIKEN cDNA E130309F12
+6.91	0.00000000	0.00000052	1436733_at	E130309F12Rik | RIKEN cDNA E130309F12
+1.64	0.00001904	0.00336759	1436544_at	Atp10d | ATPase, Class V, type 10D
+71.49	0.00000000	0.00000000	1436240_at	Sost | sclerostin
+2.06	0.00004207	0.00608153	1436239_at	Slc5a5 | solute carrier family 5 (sodium iodide symporter), member 5
+1.83	0.00012905	0.01350417	1436148_at	--- | Adult male olfactory brain cDNA, RIKEN full-length enriched library, clone:6430531K17 product:unclassifiable, full insert sequence
+2.40	0.00000005	0.00003631	1436133_at	Ccdc127 | coiled-coil domain containing 127
+1.69	0.00022250	0.01993242	1436090_at	Enpp6 | ectonucleotide pyrophosphatase/phosphodiesterase 6
+1.80	0.00003397	0.00521089	1435998_at	Gm288 | gene model 288, (NCBI)
+2.04	0.00000123	0.00042981	1435929_at	LOC677429 | similar to RIKEN cDNA 9630033F20 gene
+8.54	0.00000000	0.00000003	1435792_at	Csprs | component of Sp100-rs /// predicted gene, EG665338
+1.66	0.00003883	0.00568645	1435491_at	9830167H18Rik | RIKEN cDNA 9830167H18
+1.52	0.00002835	0.00453333	1435417_at	AI464131 | expressed sequence AI464131
+2.23	0.00000885	0.00183952	1435166_at	Cntn2 | contactin 2
+1.63	0.00205827	0.08588374	1434902_at	Rnf157 | ring finger protein 157
+2.67	0.00012662	0.01334234	1434585_at	2210038L17Rik | RIKEN cDNA 2210038L17
+1.61	0.00011075	0.01209404	1434554_at	Trim37 | tripartite motif protein 37
+1.54	0.00025478	0.02172153	1434510_at	Papss2 | 3-phosphoadenosine 5-phosphosulfate synthase 2
+1.63	0.00098303	0.05376307	1434449_at	Aqp4 | aquaporin 4
+3.12	0.00000000	0.00000288	1434375_at	B930006L02Rik | RIKEN cDNA B930006L02
+2.53	0.00000088	0.00033423	1434374_at	B930006L02Rik | RIKEN cDNA B930006L02
+1.64	0.00001581	0.00291067	1434296_at	BC049349 | cDNA sequence BC049349
+1.65	0.00000399	0.00098457	1434208_at	2900057K09Rik | RIKEN cDNA 2900057K09
+2.06	0.00000039	0.00018539	1433906_at	4933402J24Rik | RIKEN cDNA 4933402J24
+2.00	0.00006741	0.00852942	1433774_x_at	Cog1 | component of oligomeric golgi complex 1
+1.51	0.00048949	0.03380777	1432304_a_at	9030624J02Rik | RIKEN cDNA 9030624J02
+2.16	0.00000323	0.00085093	1432130_a_at	Ttc14 | tetratricopeptide repeat domain 14
+1.94	0.00000780	0.00167530	1431821_a_at	Eps8l1 | EPS8-like 1

+8.08	0.00000000	0.00000116	1431708_a_at	Tia1 | cytotoxic granule-associated RNA binding protein 1
+1.70	0.00000233	0.00067062	1431684_at	4933402J24Rik | RIKEN cDNA 4933402J2
+2.33	0.00000703	0.00153193	1431255_at	Calr3 | calreticulin 3
+1.88	0.00026684	0.02249455	1431225_at	Sox11 | SRY-box containing gene 11
+1.56	0.00006508	0.00831378	1431207_at	2900024O10Rik | RIKEN cDNA 2900024O10
+1.59	0.00056746	0.03682474	1430971_a_at	Aqr | aquarius
+1.91	0.00000092	0.00033860	1430889_a_at	Tpmt | thiopurine methyltransferase
+1.52	0.00070906	0.04275296	1430667_at	Pcdh10 | protocadherin 10
+4.04	0.00000000	0.00000279	1430485_at	3010009O07Rik | RIKEN cDNA 3010009O07
+4.21	0.00000001	0.00001259	1430352_at	A730049H05Rik | RIKEN cDNA A730049H05
+1.55	0.00130517	0.06584412	1430317_at	Ube2j2 | ubiquitin-conjugating enzyme E2, J2 homolog (yeast)
+1.94	0.00001649	0.00298617	1429926_at	6720473G16Rik | RIKEN cDNA 6720473G16
+1.66	0.00011276	0.01225490	1429784_at	C130032J12Rik | RIKEN cDNA C130032J12 gene
+1.84	0.00007349	0.00893411	1429463_at	Prkaa2 | protein kinase, AMP-activated, alpha 2 catalytic subunit
+1.79	0.00010157	0.01139489	1429443_at	Cpne4 | copine IV
+2.63	0.00000002	0.00002093	1429331_at	4632427E13Rik | RIKEN cDNA 4632427E13 gene
+1.77	0.00000652	0.00143378	1429184_at	Gvin1 | GTPase, very large interferon inducible 1
+1.75	0.00000498	0.00116425	1429076_a_at	Gdpd2 | glycerophosphodiester phosphodiesterase domain containing 2
+1.60	0.00208825	0.08659531	1429023_at	2900042E01Rik | RIKEN cDNA 2900042E01
+2.50	0.00000015	0.00008566	1428738_a_at	D14Ertd449e | DNA segment, Chr 14, ERATO Doi 449, expressed
+1.52	0.00086088	0.04946051	1428343_at	Rcor3 | REST corepressor 3
+1.67	0.00001125	0.00219733	1428302_at	Mrpl48 | mitochondrial ribosomal protein L48
+1.54	0.00259231	0.09732058	1428023_at	3110009E18Rik | RIKEN cDNA 3110009E18
+1.87	0.00029005	0.02369808	1426876_at	4732466D17Rik | RIKEN cDNA 4732466D17
+2.09	0.00000017	0.00009328	1426704_at	Gak | cyclin G associated kinase
+1.92	0.00000133	0.00045946	1426584_a_at	Sord | sorbitol dehydrogenase
+2.06	0.00000072	0.00028649	1426544_a_at	Ttc14 | tetratricopeptide repeat domain 14
+1.53	0.00013186	0.01367180	1426519_at	P4ha1 | procollagen-proline, 2-oxoglutarate 4-dioxygenase (proline 4-hydroxylase), alpha 1 polypeptide
+1.76	0.00027363	0.02289571	1426361_at	Zc3h11a | zinc finger CCCH type containing 11A
+1.75	0.00001172	0.00226883	1426360_at	Zc3h11a | zinc finger CCCH type containing 11A
+1.69	0.00004317	0.00622053	1426359_at	Zc3h11a | zinc finger CCCH type containing 11A
+1.54	0.00017490	0.01653714	1426008_a_at	Slc7a2 | solute carrier family 7 (cationic amino acid transporter, y+ system), member 2
+2.06	0.00000175	0.00055119	1425343_at	Hdhd3 | haloacid dehalogenase-like hydrolase domain containing 3
+1.73	0.00047477	0.03330108	1425099_a_at	Arntl | aryl hydrocarbon receptor nuclear translocator-like
+2.26	0.00000038	0.00018212	1425054_a_at	2510006D16Rik | RIKEN cDNA 2510006D16
+1.82	0.00026911	0.02264386	1424952_at	Ociad1 | OCIA domain containing 1
+2.58	0.00000012	0.00007455	1424877_a_at	Alad | aminolevulinate, delta-, dehydratase
+2.95	0.00000018	0.00010090	1424857_a_at	Trim34 | tripartite motif protein 34 /// similar to Tripartite motif protein 34
+1.63	0.00003072	0.00484388	1424843_a_at	Gas5 | growth arrest specific 5
+1.66	0.00016360	0.01594833	1424749_at	Wdfy1 | WD repeat and FYVE domain containing 1
+1.51	0.00012602	0.01331099	1424738_at	4932432K03Rik | RIKEN cDNA 4932432K03 gene
+1.76	0.00001641	0.00298414	1424730_a_at	Slc15a2 | solute carrier family 15 (H+/peptide transporter), member 2
+1.73	0.00004629	0.00648343	1424615_at	Frag1 | FGF receptor activating protein 1
+1.86	0.00000480	0.00114258	1424508_at	Ttc5 | tetratricopeptide repeat domain 5
+1.59	0.00017352	0.01651064	1424466_at	Ipo9 | importin 9
+1.53	0.00009101	0.01041774	1424360_at	BC019943 | cDNA sequence BC019943
+1.53	0.00022908	0.02021870	1424317_at	Slc25a19 | solute carrier family 25 (mitochondrial deoxynucleotide carrier), member 19
+1.57	0.00007712	0.00922639	1423746_at	Txndc5 | thioredoxin domain containing 5
+1.75	0.00000565	0.00127492	1423606_at	Postn | periostin, osteoblast specific factor
+2.47	0.00000003	0.00002369	1423554_at	Ggcx | gamma-glutamyl carboxylase
+1.60	0.00055969	0.03653064	1423484_at	Bicc1 | bicaudal C homolog 1 (Drosophila)

+1.52	0.00117937	0.06170602	1423424_at	Zic3 | zinc finger protein of the cerebellum 3
+1.52	0.00002089	0.00363851	1422466_at	Nxn | nucleoredoxin
+1.80	0.00000344	0.00089641	1422141_s_at	Csprs | component of Sp100-rs
+2.89	0.00000011	0.00006930	1422140_at	Sp100-rs | similar to component of Sp100-rs /// similar to component of Sp100-rs /// predicted gene, EG665338 /// predicted gene, EG665378 /// similar to component of Sp100-rs /// similar to component of Sp100-rs /// similar to component of Sp100-rs /// similar to component of Sp100-rs /// similar to component of Sp100-rs /// similar to component of Sp100-rs
+1.55	0.00111630	0.05895358	1422051_a_at	Gabbr1 | gamma-aminobutyric acid (GABA-B) receptor, 1
+3.79	0.00000002	0.00001739	1421850_at	Mtap1b | microtubule-associated protein 1 B
+1.53	0.00031589	0.02508259	1421604_a_at	Klf3 | Kruppel-like factor 3 (basic)
+1.82	0.00206109	0.08588374	1421426_at	Hhip | Hedgehog-interacting protein
+3.74	0.00000315	0.00083516	1421385_a_at	Myo7a | myosin VIIa
+3.45	0.00000000	0.00000315	1421090_at	Epb4.1l1 | erythrocyte protein band 4.1-like 1
+1.65	0.00022609	0.02005773	1421018_at	1110018J18Rik | RIKEN cDNA 1110018J18 gene
+2.70	0.00000011	0.00006930	1421011_at	Hsd17b11 | hydroxysteroid (17-beta) dehydrogenase 11
+1.53	0.00060810	0.03867460	1420984_at	Pctp | phosphatidylcholine transfer protein
+1.80	0.00063370	0.03958544	1420873_at	Twf1 | twinfilin, actin-binding protein, homolog 1 (Drosophila)
+1.56	0.00007004	0.00875047	1420849_at	Crnkl1 | Crn, crooked neck-like 1 (Drosophila)
+2.62	0.00000234	0.00067062	1420286_at	--- | Transcribed locus
+1.56	0.00006759	0.00852942	1419905_s_at	Hpgd | hydroxyprostaglandin dehydrogenase 15 (NAD)
+1.73	0.00062314	0.03914239	1419741_at	Supt16h | suppressor of Ty 16 homolog (S. cerevisiae)
+2.25	0.00000520	0.00119051	1419612_at	4632415L05Rik | RIKEN cDNA 4632415L05 gene
+2.04	0.00000165	0.00053813	1419469_at	Gnb4 | guanine nucleotide binding protein, beta 4
+2.03	0.00000933	0.00190307	1419394_s_at	S100a8 | S100 calcium binding protein A8 (calgranulin A)
+1.59	0.00007375	0.00894186	1419363_a_at	Mrpl35 | mitochondrial ribosomal protein L35
+1.52	0.00020780	0.01904856	1419362_at	Mrpl35 | mitochondrial ribosomal protein L35
+1.55	0.00186132	0.08262554	1419291_x_at	Gas5 | growth arrest specific 5
+1.72	0.00214502	0.08731293	1419157_at	Sox4 | SRY-box containing gene 4 /// similar to Transcription factor SOX-4
+1.57	0.00087697	0.05000254	1418925_at	Celsr1 | cadherin EGF LAG seven-pass G-type receptor 1
+1.59	0.00002952	0.00467149	1418903_at	Aqp2 | aquaporin 2
+1.57	0.00014155	0.01444323	1418464_at	Matn4 | matrilin 4
+1.62	0.00131036	0.06588483	1418429_at	Kif5b | kinesin family member 5B
+1.56	0.00008093	0.00958003	1418427_at	Kif5b | kinesin family member 5B
+2.89	0.00000008	0.00005377	1418310_a_at	Rlbp1 | retinaldehyde binding protein 1
+4.40	0.00000000	0.00000112	1418282_x_at	Serpina1b | serine (or cysteine) preptidase inhibitor, clade A, member 1b
+1.52	0.00032050	0.02531535	1418245_a_at	Rbm9 | RNA binding motif protein 9
+1.83	0.00024094	0.02093483	1417961_a_at	Trim30 | tripartite motif protein 30
+1.51	0.00019178	0.01776110	1417903_at	Dfna5h | deafness, autosomal dominant 5 homolog (human)
+2.74	0.00000006	0.00004203	1417764_at	Ssr1 | signal sequence receptor, alpha /// similar to signal sequence receptor, alpha
+2.57	0.00000092	0.00033860	1417600_at	Slc15a2 | solute carrier family 15 (H+/peptide transporter), member 2
+1.57	0.00266951	0.09874270	1417432_a_at	Gnb1 | guanine nucleotide binding protein, beta 1
+1.57	0.00169470	0.07830735	1416946_a_at	Acaa1a | acetyl-Coenzyme A acyltransferase 1A /// acetyl-Coenzyme A acyltransferase 1B
+1.51	0.00004820	0.00666784	1416203_at	Aqp1 | aquaporin 1
+2.19	0.00033165	0.02578924	1416136_at	Mmp2 | matrix metallopeptidase 2
+1.73	0.00005074	0.00691246	1415977_at	Isyna1 | myo-inositol 1-phosphate synthase A1